

# Complementing Automotive Haptic Shared Control with Visual Feedback for Obstacle Avoidance

W. Vreugdenhil







---

MASTER OF SCIENCE THESIS

# Complementing Automotive Haptic Shared Control with Visual Feedback for Obstacle Avoidance

BY

W. VREUGDENHIL

to obtain the degree of Master of Science  
at the department of Mechanical Engineering  
of Delft University of Technology,  
to be defended publicly on Monday January 28, 2019 at 13:00.

Student Number:	4134001	
Master Track:	Biomechanical Design	
Specialization:	Automotive Human Factors	
Thesis Committee:	Prof. dr. ir. D. A. Abbink	TU Delft ME, Supervisor
	Dr. ir. C. Borst	TU Delft AE, Supervisor
	ir. S. Barendswaard	TU Delft ME, Supervisor
	Dr. S. M. Petermeijer	TU Delft ME, Supervisor
	Dr. ir. M. M. Paassen	TU Delft AE, External Member

An electronic version of this study is available at <https://repository.tudelft.nl/>.



## Preface

This work presents the development and evaluation of a novel visual feedback system aimed at complementing the current automotive haptic feedback solutions. In this study I researched the effect of the combined feedback on driver behavior during an obstacle avoidance task.

In this section I would like to devote special attention to the people that played a key role in the establishment of my work. First of all, I would like to thank David Abbink for his positive energy, critical eye and out-of-the-box thinking. My gratitude also goes out to Clark Borst, for his determined support, patience and sharing his mutual passion for electronic music. Moreover, I would like to thank Sarah Barendswaard for her tranquility, great assistance and overall supervision of the thesis. Also, I am thanking Bastiaan Petermeijer for his humour and excellent guidance throughout the thesis, starting as far back as the literature study. Additionally, I would like to thank my supervisors for the enormous flexibility and freedom that I was given during the Master Thesis, as this allowed me to get the most out of myself, also in my personal life.

Besides my supervisors I would like to give many thanks to Sarvesh Kolekar, Dirk van Baelen and René van Paassen in particular, for the implementation and debugging of my simulator experiment. Likewise, I want to thank all members of the Delft Haptics Lab for the friendly atmosphere and the good talks.

Finally, I am thanking my friends and family for their genuine engagement in my personal and academic development. In particular, I would like to thank my parents for supporting me throughout my entire academic career, while at the same time allowing me to pursue my dreams besides my study.

*Wilco Vreugdenhil*  
*Delft, January 2019*



# Contents

<b>Nomenclature</b>	<b>3</b>
<b>1 Research Paper</b>	<b>4</b>
Abstract	
Introduction	
Visual Feedback	
Method	
Results	
Discussion	
Conclusion	
<b>Appendix</b>	<b>5</b>
<b>A Background: Literature Summary</b>	<b>6</b>
<b>B Haptic Feedback Design</b>	<b>7</b>
Four-Design-Choice Controller . . . . .	7
Human Compatible Reference . . . . .	7
Haptic Settings DUECA . . . . .	11
<b>C Visual Ecological Feedback Design</b>	<b>12</b>
Abstraction Hierarchy . . . . .	12
<b>D Implementation</b>	<b>13</b>
MATLAB Simulation . . . . .	13
DUECA Simulation . . . . .	15
<b>E Experiment Forms</b>	<b>17</b>
<b>F Conflict Torque Analysis</b>	<b>18</b>
<b>G Experimental Results</b>	<b>20</b>
Pilot Study . . . . .	20
Experimental Study . . . . .	23



## Nomenclature

Abbreviation	Description
ABS	Antilock Brake System
ACC	Adaptive Cruise Control
ADAS	Advanced Driver Assistance Systems
AR	Augmented Reality
DDT	Dynamic Driving Task
EID	Ecological Interface Design
FoST	Field of Safe Travel
HCR	Human Compatible Reference
HDD	Head-Down Display
HSC	Haptic Shared Control
HUD	Head-Up Display
LKA	Lane Keeping Assist
LoHA	Level of Haptic Authority
MFD	Multi-Function Display
RMS(E)	Root Mean Squared Error
RT	Reaction Time
SRK	Skills, Rules and Knowledge
SRR	Steering wheel Reversal Rate
THW	Time Headway
TIS	Tunnel In the Sky
TLC	Time to Line Crossing
TOR	Take-Over Request
TTC	Time To Collision
UAV	Unmanned Aerial Vehicle
VSD	Vertical Situation Display
WDA	Work Domain Analysis



# 1 Research Paper



# Complementing Automotive Haptic Shared Control with Visual Feedback for Obstacle Avoidance

W. Vreugdenhil

supervised by:

S. Barendswaard, S. M. Petermeijer, C. Borst, D. A. Abbink

**Abstract**—The technological advancements in the automotive industry have enabled the automation of numerous routine driving tasks. As a result, the art of driving has become a control task with a strong supervisory character, including the common human factor issues. Haptic Shared Control has been shown to be useful in keeping the driver in-the-loop by providing continuous haptic guidance on the steering wheel. Nonetheless, it has been reported that haptic support often induces control conflicts caused by the limited amount of information that can be conveyed through haptic forces. As a consequence, it is often burdensome to develop a correct mental model of the underlying controller and to establish accurate situation awareness. This study presents the results of the conceptual development of a novel visual feedback system inspired by the principle of Ecological Interface Design. By displaying the future trajectory with respect to both the physical limitations of the vehicle and the intentional constraints imposed by the road, the driver is able to establish a better understanding of the space of possibilities in a certain driving scenario. The new visual feedback is combined with current haptic feedback solutions, with the goal of guiding the driver through force-feedback, while visualizing the space of possibilities as defined by the work domain constraints. A human-in-the-loop experiment was conducted to evaluate the effects of the novel feedback system on driver behavior and acceptance during an obstacle avoidance task. In analogy with previous findings, the results showed that haptic guidance was beneficial during obstacle avoidance in terms of response time, control activity and effort, where the addition of EID-inspired visual feedback revealed an improved task execution, together with a significant reduction of control activity and conflicts.

**Index Terms**—Haptic Shared Control, Visual Feedback, Ecological Interface Design, multimodal feedback, evasive manoeuvres, obstacle avoidance, human-automation interaction.



## 1 INTRODUCTION

Rapid developments in the field of Advanced Driver Assistance Systems (ADAS) have led to the transformation of direct physical control tasks into assisted or even fully automated driving tasks, such as longitudinal and lateral control. The potential advantages of such systems are higher safety, comfort and reduction in control effort. However, in the last decades ample studies have shown that the challenges that come with the development of higher levels of automation are more than just technical [1]. One of the challenges are the human factor issues, such as overreliance and skill loss that emerge when operating automated systems that still require human supervision and intervention [2]. This can be explained by the fact that increasing the level of automation may be able to streamline a routine driving task, however it typically increases the total system complexity. Therefore, the driver's overall comprehension of the system is reduced, undermining the ability to intervene in case of an unanticipated event. The ability to cope with unexpected events is one of the most important reasons why drivers are still required. Successful automation design must therefore empower the driver to compensate for the limits of the automation and help the driver exploit on the capabilities of the automation [3].

Haptic Shared Control (HSC), a cooperative form of automation aimed at keeping the driver in-the-loop, has been researched in multiple studies [4]–[7]. The aim of HSC is to avoid the pitfalls of automation by providing continuous haptic feedback, giving guidance to the driver in order to complement skill-based behavior. Consequently, HSC has

proven to yield improvements in vehicle locomotion, such as reduced human variability for different control tasks [4], [6]–[9], reduced control activity [10] and improved reaction times [4]. However, these improvements frequently come at a cost of increased human torque [11], caused by conflicting directions of intent between the driver and HSC. Among other reasons ([11]–[13]) these conflicts can be explained by the limited amount of information complexity that can be conveyed through haptic forces [14], perceived by the tactile senses of the human. For example, without a visual notification, a haptic vibration in the steering wheel could be interpreted as a lane departure warning, drowsiness detection or some other warning. By visualizing the underlying message, the automation intent can be conveyed in an intuitive and comprehensive way.

### 1.1 Problem Statement

To improve automation feedback, several studies have found promising results of combining feedback modalities such as visual and auditory together with haptic feedback [15], [16], showing improved primary task performance and reduced control activity, visual and cognitive demand. In such systems the modality of the feedback is highly dependent on the complexity and time scale of the required information. For instance, direct perception (i.e. tactile senses) is highly suited for feedback on a short time scale, supporting skill-based behavior. Visual feedback however, is often used for longer time scales where interpretation is more prevalent [17], supporting skill- and rule-based behavior [18].

However, the current applications of visual-haptic feedback are solely designed to reflect the automation constraints imposed by the underlying controller, and thereby do not consider constraints beyond this envelope, [15], [16]. In other words, the current visual feedback is focused mostly on informing the operator about the operational domain of the haptic feedback, but not on the actual performance of the vehicle with respect to its surroundings. This means that visual-haptic guidance is generally well-accepted for routine tasks where the haptic feedback is reliable, yet the visual feedback becomes obsolete for non-routine tasks in which the haptics may fail, often imposing control conflicts. In this case, the visual feedback is not able to inform the operator about possible solutions beyond the automation constraints. To increase the robustness of HSC during unexpected situations and to prevent for control conflicts, a new approach is required which reflects more than just automation constraints.

Apart from [15], [16], little research has been done investigating the potential benefits of applying continuous visual-haptic feedback to vehicle locomotion and car driving in particular. Other studies investigated the effect of solely applying visual feedback for hazard detection [19], [20] and improving situation awareness during Take Over Requests (TOR) [21]. However, these applications focus mostly on providing specific advisory information rather than providing continuous holistic feedback of the driving task in order to improve robustness during unexpected scenarios. A promising design strategy to support operators in complex work domains where unexpected events may occur, is the principle of Ecological Interface Design (EID) [22]. The main goal of EID is to transform a cognitive task into a perceptual task by providing meaningful information about the work domain constraints that humans can directly perceive and act on accordingly [23]. By allowing the constraints to be directly perceptible, EID interfaces assist users in the development of their mental model of the domain. Driver support system interfaces resulting from this analysis may not only help drivers form better situation awareness, but also an improved mental model of the vehicle. It has been shown that applying EID to the driving domain can improve calibrated trust and reliance [14], [24], [25]. Other examples of work domains in which EID has been applied successfully are process control [22], [26], health care [27], command and control [28], marine [29] and aviation [30]–[33]. In the driving domain EID has already successfully been applied to reflect the operational envelope of Adaptive Cruise Control (ACC) with respect to other work domain constraints. However, it has not yet been combined with haptic feedback systems. In this study, the idea was investigated of combining the existing HSC systems together with a novel form of EID-inspired visual feedback, based on the benefits and drawbacks of both HSC and EID.

## 1.2 Research Objective

The aim of this simulator study was to quantify the benefits and drawbacks of the combined feedback in relation to their separate application, with manual driving as a baseline condition. Driving behavior was assessed for obstacle avoidance by using a previously developed continuous

haptic feedback system [34] in combination with a novel EID-inspired visual feedback system, displaying the future trajectory with respect to the physical limitations of the vehicle and the intentional constraints imposed by the road. To investigate the effect of adding visual feedback, it was hypothesized that combining HSC with EID-inspired visual feedback, compared with HSC-only, would result in: (1) improved task execution, (2) reduced control activity, (3) reduced control effort, (4) reduced conflicts in torque and (5) improved user acceptance. It was expected that these effects would be more distinct for non-critical scenarios. Argumentation for the defined hypotheses will follow in the next sections.

In particular, the rationale behind these hypotheses is that haptic feedback is highly suited for unexpected events on a short time scale, but less desired for non-critical tasks, where an increase of human torque (conflicts) can be seen [35]. The opposite holds for visual feedback, which tends to be most useful for non-critical events by transforming a complex task into a perceptual task. It is expected that both forms of feedback will complement each other in an obstacle avoidance task with different time-criticalities.

## 2 VISUAL FEEDBACK

### 2.1 Theoretical Motivation

In general, EID applies a top-down approach with the complete work domain as a starting point. Within this work domain, roughly three layers can be distinguished. The first layer is formed by (1) the physical constraints, which refer to the laws of physics that influence possible directions of the driver. Subsequently, (2) the intentional constraints reflect the rules and laws that govern driver behavior. Finally, (3) the automation constraints indicate the operational envelope of the underlying controller, which is often limited by a predetermined optimal control strategy. It has been shown that constraint-based interfaces can enhance situation awareness, which at its turn can be used to decide whether or not to follow the automation advisory. On the other hand "ecological interfaces reveal all feasible control actions within the work domain constraints, thereby increasing the chance that people will disagree with automation advice that wants to push them into one specific direction" [36]. Therefore, the design of an EID-inspired interface is highly dependent on the balance between the three different types of work domain constraints.

### 2.2 Visual Feedback Design

An overview of the EID-inspired visual feedback design is depicted in Figure 1, where the road, vehicle and performance envelope are shown. A comparable design was researched previously in the aviation domain [37], visualizing the flight envelope of an aircraft. At first, the physical constraints were implemented by showing the physical performance of the dynamic vehicle model. The performance envelope, indicated in grey consists of multiple curves that provide an estimation of the future trajectory given a constant steering wheel input, thereby representing the domain for which the vehicle remains stable at a given speed (i.e. space of possibilities). The outermost curves indicate

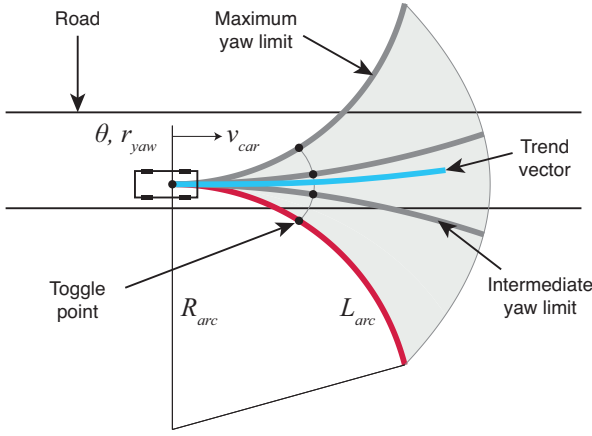


Fig. 1. Overview of visual feedback design, with future trajectory curves forming the performance envelope (grey). In the simulation only the curves are visualized, the grey envelope is presented here for clarity.

the predicted trajectory for which the vehicle reaches the maximum yaw rate at the current speed. The inner lines show an intermediate yaw rate that can be used for heading estimation. The radius of the curves is based on the current velocity  $v_{car}$  and yaw rate  $r$  corresponding to the curve (Equation 1), meaning that the higher the speed, the greater the radius of the curves. Here,  $R_{arc}$  represents the radius of the desired curve.

$$R_{arc} = \frac{v_{car}}{r} \quad [m] \quad (1)$$

TABLE 1. Definitions of physical constraints.

Constraint	Velocity	Yaw	Yaw rate [rad·s <sup>-1</sup> ]
Trend vector	variable	variable	$r_{yaw}$
Intermediate yaw limits	variable	fixed	0.08
Maximum yaw limits	variable	fixed	0.33

In Figure 1 it can be seen that there are two curves defining the maximum yaw limit and two curves for the intermediate yaw limit. This means that for the definition of the yaw limits, a fixed yaw rate was applied making these curves only velocity-dependent. The trend vector however, represents the future trajectory of the vehicle according to the actual yaw rate which is updated real-time according to both the velocity and current yaw rate of the vehicle. An overview of the curve definitions can be found in Table 1, where the maximum yaw limit corresponds to the maximum yaw rate of the vehicle model, as was used in previous studies [10]. The intermediate yaw limit was chosen such that it would match a common road curve with a radius of approximately 300 m at a speed of 24 m/s. The curves were implemented in the simulator by attaching them to the vehicle, accounting for the current heading  $\theta$ , where the Center of Gravity (CoG) of the vehicle was used as the origin of the curves. Note that the design of the physical constraints is strictly based on the internal constraints, meaning that they only provide information about the vehicle status and not of its surroundings.

TABLE 2. Definitions of constraint look ahead times (determined empirically).

Constraint	Visible	$t_{ahead}$ [s]
Trend vector	yes	3.5
Intermediate yaw limits	yes	4.5
Maximum yaw limits	yes	4.5
Toggle points	no	0.9

Secondly, the implementation of the intentional constraints (rules and laws) was done through the detection of the road boundaries, as indicated by 'road' in Figure 1. On each curve, imaginary toggle points were applied, specified by their own look ahead time  $t_{ahead}$ , see the last row in Table 2. In this table it can also be seen how the length  $L_{arc}$  of the other curves was defined, assuming that  $L_{arc} = v_{car} \cdot t_{ahead}$ . During the simulation it was constantly verified whether one of the toggle points was outside either of the two road boundaries. In case the toggle point was indeed outside the road boundary, the corresponding curve would turn from grey to red, of which an example is shown by the rightmost curve in Figure 1 and Figure 2. This should give the driver a warning that when choosing this trajectory, the lane would be departed within the specified toggle look ahead time. Therefore, the lane boundary detection informs the driver about their interaction with the intentional constraints and thus what the field of safe travel (FoST) is during a certain driving manoeuvre. It was deliberately chosen to assign the outermost road boundaries as intentional constraints, and not the road center line. Together with the fact that the external physical constraints such as obstacles were not incorporated, it is believed that the driver should be informed of all available spatial options on the road. With this information, the responsibility of visual object detection in case of an unexpected event, lies fully on the side of the driver. It is believed that this will improve situation awareness and thus decision making during an obstacle avoidance.



Fig. 2. Visual feedback design as implemented in the simulator, with future trajectory curves forming the performance envelope.

Finally, it was chosen not to incorporate any automation constraints in the visual feedback design, since this study is the first to use EID-inspired visual feedback. Therefore, it was chosen to first study the effect of combining haptic feedback with the visualization of physical and intentional constraints imposed by the driving domain, to find a re-

lation between these results and prior research. However, it should be noted that a disguised form of automation constraints is present in the visual feedback. This can be explained by the fact that the trend vector from Figure 1 represents the total output of both the human and controller. In other words, the current yaw rate is determined by both the actions of the human and HSC. This means that when the HSC follows the reference trajectory without human intervention, the trend vector displays the intentions of the controller. In the simulation however, people were asked to control the steering wheel at all times, making this effect hardly noticeable.

### 3 METHOD

#### 3.1 Participants

Twenty-six participants (4 women and 22 men) between 24 and 58 years old ( $M = 28$ ,  $SD = 6.6$ ), holding a driving license for at least 1 year ( $M = 9.0$ ,  $SD = 6.9$ ) conducted the experiment. All participants had normal to corrected eyesight and took part on a voluntary basis without a financial compensation for their effort. The study was approved by the Human Research Ethics Committee of the Delft University of Technology.

#### 3.2 Apparatus

The experiment was conducted using a fixed-base driving simulator, equipped with an actuated steering wheel, an adjustable driver seat, an LCD dashboard and three projectors visualizing the driving scene. During the experiment the vehicle's velocity was kept constant, meaning that the brake and gas pedals were inactive. The steering wheel was actuated by a Moog-FCS S-motor and controlled through a control-loading computer at a rate of 2500 Hz. This actuator was used to provide haptic guidance torques, updated at a rate of 200 Hz. The total scene projection on the front and side walls yielded a size 10.1 m x 2.1 m, which corresponds to a 180° x 40° Field of View (FoV).

The simulation was updated and logged at a rate of 100 Hz, where the visual scene was rendered at 50 Hz. The driving scene consisted of a two-lane road with straight sections and intermittent curves. To improve speed perception, engine sound, side poles and randomly placed trees were implemented. A single-track heavy sedan of 1.8 m wide was used to simulate the vehicle, with vehicle dynamics identical to those used in previous studies [10].

#### 3.3 Applied Haptic Guidance

In previous research it was shown that a control structure separating the human compatible reference (HCR) from the haptic shared controller can significantly reduce control conflicts in terms of human steering wheel torque [scholtens2018], compared to a shared controller which only uses feedback based on the road center reference. In Figure 3 an overview is given of the applied FDC controller, showing the relationship between (1) the HCR, (2) strength of the Haptic Feedback (SoHF), (3) Level of Haptic Support (LoHS) and (4) the Level of Haptic Authority (LoHA). In this study it was chosen to implement the HCR by recording several manual trails, which were used to create a generic reference

of which the behavior was consistent for each obstacle configuration for all participants. The HCR consists of four variables that are required by the HSC, including vehicle position (X and Y), heading and steering wheel input. All other control parameters of the HSC were chosen similar to prior research, [34]. Figure 4 depicts two examples of the applied haptic guidance torque during the evasive manoeuvres, showing a harmonic profile to perform a double lane change. These haptic torques are the result of the implemented HCR, which was pre-programmed to avoid obstacles. The difference between the two scenarios will be explained in subsection 3.4.

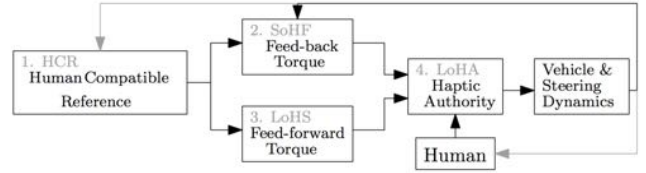


Fig. 3. Schematic overview of the applied Four-Design-Choice structure, from [34]. The HCR for this study was derived from manual recordings and made generic across all participants.

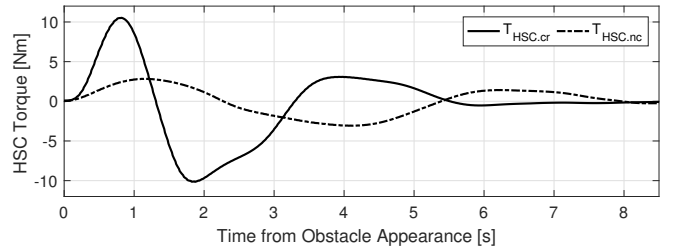


Fig. 4. Example of applied haptic guidance torques during obstacle avoidance, cr = critical and nc = non-critical.

#### 3.4 Experiment Design

Four driving conditions were evaluated among the participants, including visual feedback, haptic feedback and a combination of both, with manual control as baseline condition, see Table 3. Since the participants all experienced the four conditions, a within-subjects repeated-measures design was used. In the training session, the conditions were introduced in a generic order, being: (1) Manual, (2) EID, (3) HSC and (4) Combi. During the four main trails the driving conditions were randomized across the participants.

TABLE 3. Overview of applied driving conditions.

	Manual	EID	HSC	Combi
Visual Feedback	-	X	-	X
Haptic Feedback	-	-	X	X

The simulation trajectory was defined by a two-lane road having a total width and length of 7.2 m and 9.3 km, respectively. The driving speed was fixed at 24 m/s ( $\approx 85$  km/h), resulting in a time of 390 s per trail. The outer-lane boundaries were marked by continuous white lines, the center line by a dashed white line. The trajectory was identical for all trails and consisted of 14 straight sections

of 300 m, each alternated by two left or right curves with a center radius of 375 m, see Figure 5. No other vehicles shared the road.

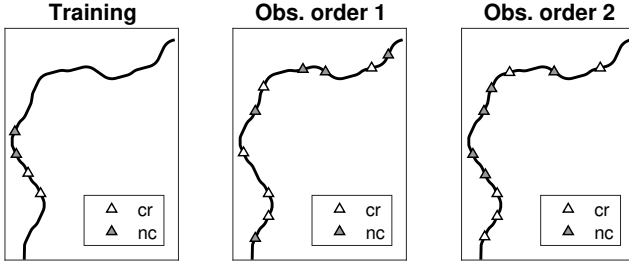


Fig. 5. Overview of simulation trajectory and applied obstacle configurations. Trajectory consists of 14 straight sections, with 5 critical and 5 non-critical obstacles for condition 1 and 2.

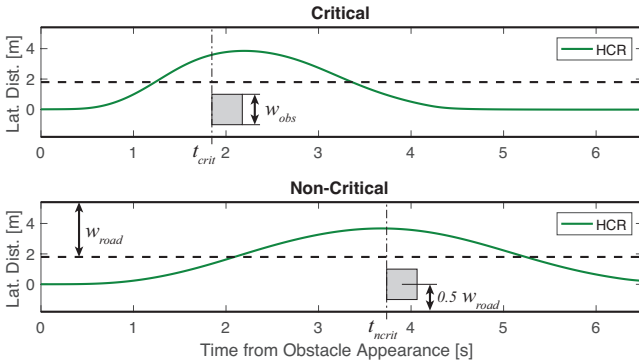


Fig. 6. Straight road sections with critical and non-critical obstacle conditions. Road width is  $w_{road} = 3.6$  m. The origin indicates the moment at which the obstacle appears on the road. Human Compatible Reference for the manoeuvre is represented by the green trajectory. Note that the lateral axis and the obstacle length are not to scale, for clarity.

Figure 6 shows the straight road sections with two obstacle conditions, including the HCR for the HSC and Combi condition. The participants had to avoid cubic obstacles having a width (length and height) of  $w_{obs} = 2.0$  m that randomly appeared in the middle of the right lane on one of the straight sections. Previous research on haptically assisted obstacle avoidance showed a tipping point of steering wheel angle and human torque at a Time To Collision (TTC) of 2.0 s. For more critical situations the control effort was reduced ( $1 < TTC < 2$ ), where the control effort increased for less critical situations ( $2 < TTC < 6$ ), [35]. Consequently, the applied time-criticalities measured from obstacle appearance to the front face of the obstacle (Figure 6) were:

- 1) Critical (cr), with  $t_{crit} = 1.85$  s
- 2) Non-critical (nc), with  $t_{ncrit} = 3.7$  s

For all training conditions, the obstacle order was defined by 2 empty sections, followed by 2 non-critical obstacles and subsequently by 2 critical obstacles, gradually increasing the level of difficulty. During the main trails, 5 critical and 5 non-critical obstacles were distributed over 14 straight sections, resulting in 4 empty sections. Anticipatory behavior in obstacle avoidance was prevented by applying two different obstacle orders among the four driving conditions, see Figure 5.

### 3.5 Procedure and instructions

Prior to the experiment, the participants were asked to read and sign a consent form, explaining the procedure, purpose and risks of the experiment. The participants were informed that they would experience either (1) no feedback, (2) visual feedback, (3) haptic feedback in the form of a steering wheel torque or (4) a combination of both. The form further stated that the car speed was held constant at 85 km/h by a cruise control system and that the participant's primary goal was to stay in the middle of the right lane on a curvy two-lane road, while avoiding objects that randomly appeared on the road. After the obstacle was avoided, the participants should turn back to the right lane at their own pace. Intentionally, the participants were not informed about the obstacle location on the road nor the evasive direction to be taken. Lastly, it was stated that they could withdraw from the experiment at any time, without any negative consequences.

Before taking place in the simulator the participants were asked to fill out a questionnaire about their demographics, driving experience and their affinity with video games. Subsequently, the participants were invited to be seated in the simulator and to adjust the driver seat to their comfort, while maintaining a ten-to-two position on the steering wheel. Next, a training session of 15 minutes was held to familiarize the participant to the different forms of vehicle feedback. During the training the experimenter repeated the primary driving goals (lane keeping and obstacle avoidance) and briefly explained the principles of the different forms of feedback. After the training session, the participants performed the four main trails (7 minutes each).

Each trail was completed by a 5-minute break, where the participants were asked to leave the simulator to fill out a NASA Controller Acceptance Rating Scale (NASA-CARS [38]) for assessing system acceptance and the Van der Laan (VDL) questionnaire [39] for assessing usefulness and satisfaction of the feedback system. Before conducting the next trail, the participants were asked whether they suffered from simulator sickness on a scale from 1 to 6 (1 = no sign of symptoms, 2 = arising symptoms, 3 = slight nausea, 4 = nauseous, 5 = very nauseous, 6 = vomiting). In case of a response of 4 or higher, the experiment would be aborted. The completion time of the experiment was approximately 1.5 hours per participant.

### 3.6 Dependent Measures

During the experiment, raw data was logged at a rate of 100 Hz regarding the steering wheel input, vehicle dynamics and vehicle position. These variables were used to analyze the effect of complementing HSC by EID-inspired feedback and thus to answer the main hypotheses. The dependent measures selected for the obstacle avoidance analysis are described in the following sections.

#### 3.6.1 Task Execution

Obstacle avoidance execution was assessed by several measures, related to the driven trajectories during the evasive manoeuvres. In Figure 7 a schematic overview of these metrics is given with an exemplary trajectory. The grey trajectory represents the car width ( $w_{car} = 1.8$  m) in time,

measured in the center of gravity (CoG) of the vehicle. Note that the origin of the lateral distance (y-axis) lies in the center of the right lane. To evaluate task execution, four dependent measures were used:

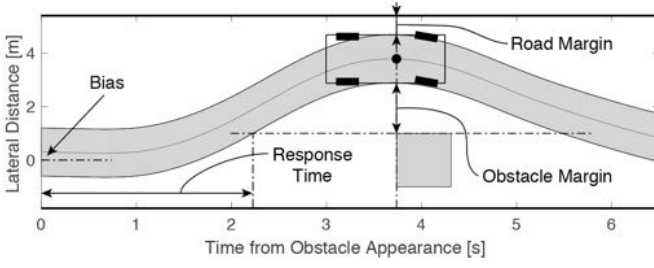


Fig. 7. Schematic overview of obstacle avoidance trajectory and the related dependent measures. Grey trajectory represents the car width in time, measured in the CoG (black dot). Note that the image is not to scale: the lane width, vehicle size and obstacle size were altered for clarity.

- *Mean lateral obstacle margin*, defined as the lateral distance between the right side of the car and the left side of the obstacle at the moment when the CoG of the vehicle passed the front face of the obstacle.
- *Standard deviation lateral obstacle margin*, describing the intra-subject variability of the lateral obstacle margin within the participants.
- *Mean lateral road margin*, defined as the lateral distance between the left side of the car and the left lane boundary at the same moment of passing the obstacle.
- *Mean lateral bias*, defined as the distance from the center of the right lane to the vehicle CoG at the instance when the obstacle appears ( $t = 0$ ).
- *Mean response time*, defined as the time at which the right side of the car exceeds the minimum lateral distance required to avoid the obstacle, equal to half the obstacle width ( $0.5 \times w_{obs} = 1.0$  m).

### 3.6.2 Control Activity

The *mean Steering wheel Reversal Rate* (SRR) was measured to analyze high frequency control activity related to both lane keeping and obstacle avoidance on the straight road sections. The SRR is defined as the number of steering direction reversals having a magnitude greater than  $2^\circ$  [40]. Since the TTC of the two obstacle conditions was different, the end time of the control activity analysis was corrected such that the remaining time after obstacle passage was equal for both conditions (Table 4), where  $t_{start}$  is defined as the moment of obstacle appearance. This was also done for measuring control effort and conflicts, considering the dependence of time-interval for these metrics.

TABLE 4. Domain of analysis for control activity, effort and conflicts.

	$t_{start}$	$t_{obs}$	$t_{end}$	$t_{end} - t_{obs}$
cr	0	1.85	6.65	4.8
nc	0	3.7	8.5	4.8

### 3.6.3 Control Effort

The *mean total rotational work*  $W_{tot}$  was calculated to determine the control effort during the evasive manoeuvre. This was done by summing the multiplication of the average human torque with the change in steering wheel input per time-step. The applied time domain for the analysis is similar to the domain for the control activity, see Table 4.

$$W(i) = \frac{|T_{hum}(i+1) + T_{hum}(i)|}{2} \quad (2)$$

$$\delta\theta_{st}(i) = ||\theta_{st}(i+1)| - |\theta_{st}(i)|| \quad (3)$$

$$W_{tot} = \sum_{n=1}^{n-1} W(i) \cdot \delta\theta_{st}(i) \quad (4)$$

### 3.6.4 Conflicts in Torque

Conflicts were exclusively evaluated for the two conditions with haptic support, being HSC and Combi. The occurrence and amount of conflicts were evaluated by determining whether the human and HSC torque were in opposite direction during the straight sections in which obstacles were avoided. Conflicts in other situations during the trails were not in the scope of this study. In case of a conflict, the time-instance was flagged as 1, where a flag of 0 indicated that the HSC torque supported the driver intentions. The occurrence and absolute difference between human and HSC torque was used to determine the *mean conflicting rotational work*  $W_{con}$ , *mean conflict peak torque*  $T_{con.p}$  and the *mean percentage of time in conflict*. For the applied time domain of the conflict analysis, see Table 4.

### 3.6.5 Subjective Acceptance

Acceptance of the vehicle feedback systems was subjectively determined by the NASA-CARS questionnaire. Based on the schematic Cooper-Harper rating scale [41], the participants were asked to provide an *acceptance rating* from 1 to 10 for each driving condition. Additionally, a *confidence rating* was given that reflected the ratio of information available to the driver in the simulation to the information necessary to obtain a realistic rating, where A = high, B = moderate, C = low.

Secondly, *usefulness* and *satisfaction* was measured after every driving condition by the VDL questionnaire, consisting of nine questions per condition, with scores ranging from -2 to +2. The usefulness was calculated by averaging the scores of question 1, 3, 5, 7 and 9, where the satisfying rate was obtained by averaging the scores of question 2, 4, 6 and 8.

## 3.7 Statistical Analyses

For all dependent measures, a matrix of data points was obtained, consisting of 26 entries x 8 conditions. The eight conditions were formed by two within-subject factors, of which the four driving conditions were categorized as ADAS factor, where time-criticality (critical and non-critical) was categorized as Time factor. Before submitting the matrices to a statistical test, all measures were checked for the assumption of normality and sphericity. In case the

assumption was violated, the values were corrected by the Greenhouse-Geisser correction. Subsequently, a two-way repeated measures ANOVA was used to verify the overall significance of the test conditions between the participants. To perform pair-wise comparisons, a post hoc test was done comparing the main effects with a Bonferroni adjustment. Note that for the measures defining the conflicts in torque, only four (2 ADAS  $\times$  2 Time) conditions were analyzed, since conflicts were only present in the HSC and Combi condition. The significance of the subjective measures was verified using the non-parametric Friedman test, based on the final rating of acceptance, confidence, usefulness and satisfaction per condition.

## 4 RESULTS

In this section the experimental results are presented according to the dependent measures as defined in subsection 3.6. Since many measures are derived from the trajectories driven during the obstacle avoidance, an example showing the characteristic behavior found during the experiments is given in Figure 8. The figure is based on the mean and standard deviation of the trajectories per condition of one participant. Note that the figure is corrected for the width of the car, meaning that both lanes are subtracted by the car width and that the obstacle size here is  $w_{obs} - w_{car}$ . By visualizing the results in this form, the lateral obstacle and road margins can directly be determined. In brief, the results indicate that the addition of visual feedback (in EID and Combi) reduces the lateral obstacle margin (while increasing road margin) compared to the Manual or HSC condition, for both critical and non-critical scenarios. Moreover, the standard deviation shows that the addition of visual feedback leads to increased intra-subject variability, where haptic feedback seems to impose a reduction of this metric.

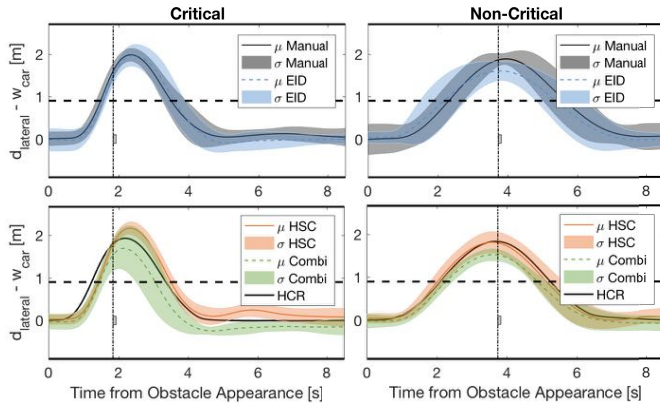


Fig. 8. Mean and standard deviation of trajectories for one participant (nr. 16) per condition. The road and obstacle width are corrected for the car width, such that the obstacle and road margin can be determined in relation to the mean trajectory. For clarity, Manual-EID and HSC-Combi are separated in the figures. The HCR represents the desired position of the vehicle, used by the haptic controller.

An overview of all resulting dependent measures of the participants, including mean and standard deviation is given in Table 5. The table also summarizes the statistical significance of the measures in conjunction with the pairwise comparisons. In general, significance was confirmed

for p-values below the alpha-threshold of 0.05. In this section box-plots will be presented to visualize the trend of the dependent measures. In each box-plot, the horizontal bars represent the median values, where the filled areas indicate the first and third quartile. The minimum and maximum recorded value is shown by the end of the whiskers (thin line). Lastly, participants and outliers are indicated by an x and +, respectively.

## 4.1 Task Execution

### 4.1.1 Lateral Obstacle Margin

The characteristic behavior as depicted in Figure 8 is analyzed in more detail by several task execution measures. Starting with the *mean lateral obstacle margin*, it was shown that there was a significant effect imposed by the driving conditions  $F(2.34, 58.56) = 19.57, p < 0.05$ . An overview of the results is depicted by the probability density functions in Figure 9. The figure displays the inter-subject distribution of the mean obstacle margin for all conditions, hence it does not show the distribution of all raw data points. Since the assumption of normality was confirmed for this measure, the densities were fitted with a normal distribution. Note that the horizontal axes of the figure were reversed to match the perspective of the driver during the avoidance, having the obstacle on the right side. The dashed line in Figure 9 indicates the distance for which the vehicle is located in the center of the left lane, corrected for the vehicle width. This was determined according to  $d_c = w_{road} - 0.5 \cdot w_{obs} - 0.5 \cdot w_{car} = 1.7$  m. Except for Manual-Combi, significance was confirmed by pairwise comparisons among all other conditions, see Table 5.

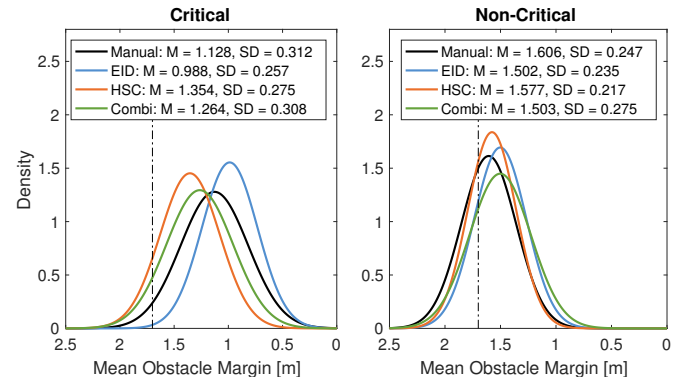


Fig. 9. Fitted normal distributions of the mean lateral obstacle margin of all participants (between subjects), for critical and non-critical obstacles. Obstacle margin defined as the distance between the obstacle and vehicle during obstacle passage, where zero indicates the left side of the obstacle. Note that the x-axis is reversed to match with the driver perspective. Y-axis does not represent distance but density of the x-value. Dashed line indicates the distance  $d_c$  for which the vehicle is located in the center of the left lane.

The results show a significant reduction of mean obstacle margin by the addition of visual feedback (compare with characteristic behavior in Figure 8), when comparing Manual-EID and HSC-Combi, for both critical and non-critical events. This phenomenon can be explained by two factors: (1) the visualization of the physical constraints provided the drivers with more direct insight in their future trajectory in relation to the obstacle, leading to a tendency

TABLE 5. Means and standard deviations of dependent measures, including significance tests.

Measure	Manual (1)				EID (2)				HSC (3)				Combi (4)				Pairwise Comparison							
	critical	non-critical	critical	non-critical	critical	non-critical	critical	non-critical	critical	non-critical	critical	non-critical	critical	non-critical	critical	non-critical	1-2	1-3	1-4	2-3	2-4	3-4		
Mean lateral obstacle margin [m]	M	1.128	1.606	0.988	1.502	1.354	1.577	1.264	1.503	1.264	1.503	1.264	1.503	1.264	1.503	1.264	1.503	X	X	-	X	X	X	X
SD lateral obstacle margin [m]	SD	0.312	0.247	0.257	0.235	0.275	0.217	0.308	0.275	0.308	0.275	0.308	0.275	0.308	0.275	0.308	0.275							
Mean lateral road margin [m]	M	0.223	0.181	0.309	0.202	0.165	0.153	0.169	0.162	0.169	0.162	0.169	0.162	0.169	0.162	0.169	0.162	-	-	-	X	X	-	-
SD lateral road margin [m]	SD	0.101	0.065	0.116	0.107	0.060	0.090	0.080	0.064	0.080	0.064	0.080	0.064	0.080	0.064	0.080	0.064							
Mean lateral bias [m]	M	1.482	0.994	1.624	1.098	1.256	1.023	1.344	1.098	1.256	1.023	1.344	1.098	1.256	1.023	1.344	1.098	X	X	-	X	X	-	-
SD lateral bias [m]	SD	0.313	0.247	0.257	0.236	0.274	0.217	0.308	0.275	0.308	0.275	0.308	0.275	0.308	0.275	0.308	0.275							
Mean response time [s]	M	0.074	0.082	0.114	0.123	0.087	0.096	0.156	0.130	0.156	0.130	0.156	0.130	0.156	0.130	0.156	0.130	-	-	X	-	-	-	-
SD response time [s]	SD	0.183	0.148	0.177	0.192	0.170	0.142	0.187	0.156	0.187	0.156	0.187	0.156	0.187	0.156	0.187	0.156				X	X	-	-
Mean SRR obstacle [s <sup>-1</sup> ]	M	0.087	0.236	0.079	0.238	0.065	0.189	0.071	0.201	0.065	0.189	0.071	0.201	0.065	0.189	0.071	0.201				X	X	-	-
SD SRR obstacle [s <sup>-1</sup> ]	SD	0.089	0.707	0.819	0.675	0.733	0.653	0.771	0.621	0.733	0.653	0.771	0.621	0.733	0.653	0.771	0.621				X	X	-	-
Mean SRR straight [s <sup>-1</sup> ]	M	0.117	0.141	0.138	0.147	0.136	0.149	0.117	0.122	0.136	0.149	0.117	0.122	0.136	0.149	0.117	0.122	X	X	-	X	X	-	X
SD SRR straight [s <sup>-1</sup> ]	SD	0.486	0.260	0.185	0.250	0.486	0.260	0.185	0.250	0.486	0.260	0.185	0.250	0.486	0.260	0.185	0.250							
Mean tot. rotational Work [Nm]	M	33.753	3.506	34.146	3.311	24.736	2.470	23.799	2.171	24.736	2.470	23.799	2.171	24.736	2.470	23.799	2.171				X	X	-	-
SD tot. rotational Work [Nm]	SD	16.093	1.416	16.930	1.360	11.960	1.183	10.945	1.126	11.960	1.183	10.945	1.126	11.960	1.183	10.945	1.126							
Mean conflicting rot. Work [Nm]	M	-	-	-	-	41.695	3.010	40.135	2.775	41.695	3.010	40.135	2.775	41.695	3.010	40.135	2.775							X
SD conflicting rot. Work [Nm]	SD	-	-	-	-	5.165	0.870	5.618	0.669	5.165	0.870	5.618	0.669	5.165	0.870	5.618	0.669							
Mean conflict peak torque [Nm]	M	-	-	-	-	1.166	0.965	1.402	0.613	1.166	0.965	1.402	0.613	1.166	0.965	1.402	0.613							
SD conflict peak torque [Nm]	SD	-	-	-	-	0.500	1.310	0.732	0.419	0.500	1.310	0.732	0.419	0.500	1.310	0.732	0.419							
Mean percentage of time in conflict [s]	M	-	-	-	-	48.754	37.342	51.200	39.666	48.754	37.342	51.200	39.666	48.754	37.342	51.200	39.666							X
SD percentage of time in conflict [s]	SD	-	-	-	-	8.714	11.132	8.174	12.890	8.714	11.132	8.174	12.890	8.714	11.132	8.174	12.890							
CARS acceptance rating [1-10]	M	6.385	7.154	7.615	8.231	8.231	8.231	8.231	8.231	8.231	8.231	8.231	8.231	8.231	8.231	8.231	8.231				X	X	-	-
SD acceptance rating [1-10]	SD	1.577	1.223	1.416	1.243	1.577	1.223	1.416	1.243	1.577	1.223	1.416	1.243	1.577	1.223	1.416	1.243							
CARS confidence rating [A-C = 3-1]	M	2.462	2.462	2.462	2.462	2.462	2.462	2.462	2.462	2.462	2.462	2.462	2.462	2.462	2.462	2.462	2.462							
SD confidence rating [A-C = 3-1]	SD	0.582	0.582	0.582	0.582	0.582	0.582	0.582	0.582	0.582	0.582	0.582	0.582	0.582	0.582	0.582	0.582							
Van der Laan usefulness [-2 - 2]	M	0.762	0.970	0.455	0.752	0.831	0.877	0.877	0.877	0.831	0.877	0.877	0.877	0.831	0.877	0.877	0.877							
SD usefulness [-2 - 2]	SD	0.731	0.455	0.752	0.870	0.731	0.455	0.752	0.870	0.731	0.455	0.752	0.870	0.731	0.455	0.752	0.870							
Van der Laan satisfaction [-2 - 2]	M	0.625	0.817	0.827	1.115	0.827	1.115	1.115	1.115	0.827	1.115	1.115	1.115	0.827	1.115	1.115	1.115				X	X	-	-
SD satisfaction [-2 - 2]	SD	0.782	0.763	0.830	0.850	0.782	0.763	0.830	0.850	0.782	0.763	0.830	0.850	0.782	0.763	0.830	0.850							

Note. The assumption of sphericity was confirmed when Mauchly's test resulted  $p > 0.05$ . Values were corrected with Greenhouse-Geisser estimates of sphericity when the assumption was violated. The p-values in the table only represent the significance of the effect imposed by the driving (ADAS) condition. The significance criteria of the driving conditions are listed below. The effect of time-criticality on the dependent measures is not incorporated in this table, since this independent measure showed significance for all metrics. Significance for pairwise comparisons among driving conditions was rejected for  $p > 0.05$ . The last entries in the table represent the subjective measures, for which the rating scales are given. Note that the alphabetic ratings for the CARS confidence were converted to numerical values for statistical analyses.

\*  $p \leq 0.05$   
 \*\*  $p \leq 0.01$   
 \*\*\*  $p \leq 0.001$

of moving towards the limits of ‘safe’ avoidance. This corresponds to previous findings in which aircraft pilots showed a similar tendency of moving towards system limitations [42]. Conversely, (2) the visualization of intentional constraints warned the participants of potential lane departure during the obstacle avoidance (by means of red curves), promoting greater road margins compared to having no visualization. Either way, it is worth noting visual feedback affected task execution for both critical and non-critical cases. This indicates that short-term decision making can also be significantly affected by adding visual feedback, which is in contrast to the expectation that the effect of adding visuals to HSC would be more distinct for non-critical cases.

Furthermore, the results confirm previous research on haptic guidance during obstacle avoidance [35], showing that the effect of haptic feedback is most distinct for critical cases, where an increase of obstacle margin can be seen for HSC and Combi, compared to Manual and EID. This can be explained by the nature of the implemented HCR and the resulting haptic guidance, which responded inherently faster than the human ability. Secondly, in Figure 9 it can be seen that the inter-subject variability is greatly reduced for the HSC condition, indicated by a higher narrowness of the density function. On the other hand it can be seen that the addition of visual feedback to HSC (Combi) imposes an increased variability between the subjects (reduced narrowness in the figure). The increased variability between subjects can be explained by the fact that EID-inspired interfaces do not advocate for an optimal control strategy, leading to an increased number of options.

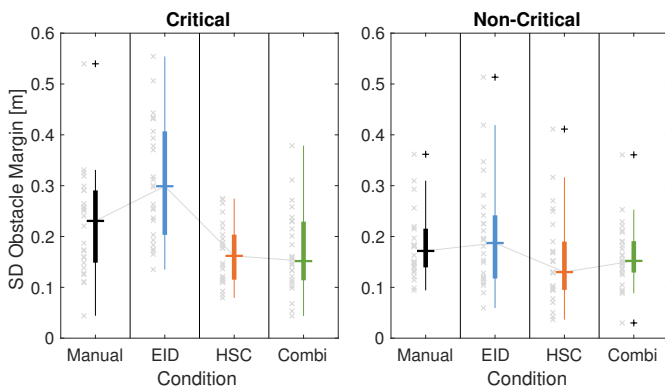


Fig. 10. SD of lateral obstacle margin during obstacle passage, for critical and non-critical obstacles. These figures reflect the intra-subject variability within all participants. Participants and outliers are indicated by an x and +, respectively.

Apart from the inter-subject (between) variability in Figure 9 an analysis was also done on the intra-subject (within) variability of the lateral obstacle margin. The intra-subject variability describes the difference in behavior in the same participant given the experienced driving conditions. The results of the *standard deviation lateral obstacle margin* revealed a significant effect due to the driving conditions,  $F(3, 75) = 12.46, p < 0.05$ . An overview of the results is given in Figure 10, where pairwise comparisons confirmed significance only between EID-HSC and EID-Combi. From this it can be concluded that the addition of haptic feedback

significantly reduces intra-subject variability, compared to EID-only. In analogy with the inter-subject variability, this can be explained by the fact that haptic guidance dictates a more specific control strategy. In the next sections it will be elaborated whether this increased variability has a negative effect on control effort and control conflicts.

#### 4.1.2 Lateral Road Margin

The third task execution measure, *mean lateral road margin*, is inversely related to the obstacle margin. This means that the greater the obstacle margin, the smaller the lateral road margin, see Figure 7. Therefore, similar interpretations can be made as done for the obstacle margin. The results show a significant effect of the driving condition on the mean lateral road margin  $F(2.35, 58.73) = 19.84, p < 0.05$ . To match the perspective of Figure 9, the results in Figure 11 were shown horizontally, having the left lane boundary on the left side. The results indicated a significant increase of road margin by the addition of visual feedback, when comparing Manual-EID and HSC-Combi, for both critical and non-critical events. Therefore, it can be deduced that applying visual feedback positively affects road margins and thus improves safety in terms of lane departure risk. At the same time it was shown that drivers moved to the boundaries of ‘safe’ avoidance by maintaining smaller obstacle margins. Accordingly, it can be said that due to the addition of visual feedback, participants adhered to the intentional constraints (increased road margins), while respecting the physical constraints (reduced obstacle margins). This holds for both EID and Combi, where the largest effect can be seen for critical tasks. Lastly, it was shown that the application of haptic feedback during critical events induces a considerable reduction of road margins compared to Manual and EID. This effect is significant, but less visible for non-critical situations. The increased road margins for critical cases show that a fast response of haptic feedback can result in overshooting behavior, resulting from participants being overwhelmed by the system. It can be seen that the visual feedback is able to reduce this overshooting behavior, revealing a positive outcome of combining the two forms of feedback.

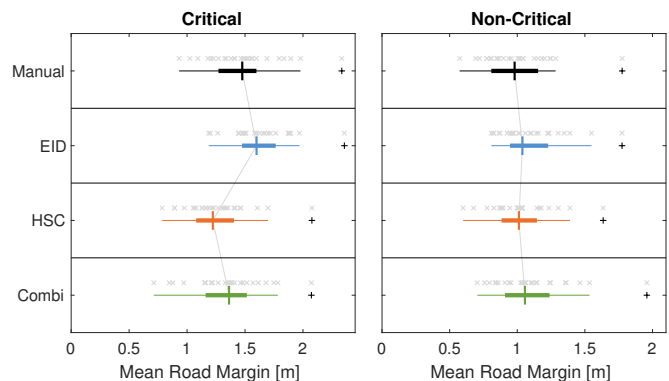


Fig. 11. Mean lateral road margin during obstacle passage, for critical and non-critical obstacles. Road margin defined as the distance between the left lane boundary and vehicle, where zero indicates the left lane boundary.

#### 4.1.3 Lateral Bias

Fourthly, the *mean lateral bias* measured at the moment of obstacle appearance revealed a significant effect imposed by

the driving condition  $F(1.90, 47.53) = 4.31, p < 0.05$ . However, pairwise comparisons only showed a significant result between Manual-Combi, indicating an increase of lateral bias for the Combi condition ( $0.156 \pm 0.187$  m) compared to Manual ( $0.074 \pm 0.183$  m), see Table 5. These two values represent the mean bias for the critical events, showing the strongest effect. However, a similar trend is visible for the non-critical cases. The increased bias (towards the left) can partially be explained by the improved ability of lane center determination by the trend vector originating from the middle of the vehicle, see Figure 1. It is likely that due to learning-effects the participants used this information to maintain a more favorable initial position on the straight road sections, even when they were guided towards the lane center by the haptic feedback. The relation between other conditions is not elaborated, since this effect was only proven significant between Manual-Combi.

#### 4.1.4 Response Time

The results of the fifth task execution measure, *mean response time* revealed a significant effect,  $F(3, 75) = 20.23, p < 0.05$ , induced by the different driving conditions. An overview of the resulting response times is illustrated in Figure 12. By means of pairwise comparisons, significant results were found between all conditions, except between Manual-EID and HSC-Combi, see Table 5. When regarding the results for the critical obstacles, it is evident that the addition of haptic feedback established reduced response times for both HSC as Combi, compared to Manual and EID. This is in analogy with the trend that was found for the mean lateral obstacle margin, showing increased obstacle margins for reduced response times, again confirming prior research [35]. To a smaller extent the effect of haptic feedback is also visible in the response times of the non-critical events. Moreover, in contrast to the hypothesis, the addition of visual feedback did not significantly improve mean response times. This could be an indication of the participants relying more on the haptic feedback to act in case of an obstacle, rather than starting the manoeuvre themselves.

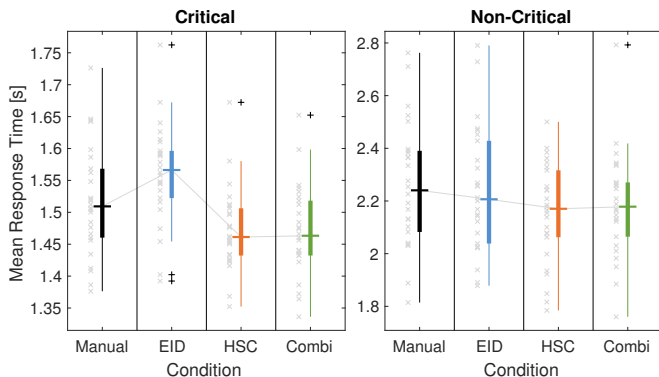


Fig. 12. Mean response time from obstacle appearance, for critical and non-critical obstacles. Response time defined as moment when vehicle exceeds the minimum lateral distance to avoid obstacle.

## 4.2 Control Activity

Control activity was analyzed for all straight sections, including those with no obstacles. At first, the *mean SRR for*

*obstacle avoidance* showed a significant effect of the experienced driving condition  $F(3, 75) = 8.96, p < 0.05$ . Pairwise comparisons showed only significant effects between Manual-HSC and Manual-Combi. The results in Figure 13 reveal a significant reduction of control activity due to the addition of haptic feedback (HSC and Combi), compared to Manual. This is in analogy with prior research, [8], [43], [44]. Although not significant, it can be seen that while comparing HSC to Combi, the addition of visual feedback increased control activity for critical events, where a reduction was found for the non-critical cases.

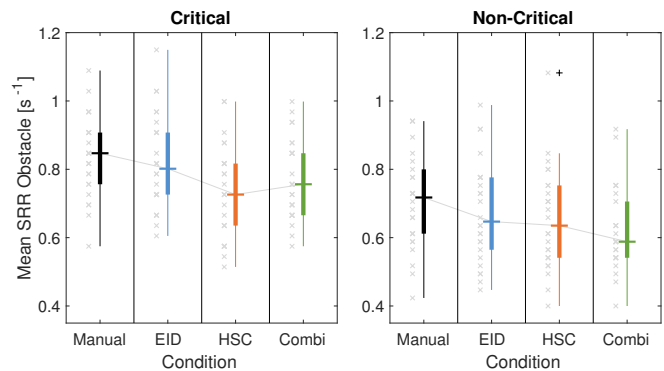


Fig. 13. Mean Steering Reversal Rate for critical and non-critical obstacles, measured during obstacle avoidance.

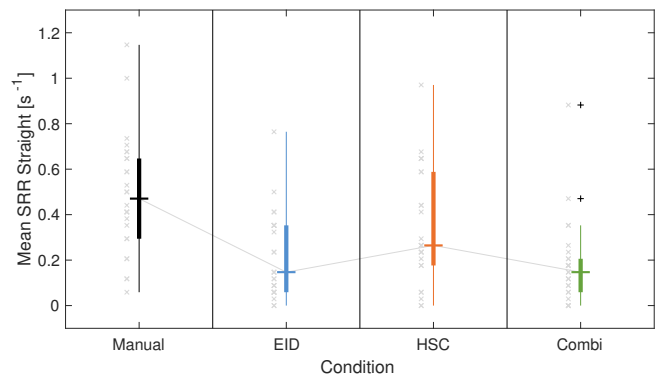


Fig. 14. Mean Steering Reversal Rate for straight road sections without obstacles. Hence, no distinction is made between critical and non-critical.

To further investigate the effect of visual feedback during non-critical events, the *mean SRR for straight sections* was evaluated (i.e. straight sections without obstacles). The results of this measure indicated a significant effect imposed by the driving condition,  $F(3, 75) = 25.77, p < 0.05$ . An overview of the results is presented in Figure 14, for which pair-wise comparisons showed significant effects between all conditions, except for EID-Combi. Compared to the non-critical results (right) in Figure 13, a similar reduction of control activity was found between HSC and Combi, confirming the hypothesis that control activity can be reduced by the addition of visual feedback. Moreover, the addition of visuals also revealed a considerable reduction of SRR for EID, compared to Manual. As a result it was found that compared to Manual, control activity was reduced by a factor 2.5 for both EID and Combi, as opposed to a

reduction factor of 1.4 for HSC. Similar to the lateral bias, this result can be justified by the fact that the trend vector represents an immediate response to the steering wheel input, meaning that every steering action is amplified by the future trajectory prediction. During straight sections with no obstacles (lane keeping), the control activity is therefore reduced by improved lane center detection, requiring less steering wheel corrections and thus less oscillations. In conclusion, the control activity is mostly reduced for non-critical tasks (including straight sections) by the addition of visual feedback, while the SRR is reduced most significantly by HSC during critical tasks. This indicates the power of HSC and EID-inspired feedback for short and long-term decision making, respectively.

### 4.3 Control Effort

The results of the *mean total rotational work* (Figure 15), indicated a significant outcome due to the driving condition,  $F(2.43, 60.65) = 17.68, p < 0.05$ . Through pair-wise comparisons, a significant effect was found between all conditions, except for Manual-EID and HSC-Combi. Control effort was reduced significantly by adding haptic feedback, which corresponds previous findings [10]. The effect of visual feedback showed no significance. However, when comparing HSC and Combi, increased control effort was found for critical, with slightly reduced control effort for non-critical tasks. This corresponds to the increased control activity in terms of SRR for obstacle avoidance, as depicted in Figure 13 (notice the similarity of the results). Most likely, this phenomenon can be explained by a higher corrective behavior for critical cases as opposed to non-critical scenarios, when comparing HSC and Combi. Although not significant, this could be an indication that adding visuals to HSC can reduce control effort for non-critical tasks, where it can increase control effort for critical cases.

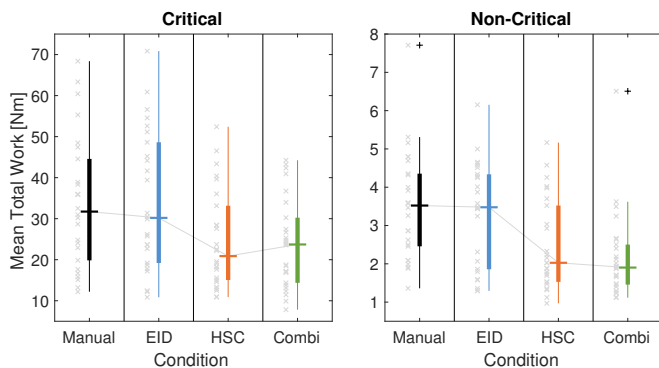


Fig. 15. Mean total rotational work during obstacle avoidance, for critical and non-critical obstacles.

### 4.4 Conflicts in Torque

In this section, conflicts in torque are evaluated only between HSC and Combi. For the Manual and EID condition, no conflicts were present, since no haptic feedback was applied here. Conflicts in terms of *mean conflicting rotational work* indicated a significant effect by the applied driving condition  $F(1, 25) = 4.96, p < 0.05$ . As hypothesized, the

addition of visual feedback to haptics imposed a significant reduction of conflicting work compared to HSC-only, especially for non-critical cases, see Figure 16. As previously argued, this effect can be explained by a reduction of corrective behavior, indicating improved coherence between driver and HSC intent.

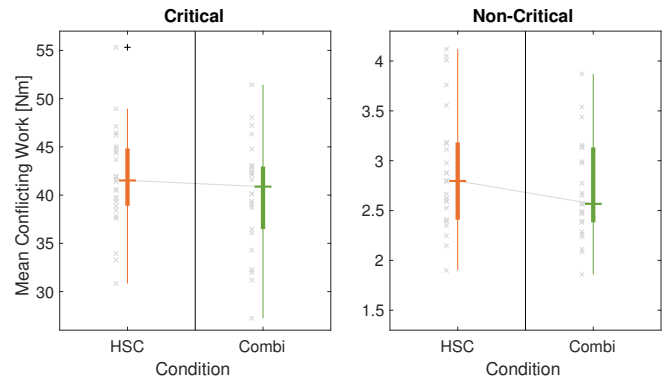


Fig. 16. Mean conflicting work during obstacle avoidance, for critical and non-critical obstacles.

For the second conflict measure, *mean conflict peak torque*, no significant effect was found between HSC and Combi. In other words, the peak conflict torques were not affected by the addition of visual feedback. The final conflict measure, *mean percentage of time in conflict*, resulted in a significant increase from the HSC to Combi condition (Figure 17), with  $F(1, 25) = 5.11, p < 0.05$ . From the results in Figure 16 it appears that given an increased percentage of time in conflict, the conflicting work (energy) could still be reduced by the addition of visual feedback.

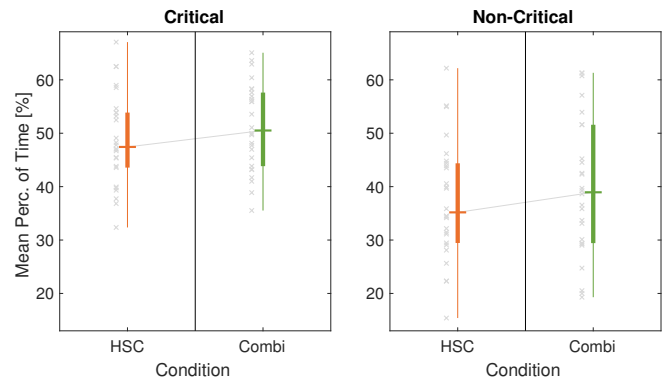


Fig. 17. Mean percentage of time in conflict, based on human and HSC torque, for critical and non-critical obstacles.

### 4.5 Subjective Acceptance

System acceptance was measured through both the NASA-CARS as well as the Van der Laan questionnaire. The CARS results were subdivided by two rating scales. The first measure, *acceptance rating*, indicated a significant effect imposed by the driving condition,  $F(3, 26) = 20.89, p < 0.05$ . By means of pair-wise comparisons, significant effects were only found between Manual-Combi and EID-Combi, see Table 5. An overview of the acceptance ratings per condition, including the mean rating, is depicted in

Figure 18. An increased score for each condition can be seen, with the highest subjective acceptance for the Combi condition. Interestingly, HSC scored higher than EID, which can be argued by the fact that haptic feedback provided rather active support, compared to the informative feedback presented by the implemented visuals. It is likely that the participants benefited more from the haptic feedback and thus provided higher ratings for HSC, compared to EID. The second CARS measure, *confidence rating*, showed an overall significant effect by the conditions,  $F(3, 26) = 7.95$ ,  $p < 0.05$ . However, pair-wise comparisons revealed no significant effect between the conditions.

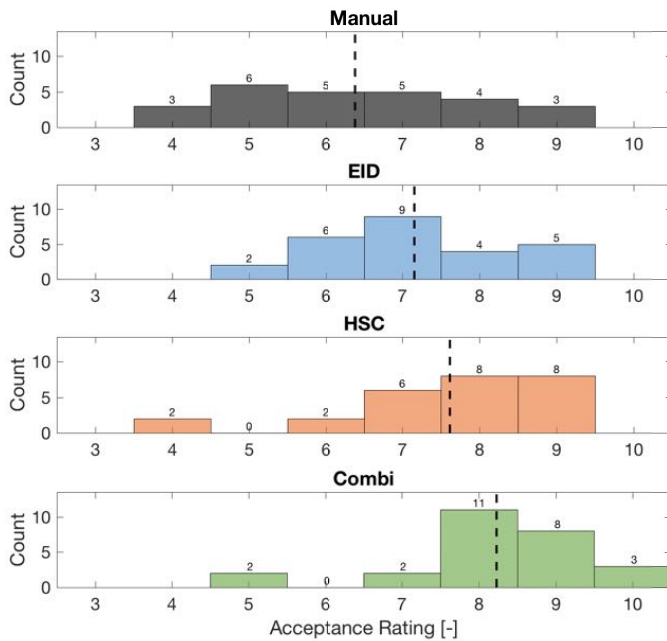


Fig. 18. Histograms of NASA-CARS acceptance ratings per condition. The number of participants with a specific rating is denoted on top of the bars, where  $n = 26$ . Mean ratings are indicated by a dashed line.

Similar to the CARS, the VDL results were formed by two ratings. At first the *usefulness* with respect to the driving condition was verified. However, as summarized in Table 5 this measure did not result in a significant effect. Secondly, the *satisfaction* indicated an overall significant effect by the applied condition,  $F(3, 26) = 10.93$ ,  $p < 0.05$ . Nonetheless, pair-wise comparisons only showed a significant effect between Manual and Combi, see Table 5. An overview of the VDL results is depicted in Figure 19, showing at least significant increase of satisfaction rating between Manual and Combi. An explanation of the low significance for most subjective measures could be given by the difficulty of rating the experienced 'feedback system' for obstacle avoidance, which consisted of both critical and non-critical tasks. For example, some participants reported that the visual feedback was most desired for non-critical tasks such as lane keeping, curve negotiation and 'far' obstacles, but not for critical obstacle avoidance. The questionnaires however, constrained them to provide just one rating per condition. In conclusion, the subjective acceptance was only evaluated by the CARS acceptance rating, showing increased acceptance when adding visual feedback to HSC.

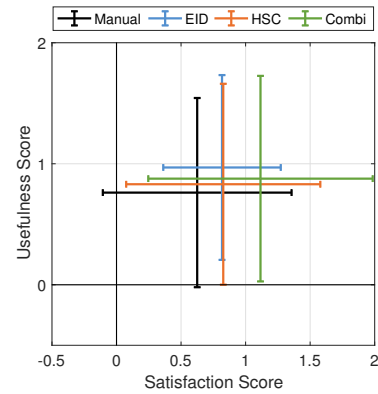


Fig. 19. VDL results shown by error bars per condition. The mean value is obtained in the center of the error bars. No significance was found for the usefulness score.

## 5 DISCUSSION

The aim of this research was to investigate the effect of complementing HSC by EID-inspired visual feedback on driver behavior during an obstacle avoidance task, in terms of task execution, control activity / effort, conflicts and user acceptance. The measures describing this effect were elaborated in the previous section, including interpretations of the results. This section will focus on highlighting the answers to the predefined hypotheses. Furthermore, an elaboration is given of the study limitations and the proposed recommendations for future work.

Reflecting on subsection 1.2, the results showed that task execution was indeed affected significantly by the addition of EID-inspired visual feedback to HSC. This effect was most evident from the improved road margins imposed by the addition of visual feedback. Interestingly, this effect was also shown for time-critical tasks, indicating that short-term decision making can be significantly affected as well. Additionally, the results based on the SRR revealed a significant reduction of control activity for non-critical events, confirming the second hypothesis. Despite the lack of significance between HSC and Combi in terms of control effort, the results of control activity and effort showed remarkably similar trends. Consequently, it can be assumed that both control activity and effort are negatively affected by the addition of visual feedback in critical cases, as opposed to a positive effect (reduction) for non-critical events. Regarding the conflicts in torque, it was shown that while the percentage of time in conflict increased marginally (but significantly), the conflicting work could still be reduced, especially for non-critical cases. This partially confirms the fourth hypothesis. With regards to subjective acceptance, no significant effects were found by the addition of visual feedback on top of HSC. However, the results lead to believe that system acceptance and satisfaction can be improved by the addition of EID-inspired visual feedback.

The reduced obstacle margins as imposed by the visual feedback may raise concerns about the likelihood of accidents and the added benefit in terms of driving safety. However, throughout the experiment no accidents in terms of obstacle collisions occurred, which does not allow for proper 'safety' comparisons between the conditions. At the same time road margins were significantly improved, resulting in

a reduced risk of lane departures. Hence, it is believed that EID-inspired feedback confirms driver assumptions, leading to a higher certainty of their actions. Consequently, it can be said that the visuals improve adherence to the intentional constraints, while respecting the physical constraints, when comparing to HSC-only. In addition, prior research has shown that the tendency of pushing the envelope does not necessarily imply a higher likelihood of accidents [42]. Therefore, it is argued that the addition of EID-inspired feedback does not negatively affect execution of an obstacle avoidance task.

More interestingly, the results revealed that when offered visual feedback, the participants indeed showed a tendency of disagreement with the haptic feedback, forcing them to follow one particular trajectory. This is in analogy with previous findings for air traffic controllers [36]. On the one hand the disagreement would be disadvantageous in case this would lead to increased control conflicts. On the other hand it could be highly beneficial in case of haptic feedback failure, since a higher situation awareness would yield improved human interventions. While the participants of this study showed a tendency of disagreement with the haptics, a reduction of control conflicts was found. However, during this experiment the haptic guidance operated with a maximum consistency (no failures), meaning that human interventions were not necessarily required.

## 5.1 Study Limitations

The first limitation of this study was the fairly uncomplicated driving task of the experiment, where the vehicle speed was fixed, no other traffic shared the road and the obstacles always appeared on the right side of the straight sections. This means that the unexpectedness in terms of obstacle avoidance was relatively low, resulting in a higher learning effect and thus less variability of the chosen path within the solution space. For example, it was shown that even though not instructed, the participants consistently chose to evade the obstacle on the left side. Increasing the complexity of the driving task by for instance implementing oncoming traffic would therefore increase the variability of driving patterns and may reveal other interesting driving behavior that could not be found in this study. Additionally, with an increased complexity the benefits of EID-inspired feedback will be manifested even more, since this principle is mainly focused on improving decision-making during complex tasks where unexpected events might occur.

As concluded in previous studies, the application of a one-size-fits-all control strategy for haptic feedback can cause disagreements, resulting in control conflicts [11]. To reduce possible disagreements between the operator and controller, it was shown beneficial to change the structure of haptic feedback and to adapt the reference of the controller to the individual behavior of the driver [34]. In this study, use is made of the newly proposed haptic control structure. However, to prevent for high experimental variability it was chosen to implement a generic HCR, similar for all participants. As a result, the applied HCR resulted in overshooting reactions of the participants, resulting from participants being overwhelmed by the system. In other words, the total sum of the haptic and human torque resulted in a

torque which exceeded the required torque for the evasion, imposing countersteering and thus disagreements. For this reason, it is likely that individualizing the HCR would improve the synergy and acceptance of the combined feedback. However, it is questionable whether this would attribute to the comparison between haptic and visual-haptic feedback. In this case it is not about comparing between feedback modalities, but rather the feedback design in itself, which involves a different kind of research.

On another note, the implementation of the visual feedback was done through displaying the performance envelope on the same projection screens as the driving scene. In reality, these visuals are more likely to be implemented by projecting them on a Head Up Display (HUD) in the wind screen, by means of augmented reality [21]. During this experiment, participants reported that the implemented visual feedback considerably reduced their field of view from far sight to near sight, which resulted in decreased awareness with respect to the surroundings. Therefore, the visuals were sometimes shown to be informative (positive) and distracting (negative) at the same time. The phenomenon of visual interference between the driving scene and overlaying visual feedback is also known as cognitive tunneling [45], which could be prevented by improving the design of the visual feedback. To solve this problem, one could think of situation adaptation of the visual feedback, meaning that the visual information is tailored to the current driving situation, improving the usefulness of the provided information. A simple example could be to apply a yaw-threshold to the trend vector, such that the curve remains stable for straight sections, while the curve starts to bend when the threshold is exceeded (e.g. curve negotiation). The difficulty of constraint based interfaces however, lies in the fact that the design should provide information from a holistic perspective rather than a fragmented view, since the former is more suited to improve robustness during unexpected events.

## 5.2 Future Work

Based on the findings of this study, recommendations can be given regarding potential future work. After showing that visual feedback significantly affects driving behavior, the first recommendation is directed to investigating the relation between the physical constraints and intentional constraints, and their effect on driving behavior. In other words, it would be interesting to quantify the additional effect that the intentional imposed on top of the physical constraints, by turning off the intentional constraints for one driving condition. With this research, a better understanding of the contribution by different types of constraints within the driving domain can be obtained.

Secondly, it was explained in subsection 2.2 that the automation constraints were not incorporated for this study. However, it is believed that by showing the automation intentions, a better understanding of the underlying controller can be developed (i.e. automation awareness). The implementation of these constraints could for example be accomplished by visualizing the proposed automation advisory on the road, together with the performance envelope. Another way to visualize the automation intent could be

through presenting a future trajectory (curve) based on the desired yaw rate imposed by the controller, together with the existing trend line that is based on the current yaw rate of the vehicle. This visualization should give the driver more direct insight in the difference between the automation and his/her intent.

The third recommendation is based on the correlation between velocity and the corresponding behavior of the work domain constraints, which could be made more intuitive through EID-inspired visual feedback. In this study, a fixed speed was applied throughout the simulations. This means that apart from the trend vector, the performance envelope was experienced as a static entity. The performance envelope is however designed to dynamically change shape, becoming wide for low speeds and narrow for high speeds. For future work it could be highly interesting to investigate driving behavior under variable speed, meaning that the dynamic performance envelope will provide new insights in the consequences of applying different velocities by the driver. This could again be used for obstacle avoidance, but also for curve negotiation (or a combination of the two), tasks for which vehicle velocity plays an important role.

As a fourth recommendation, investigating the use of EID-inspired visual feedback for fault detection, diagnosis and intervention could be an interesting topic when combined with haptic feedback. Throughout this study, the haptic guidance operated with a maximum reliability, meaning that no serious interventions were required by the driver. However, since the reliability of such systems is never perfect, it is worth investigating whether visual feedback can improve fault detection of drivers during haptic guidance failures. As an example, fault detection could be researched by obstacle avoidance experiments in which the haptic feedback sometimes fails to work. Together with the second recommendation, this could be a good way to investigate driver behavior. Note that prior research has shown that fault detection and diagnosis can significantly be improved through visual feedback [36].

The last recommendation is not specifically aimed at continuous haptic guidance, but rather at traded control, where the automation takes over a task completely, while sometimes imposing a Take Over Request (TOR). For these applications the principle of EID-inspired visual feedback could be interesting, by improving situation awareness of the driver in case an intervention is required. The strategy of visualizing the available spatial fields during obstacle avoidance has already been proven beneficial in terms of driving safety, [21]. By visualizing the work domain constraints in a comprehensive and intuitive manner, the driver could gain a better understanding of the current situation and act accordingly, possibly improving safety during unexpected scenarios.

## 6 CONCLUSION

In this research a novel visual feedback system inspired by the principle of EID is presented and combined with the existing haptic guidance solutions. By means of a driving simulator study it was demonstrated that the addition of EID-inspired visual feedback was beneficial to drivers in

maintaining safety during obstacle avoidance, while reducing control activity and torque conflicts. This was reflected by the experimental results, which revealed that compared to HSC, the addition of visual feedback imposed:

- Improved task execution in terms of road margins
- Reduced control activity for non-critical tasks
- No significant effect on control effort
- Reduced conflicts in terms of conflicting Work
- An insignificant improvement of user acceptance

This suggests that drivers can be supported in forming their own strategy, while at the same time promoting an improved compliance with the existing haptic guidance systems. The combination between haptic guidance and visual feedback offers a beneficial synergy worth exploring further.

## REFERENCES

- [1] R. Parasuraman and V. Riley, "Humans and automation: Use, misuse, disuse, abuse," *Human factors*, vol. 39, no. 2, pp. 230–253, 1997.
- [2] M. Saffarian, J. C. de Winter, and R. Happee, "Automated driving: human-factors issues and design solutions," in *Proceedings of the Human Factors and Ergonomics Society Annual Meeting*, vol. 56, no. 1. Sage Publications Sage CA: Los Angeles, CA, 2012, pp. 2296–2300.
- [3] J. D. Lee and B. D. Seppelt, "Human factors in automation design," in *Springer handbook of automation*. Springer, 2009, pp. 417–436.
- [4] M. Mulder, M. Mulder, M. van Paassen, S. Kitazaki, S. Hijikata, and E. Boer, "Car-following support with haptic gas pedal feedback," in *Proceedings of IFAC Symposium on Analysis, Design, and Evaluation of Human-Machine Systems*, 2004.
- [5] M. Enriquez and K. E. MacLean, "Impact of haptic warning signal reliability in a time-and-safety-critical task," in *Haptic Interfaces for Virtual Environment and Teleoperator Systems, 2004. HAPTICS'04. Proceedings. 12th International Symposium on*. IEEE, 2004, pp. 407–414.
- [6] P. G. Griffiths and R. B. Gillespie, "Sharing control between humans and automation using haptic interface: primary and secondary task performance benefits," *Human factors*, vol. 47, no. 3, pp. 574–590, 2005.
- [7] D. A. Abbink, E. R. Boer, and M. Mulder, "Motivation for continuous haptic gas pedal feedback to support car following," in *2008 IEEE Intelligent Vehicles Symposium*. IEEE, jun 2008. [Online]. Available: <https://doi.org/10.1109/ivs.2008.4621325>
- [8] K. K. Tsoi, M. Mulder, and D. A. Abbink, "Balancing safety and support: Changing lanes with a haptic lane-keeping support system," in *Systems Man and Cybernetics (SMC), 2010 IEEE International Conference on*. IEEE, 2010, pp. 1236–1243.
- [9] B. A. Forsyth and K. E. MacLean, "Predictive haptic guidance: Intelligent user assistance for the control of dynamic tasks," *IEEE transactions on visualization and computer graphics*, vol. 12, no. 1, pp. 103–113, 2006.
- [10] M. Mulder, D. A. Abbink, and E. R. Boer, "The effect of haptic guidance on curve negotiation behavior of young, experienced drivers," in *Systems, Man and Cybernetics, 2008. SMC 2008. IEEE International Conference on*. IEEE, 2008, pp. 804–809.
- [11] R. Boink, M. M. van Paassen, M. Mulder, and D. A. Abbink, "Understanding and reducing conflicts between driver and haptic shared control," in *Systems, Man and Cybernetics (SMC), 2014 IEEE International Conference on*. IEEE, 2014, pp. 1510–1515.
- [12] M. H. Martens and A. P. van den Beukel, "The road to automated driving: Dual mode and human factors considerations," in *Intelligent Transportation Systems-(ITSC), 2013 16th International IEEE Conference on*. IEEE, 2013, pp. 2262–2267.
- [13] C. Westin, C. Borst, and B. Hilburn, "Strategic conformance: Overcoming acceptance issues of decision aiding automation?" *IEEE Transactions on Human-Machine Systems*, vol. 46, no. 1, pp. 41–52, 2016.
- [14] J. Lee, J. Hoffman, H. Stoner, B. Seppelt, and M. Brown, "Application of ecological interface design to driver support systems," in *Proceedings of IEA 2006: 16th World Congress on Ergonomics*, 2006.

- [15] D. Beeftink, C. Borst, M. Van Paassen, and M. Mulder, "Increasing task-sharing performance by haptically assisting a tunnel-in-the-sky approach," *submitted to IEEE*, 2018.
- [16] M. Razzanelli, S. Aringhieri, G. Franzini, G. Avanzini, F. Giuliotti, M. Innocenti, and L. Pollini, "A visual-haptic display for human and autonomous systems integration," in *International Workshop on Modelling and Simulation for Autonomous Systems*. Springer, 2016, pp. 64–80.
- [17] J.-M. Hoc, M. S. Young, and J.-M. Blosseville, "Cooperation between drivers and automation: implications for safety," *Theoretical Issues in Ergonomics Science*, vol. 10, no. 2, pp. 135–160, 2009.
- [18] J. Rasmussen, "Skills, rules, and knowledge; signals, signs, and symbols, and other distinctions in human performance models," *IEEE transactions on systems, man, and cybernetics*, no. 3, pp. 257–266, 1983.
- [19] M. L. Rusch, M. C. Schall Jr, P. Gavin, J. D. Lee, J. D. Dawson, S. Vecera, and M. Rizzo, "Directing driver attention with augmented reality cues," *Transportation research part F: traffic psychology and behaviour*, vol. 16, pp. 127–137, 2013.
- [20] M. C. Schall Jr, M. L. Rusch, J. D. Lee, J. D. Dawson, G. Thomas, N. Aksan, and M. Rizzo, "Augmented reality cues and elderly driver hazard perception," *Human factors*, vol. 55, no. 3, pp. 643–658, 2013.
- [21] L. Lorenz, P. Kerschbaum, and J. Schumann, "Designing take over scenarios for automated driving: How does augmented reality support the driver to get back into the loop?" in *Proceedings of the Human Factors and Ergonomics Society Annual Meeting*, vol. 58, no. 1. SAGE Publications Sage CA: Los Angeles, CA, 2014, pp. 1681–1685.
- [22] J. Rasmussen and K. J. Vicente, "Coping with human errors through system design: implications for ecological interface design," *International Journal of Man-Machine Studies*, vol. 31, no. 5, pp. 517–534, 1989.
- [23] C. Borst, "Ecological approach to pilot terrain awareness," 2009.
- [24] H. A. Stoner, E. E. Wiese, and J. D. Lee, "Applying ecological interface design to the driving domain: the results of an abstraction hierarchy analysis," in *Proceedings of the Human Factors and Ergonomics Society Annual Meeting*, vol. 47, no. 3. SAGE Publications Sage CA: Los Angeles, CA, 2003, pp. 444–448.
- [25] B. D. Seppelt and J. D. Lee, "Making adaptive cruise control (ACC) limits visible," *International Journal of Human-Computer Studies*, vol. 65, no. 3, pp. 192–205, mar 2007. [Online]. Available: <https://doi.org/10.1016/j.ijhcs.2006.10.001>
- [26] K. J. Vicente, K. Christoffersen, and A. Perekhita, "Supporting operator problem solving through ecological interface design," *IEEE transactions on systems, man, and cybernetics*, vol. 25, no. 4, pp. 529–545, 1995.
- [27] T. R. McEwen, J. M. Flach, and N. C. Elder, "Interfaces to medical information systems: Supporting evidenced based practice," in *Systems, Man and Cybernetics (SMC), 2014 IEEE International Conference on*. IEEE, 2014, pp. 335–340.
- [28] D. S. Hall, L. G. Shattuck, and K. B. Bennett, "Evaluation of an ecological interface design for military command and control," *Journal of Cognitive Engineering and Decision Making*, vol. 6, no. 2, pp. 165–193, 2012.
- [29] M.-C. Ostendorp, J. C. Lenk, and A. Lüdtkke, "Smart glasses to support maritime pilots in harbor maneuvers," *Procedia Manufacturing*, vol. 3, pp. 2840–2847, 2015.
- [30] N. Dinadis and K. J. Vicente, "Designing functional visualizations for aircraft systems status displays," *The international journal of aviation psychology*, vol. 9, no. 3, pp. 241–269, 1999.
- [31] C. Borst, H. Suijkerbuijk, M. Mulder, and M. Van Paassen, "Ecological interface design for terrain awareness," *The International Journal of Aviation Psychology*, vol. 16, no. 4, pp. 375–400, 2006.
- [32] S. B. Van Dam, M. Mulder, and M. Van Paassen, "Ecological interface design of a tactical airborne separation assistance tool," *IEEE Transactions on Systems, Man, and Cybernetics-Part A: Systems and Humans*, vol. 38, no. 6, pp. 1221–1233, 2008.
- [33] C. Borst, M. Mulder, and M. Van Paassen, "Design and simulator evaluation of an ecological synthetic vision display," *Journal of Guidance, Control and Dynamics*, vol. 33, no. 5, pp. 1577–1591, 2010.
- [34] W. Scholtens, S. Barends, D. M. Pool, M. M. van Paassen, and D. Abbink, "A new haptic shared controller reducing steering conflicts," *submitted*.
- [35] M. Della Penna, M. M. van Paassen, D. A. Abbink, M. Mulder, and M. Mulder, "Reducing steering wheel stiffness is beneficial in supporting evasive maneuvers," in *Systems Man and Cybernetics (SMC), 2010 IEEE International Conference on*. IEEE, 2010, pp. 1628–1635.
- [36] C. Borst, V. A. Bijsterbosch, M. van Paassen, and M. Mulder, "Ecological interface design: supporting fault diagnosis of automated advice in a supervisory air traffic control task," *Cognition, Technology & Work*, vol. 19, no. 4, pp. 545–560, 2017.
- [37] T. Rijndorp, C. Borst, C. C. de Visser, O. Stroosma, M. Mulder, and M. van Paassen, "Aviate, navigate: Functional visualizations of asymmetric flight envelope limits," in *AIAA Information Systems-AIAA Infotech@ Aerospace*, 2017, p. 1297.
- [38] K. Lee, K. Kerns, R. Bone, and M. Nickelson, "Development and validation of the controller acceptance rating scale (cars): Results of empirical research," in *Proceedings of the 4th USA/Europe Air Traffic Management R&D Seminar*, 2001.
- [39] J. D. Van Der Laan, A. Heino, and D. De Waard, "A simple procedure for the assessment of acceptance of advanced transport telematics," *Transportation research. Part C, Emerging technologies*, vol. 5, no. 1, pp. 1–10, 1997.
- [40] J. R. McLean and E. R. Hoffmann, "Steering reversals as a measure of driver performance and steering task difficulty," *Human Factors*, vol. 17, no. 3, pp. 248–256, 1975.
- [41] G. E. Cooper and R. P. Harper Jr, "The use of pilot rating in the evaluation of aircraft handling qualities," Advisory Group for aerospace research and development Neuilly-Sur-Seine (France), Tech. Rep., 1969.
- [42] C. Borst, J. M. Flach, and J. Ellerbroek, "Beyond ecological interface design: Lessons from concerns and misconceptions," *IEEE Transactions on Human-Machine Systems*, vol. 45, no. 2, pp. 164–175, 2015.
- [43] M. Mulder, D. A. Abbink, and E. R. Boer, "Sharing control with haptics: Seamless driver support from manual to automatic control," *Human factors*, vol. 54, no. 5, pp. 786–798, 2012.
- [44] A. Balachandran, M. Brown, S. M. Erlien, and J. C. Gerdes, "Predictive haptic feedback for obstacle avoidance based on model predictive control," *IEEE Transactions on Automation Science and Engineering*, vol. 13, no. 1, pp. 26–31, 2016.
- [45] L. C. Thomas and C. D. Wickens, "Visual displays and cognitive tunneling: Frames of reference effects on spatial judgments and change detection," in *Proceedings of the Human Factors and Ergonomics Society Annual Meeting*, vol. 45, no. 4. SAGE Publications Sage CA: Los Angeles, CA, 2001, pp. 336–340.



## **Appendix**



## **A Background: Literature Summary**



# **An Ecological Approach to Complement Haptic Shared Control Driving**

A LITERATURE REVIEW (SUMMARY)

BY

WILCO VREUGDENHIL  
4134001

in partial fulfillment of the requirements for the degree of

**MSc Mechanical Engineering**

Delft Haptics Lab  
Department of BioMechanical Engineering  
Delft University of Technology

Supervised by:  
Dr. ir. David Abbink  
Dr. ir. Clark Borst  
ir. Bastiaan Petermeijer  
ir. Sarah Barendswaard

March 14, 2018

## **Abstract**

The increasing level of automation in car driving has enabled the automation of simple physical tasks, while leaving the driver with complex cognitive tasks. This has caused the art of driving to become a control task having a strong supervisory character, including the common human factor issues. In literature, multiple strategies have been proposed to keep the driver in-the-loop by means of cooperative control, with the collective goal to improve safety, performance and comfort. One control strategy that has recently gained popularity is called Haptic Shared Control, which aims to assist driver subtasks such as longitudinal and lateral control by providing continuous haptic guidance, supporting skill-based behavior. The benefits of this form of control are good communication of the driver's intentions and a smooth transition to human intervention in case the automation fails to work. Nonetheless, due to the limited level of information complexity provided by haptic feedback it can be burdensome to develop a mental model of the underlying controller and proper situation awareness, which can lead to control conflicts, errors and deteriorated user acceptance. Haptic Shared Control has already been successfully combined with other feedback modalities such as auditory and visual feedback, supporting skills-, rules- and knowledge-based behavior of the driver. However, these studies are mostly focused on reflecting the operational envelope (automation constraints) of the haptic shared controller and do not consider the influence of other work domain constraints, being intentional and physical constraints. On the basis of other research domains, this study proposes to complement Haptic Shared Control with the use of Ecological Interface Design and thus to encourage a constraint-based approach. The goal of this synergy is to visualize the automation advisory in combination with the space of possibilities for the control task, defined by the work domain constraints. In other words, where HSC assists the driver by suggesting an optimal path, EID-inspired feedback aims to satisfy the driver by presenting multiple trajectories. With the EID-approach the work domain constraints are reflected in an intuitive way that activates the higher levels of cognition, such that a better mental model is developed, a higher situation awareness is established and more automation acceptance can be achieved.

# Contents

<b>1</b>	<b>Introduction</b>	<b>3</b>
1.1	Background . . . . .	3
1.2	Problem Statement . . . . .	3
1.3	Research Questions . . . . .	4
1.4	Method . . . . .	4
<b>2</b>	<b>Theoretical Background</b>	<b>5</b>
2.1	Haptic Shared Control . . . . .	5
2.2	Ecological Interface Design . . . . .	5
<b>3</b>	<b>Experimental Results: HSC</b>	<b>7</b>
3.1	Haptic feedback . . . . .	7
3.2	Visual-Haptic Feedback . . . . .	8
<b>4</b>	<b>Experimental Results: EID</b>	<b>9</b>
4.1	Physical Constraints . . . . .	9
4.2	Intentional Constraints . . . . .	10
4.3	Automation Constraints . . . . .	10
4.4	Summary . . . . .	11
<b>5</b>	<b>Discussion</b>	<b>11</b>
A	Benefits and risks of HSC . . . . .	11
B	How can EID be applied to the driving domain? . . . . .	12
C	In what way can HSC and EID be applied practically? . . . . .	12
<b>6</b>	<b>Conclusions and Future Work</b>	<b>14</b>
	<b>References</b>	<b>15</b>

# 1 Introduction

## 1.1 Background

In the past vehicle locomotion was achieved by manually controlling the vehicle, relying on the direct physical cues of the vehicle itself and the driving environment. Inspired by the aviation domain this mechanical coupling has gradually been transformed into an electronically coupled human-machine interaction called drive-by-wire [56]. This development greatly contributed to the evolution of ADAS, introducing automation of simple physical tasks, yet leaving the driver with complex cognitive tasks that have a strong supervisory character. Research in high-risk domains has shown that highly automated systems often lead to the well-known pitfalls of automation, such as complacency, loss of skills and over-reliance [2].

To keep the driver in-the-loop a cooperative form of automation called Haptic Shared Control (HSC) has been proposed in multiple studies [35, 14, 19, 1]. The aim of HSC is to avoid the pitfalls of automation by providing continuous haptic feedback, giving guidance to the driver in order to complement the skill-based behavior. Consequently, HSC has proven to yield improvements in vehicle locomotion, such as improved performance on different control tasks [1, 19, 51, 18, 35], reduced control activity [34] and improved reaction times [35].

## 1.2 Problem Statement

In the context of transportation automation Flemisch [16] describes the relationship between situation awareness and the mental model as follows: “In order to gain and maintain situation awareness, there has to be a sufficient representation, a mental model of the automation inside the operator”. Conflicts in automation systems such as HSC could occur when the mental model of the driver does not reflect the model of the underlying automation, resulting in a deteriorated situation awareness and reliance [16, 39]. The control conflicts can be explained in three ways, where (1) is the finite operational envelope of the automation [30]. Within this region the automation is supposed to function properly, whereas outside this region the automation behaves unpredictably, causing control conflicts perceived by the operator. Another reason for conflicts is (2) the difference between the desired assistance and the actual automation programmed into the controller [57]. A last reason is (3) the limited level of information complexity that can be conveyed through haptic feedback [27], since this type of feedback can only be perceived through the tactile senses and thus mainly complements skill-based behavior.

To improve automation feedback, several studies have shown promising results of combining feedback modalities such as visual and auditory together with haptic feedback [5, 44]. A promising method to visualize the system boundaries of automation is the concept of Ecological Interface Design (EID), a framework that prioritizes the work environment with the goal to visualize the space of possibilities in a way that supports people’s skill-, rule- and knowledge (SRK) based behavior [8]. This method has been successfully applied in fields like the process industry, aviation and automotive, where EID has been used to reflect the limits of the ACC automation controller [45]. Where HSC mainly complements skill-based behavior, EID can be used to provide insight about the automation behavior on a higher cognitive level, such that the behavior is visualized in a way that supports people’s SRK-based behavior. By reflecting the operational envelope of the automation in this way, the driver will develop a better understanding (i.e. mental model) of the underlying controller, improving situation awareness and thus supporting operator trust, reliance and acceptance.

### 1.3 Research Questions

In accordance with the introduction given in the previous section, the research question answered in this review can be posed as:

*How can Ecological Interface Design be used to reflect the operational envelope of Haptic Shared Control in assisted driving?*

To answer the main research question and in order to structure the literature review, the following sub-questions will be addressed:

- A. *What are the benefits and risks of the currently applied HSC models in car driving and how can these systems possibly be improved?*
- B. *In what way have EID-inspired systems been applied to mitigate human factor issues in human-machine systems and to what end can these principles potentially be combined with HSC?*
- C. *In what way could the combination of HSC and visual EID be applied practically and what are the potential problems of this application?*

### 1.4 Method

For the literature review an initial search was performed in the digital libraries of Web of Science, Science Direct, Google Scholar and IEEE Xplore using keywords as "vehicle locomotion", "driver assistance", "shared control", "haptic feedback", "visual feedback", "situation awareness", "Ecological Interface Design" and "augmented reality". Afterwards, a more detailed search was performed based on the references cited by these papers. The relevance of the publications with respect to the subject of this review was validated by consulting the following inclusion criteria:

1. The main goal to be achieved should be vehicle locomotion: to move the individual from one space to another by means of a vehicle either in a real or in a simulated environment.
2. Continuous feedback is to be given to the operator in the form of haptic forces, visual cues or a combination, providing continuous guidance for the control task.
3. The level of automation should be such that the environment is monitored by the system, the dynamic operating task is performed by both operator and system and the human operator is responsible for the fallback scenario (i.e. hands-on-wheel - SAE level 3).
4. The system should have a hierarchical task level categorized as operational or tactical: reaching a steady state target (longitudinal/lateral position) or performing a vehicle manoeuvre (lane change), respectively.
5. The study is to be performed within the operational envelope of the automation, meaning that the operator is only supported in maintaining situation awareness and understanding of the system within the system boundaries during regular operations.
6. In the field of Ecological Interface Design, only the visual representation of this framework is to be considered.

## 2 Theoretical Background

This chapter elaborates on the fundamental theory required to understand the outline of this study. An introduction will be given on the developments of automation systems in general and more specifically in the driving domain, including several classification methods that are used to describe the level of automation. Moreover, it is described what the common human factor issues are associated to these automation systems and which current control strategies have been developed to solve these issues. In particular this study puts a focus on HSC as a cooperative control strategy and the implementation of EID to enhance the automation feedback during a complex control task.

### 2.1 Haptic Shared Control

HSC has successfully been applied to work domains such as robotic surgery, teleoperation and aviation. The application to the driving domain has been researched in several studies starting as early as 1966 [15]. Initially, researchers investigated the implementation of haptic guidance for longitudinal control by applying haptic forces to the gas pedal [35, 14, 1]. These studies have shown that providing continuous feedback yields (1) better task performance, (2) reduced visual effort and (3) decreased control activity. Further research was done on applying HSC to lateral control by exerting haptic guidance on the steering wheel [19, 33, 40, 4], showing (1) reduction of lateral errors, (2) lower reaction time in a secondary task and (3) in some cases increased control effort. Other HSC research subjects considering driving subtasks are lane changing [51], Eco-friendly driving and navigation, see [41] for an overview of these systems and their effect on driver performance and behavior.

Despite that fact that research in HSC has shown promising results, it can be seen that there are still related human factor issues such as loss of skills, overreliance, decreased situation awareness and increased control effort [58, 6]. A first reason for this could be that previous research focused mostly on evaluating HSC by implementing a 'one-size-fits-all' model of guidance. Recent studies have started to conduct research on adaptive haptic guidance systems in routine tasks [6, 46, 22, 38, 53]. Where traditional HSC systems are aimed at optimizing control tasks with respect to a certain target value, the adaptive systems are designed to accommodate for the driver's preferences, often having a satisficing character. The objective of such systems is to eliminate control conflicts and thus to achieve a higher automation acceptance. Another major reason for automation control conflicts can be explained by the fact that the underlying automation of HSC has a finite operational envelope, meaning that the system behaves normally in routine tasks and unpredictably in non-routine tasks, causing control conflicts perceived by the operator. This effect is strengthened by the second reason, the limited level of information complexity that can be conveyed through haptic feedback, since this type of feedback can only be perceived through the tactile senses. During routine tasks the operator may be able to adapt to this type of feedback, yet during non-routine tasks it becomes impossible to develop correct automation awareness, both due to the unexpected behavior of the controller as well as the limited information haptic feedback can provide. The understanding of the automation intents is a major contributor to the user acceptance of a system. To improve the automation awareness it could be interesting to combine haptic feedback with other modalities, such that task performance and user acceptance are enhanced in both routine and non-routine tasks.

### 2.2 Ecological Interface Design

Rasmussen and Vicente introduced and applied the concept of EID for the first time in the process control domain [43], defined as interface design based on a work domain analysis (WDA) that starts with,

and gives priority to environmental constraints. The difference between EID and classical design strategies is the fact that EID prioritizes the behavior-shaping constraints introduced by the work domain, incorporating the laws of physics and other fundamental rules and principles. This is different from strategies as technology- and user-centered design, that take technology and the human as a starting point, respectively. EID is therefore able to complement these strategies by taking the work domain constraints as a starting point. The advantage of this approach is that the work domain constraints always need to be obeyed and are therefore independent of human and/or automation capabilities.

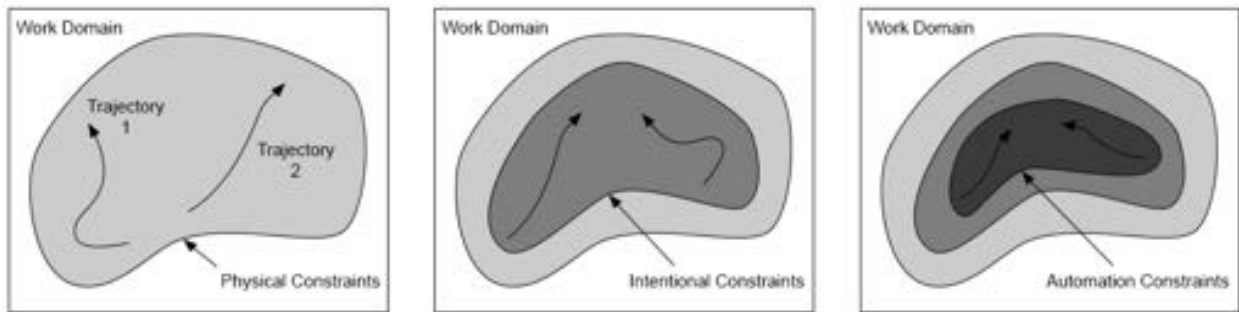


Figure 1: Overview of work domain constraints in complex sociotechnical systems, adapted from [54].

The EID-approach to complex sociotechnical systems can be defined as "a design framework that encourages a constraint-based approach with the goal to visualize the space of possibilities in a way that supports people's skill-, rule- and knowledge (SRK) based behavior" [8]. This means the goal is to determine the work domain constraints and to represent them in a visual form to support the SRK based behavior of the human operator [42]. In other words, EID aims to transform a cognitive task into a perceptual task by providing meaningful information about the work domain that humans can directly perceive and act on accordingly [8]. An overview of the general constraints imposed by a complex sociotechnical systems is depicted in Figure 1. The EID approach uses a top-down method, considering the full work domain at first, followed by the physical, intentional and automation constraints that are enclosed by the work domain. "Physical constraints refer to the laws of physics that influence possible directions of the driver. Intentional constraints reflect the laws and etiquette that govern driver behavior" [48]. Finally, the automation constraints indicate the operational envelope of the underlying controller, which is often limited by one optimal trajectory within the domain of the intentional constraints. In the case of haptic guidance this could be a single type of action supported by a predetermined control strategy. Compared to approaches such as technology- or user-centered design, EID is intended to reflect the bigger picture by satisficing rather than optimizing a complex control task.

When applying EID appropriately, it becomes especially useful for complex, safety-critical and open (subject to disturbances) work environments. By allowing the work domain constraints to be directly perceptible, EID interfaces assist users in the development of their mental model of the domain. Driver support system interfaces resulting from this analysis may not only help drivers form better mental models of the driving domain but also of vehicle automation, such as adaptive cruise control. It has already been shown that applying EID to the driving domain can improve calibrated trust and reliance [48, 45, 27]. Other examples of work domains in which EID has been applied successfully are process control [43, 55], health care [31], command and control [20], marine [37] and aviation [13, 10, 52, 7]. As with most new frameworks, EID has not only gained support, but also opponents that have expressed their concerns regarding the effects that EID may introduce. A complete list of the lessons learned from these concerns and misconceptions about EID can be found in [9].

### 3 Experimental Results: HSC

Depicted in Figure 2 are the available levels of human-machine compatibility, indicating that HSC systems focus on guiding the driver at a skill-based level, thereby reducing human workload in optimal conditions. This means that HSC is mostly applied in routine driving tasks, where no control conflicts are present. In contrast, EID-inspired automation systems support the driver on all cognitive levels, including skills-, rules- and knowledge-based behavior, which can be used for both routine and non-routine tasks. The improvements achieved with HSC in the driving domain (see subsection 2.1) can be explained by the fact that the continuous interaction and communication between driver and automation keeps the driver in-the-loop, which can for example reduce undesired human variability. Based on the experimental results of previous HSC studies, this chapter will elaborate on the strengths and weaknesses of HSC in driving. In the first section it is focused on pure HSC systems that only provide continuous haptic guidance during driving, supporting motor skills, perception, communication an interaction, see Figure 2. On the basis of experimental results, the second section describes the benefits of adding visual feedback to HSC aimed to improve automation awareness and acceptance.

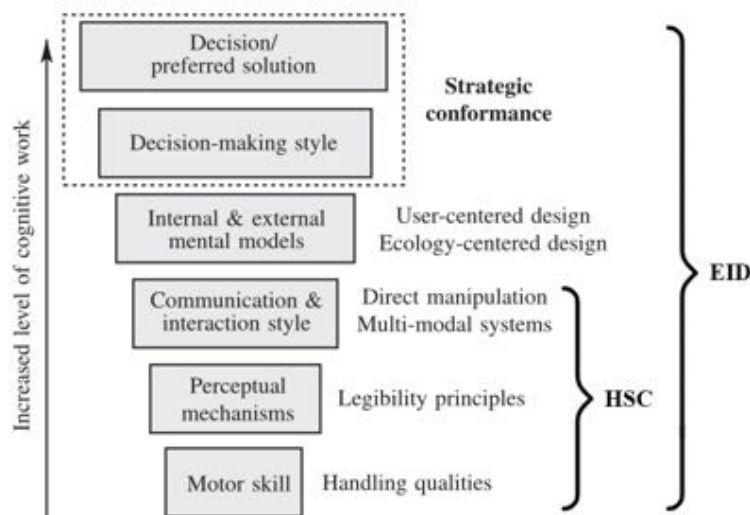


Figure 2: Levels of human-machine compatibility, and their respective constructs found in cognitive engineering research, ordered by increased levels of cognitive work for both HSC and EID, adapted from [57].

#### 3.1 Haptic feedback

In this section it is described what the effects of continuous haptic guidance on driver performance and behavior are during several driving subtasks, such as lane keeping, curve negotiation, car following and collision avoidance. A clear overview of the experimental studies involved to determine the effect of haptic support systems on driver performance and behavior, is given in [41]. In the cited paper a distinction is made between haptic warning and guidance systems, where the focus of this literature study is solely on continuous guidance systems. From the results of previous research, three conclusions can be drawn. Haptic guidance can improve (1) performance for lane keeping, curve negotiation, car following, collision avoidance and lane-changing. Furthermore, it reduces (2) the control activity during most driving subtasks, measured by steering and pedal activity. Lastly HSC reduces (3) the visual demand of lane keeping, indicated by the score of performing a secondary task. Likewise, a decrease in cognitive demand was found in three studies comparing manual to haptically guided driving, measured by secondary task performance [19, 17, 36]. Besides the positive effects, some studies also found unfavorable effects in terms of user acceptance. For example, two studies reported an increased number of obstacles

hit compared to manual driving [19, 23], where De Winter et al. [58] indicated potential pitfalls, such as complacency, increased workload and undesired after-effects in case of manual fallback. The most profound drawback reported in literature are the control conflicts that occur between human and machine [6, 21, 22], a trend which is comparable to the increased physical control effort reported by four different studies [35, 34, 51, 33]. In [21] seven types of possible control conflicts are elaborated. It is believed that some of these conflicts can be reduced by implementing EID to visualize the operational envelope of HSC with respect to the space of possibilities in the work domain. For example, conflicts caused by reverse inputs can be prevented when the direction of the control conflict is made clear through an intuitive display showing the suggested HSC direction in combination with all possible directions within the work domain.

### **3.2 Visual-Haptic Feedback**

This section elaborates on the effects of combining haptic and visual feedback by presenting the experimental results of several research domains. In previous driving studies, feedback modalities such as auditory and visual cues have already been combined together with haptic feedback [28, 29], showing varying results in terms of task performance. Although these studies have implemented multimodal feedback, they focused mostly on feedback cues (i.e. warnings) and not on continuous feedback provided to the driver, which is the focus of this paper. Due to the limited amount of studies on the implementation of continuous visual-haptic feedback for driving control tasks, other research domains such as robotics and aviation have been consulted to describe the global trend of applying this form of multimodal feedback. The first example studied the effect of haptically assisting a Tunnel-in-the-Sky approach for the control of an Unmanned Aerial Vehicle (UAV) in a restricted airspace [44]. The second example originates from the aviation domain and evaluates task-sharing performance by haptically assisting a TIS-approach on a more detailed level than the first example [5].

In summary it can be said that the application of both haptic and visual-haptic feedback can improve primary performance in vehicle locomotion control tasks, measured in terms of translational errors and acceleration rates. The true effectiveness and acceptance of these systems can be determined by considering measures such as control activity, control conflicts, cognitive demand and visual demand, indicating secondary task performance. The combination of haptic and visual feedback will only increase user acceptance when both primary and secondary task performance are enhanced. The experiments elaborated in the previous sections show that primary task performance can be improved, while reducing control activity, visual and cognitive demand. However, multiple studies have found participants to be fighting the system, indicating control conflicts that have a negative influence on user acceptance. These control conflicts could be solved in four ways: either by (1) individualizing or adapting the controller to the driver's preferences [22, 38], by (2) changing the structure of the underlying controller [53], by (3) decreasing the level of haptic authority [46] or by (4) integrating different feedback modalities (sensor fusion). In this chapter it is explained that applying visual-haptic feedback can increase the level of cognitive information, such that not only skill- but also rule-based behavior is supported. This can be explained by the fact that visual feedback has the ability to reflect complex control parameters in an intuitive manner. However, the current applications of visual-haptic feedback are solely designed to reflect the operational envelope of the underlying controller, and thereby do not consider constraints beyond this envelope. This means that visual-haptic guidance is generally well-accepted for routine tasks, yet not in the case of non-routine tasks where control conflicts may occur. To increase the robustness of HSC during unexpected situations and to prevent for the common pitfalls, a new approach is required which reflects more than just the automation constraints.

## 4 Experimental Results: EID

The theoretical background of EID is elaborated in subsection 2.2, where it is stated that EID can improve control tasks in complex sociotechnical systems by transforming a cognitive task into a perceptual task, such that all cognitive levels in Figure 2 are supported. The power of EID lies in the fact that it can significantly enhance the development of a mental model, representing the underlying automation system. The ecological approach to automation design is also believed to enhance the robustness of the human-machine system, especially in unexpected situations. This chapter is focused on how EID can be used to support human operators in car driving, by elaborating on the work domain analysis (WDA) and the corresponding work domain constraints. Experimental examples and results are given per constraint type to show the effect of different forms of EID on operator performance, control activity and cognitive demand.

### 4.1 Physical Constraints

Within the complete work domain of vehicle locomotion, the physical constraints can be defined as the physical elements of a system and their relationship to the physical environment. Examples of these constraints in the driving domain are: environment type, weather conditions and other road users, which can be subdivided into physical properties such as road types, road boundaries, road surface, etc. [48]. The physical constraints of vehicle locomotion can be split into two categories, being external and internal constraints. The former type of constraints are formed by the properties of the physical environment, where the internal constraints describe the physical performance of the vehicle, which depend directly on the external constraints. Examples of internal physical constraints are minimum stopping distance, Time to Line Crossing (TLC) and Time To Collision (TTC). Based on research done in the aviation domain, the two different types of physical constraints and their effect on operator performance will be described.

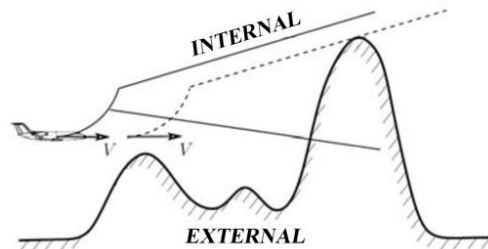


Figure 3: Physical constraints during a terrain avoidance control task, adapted from [10]. The internal constraints are formed by the physical limitations of the vehicle, the external constraints by physical elements such as terrain.

The influence of visualizing the internal and external physical constraints was experimentally evaluated in a terrain avoidance flight task, where the external constraints were formed by the physical terrain and the internal constraints by the climbing performance of the airplane, see Figure 3. Although the visualization of external constraints had already been implemented successfully in the aviation domain, the idea behind this experiment was to prove that the situation awareness of the pilots could be improved even more by showing the aircraft's performance and thus by showing the internal constraints. With this experiment it was shown that visualizing the internal and external physical constraints of a system can improve task performance and situation awareness, while reducing the perceived workload and number of accidents. However, it has also been shown that solely presenting the physical constraints can lead to risky behavior [12, 9], explained by the fact that the pilots could better estimate the performance of the airplane and therefore reduced their safety margin.

## 4.2 Intentional Constraints

The intentional constraints are the limitations of a system imposed by rules, procedures and regulations, either enforced by law or by the operator himself. The strengths and weaknesses of this approach are described by an example from the aviation domain, investigating the effect of an enhanced synthetic display for a terrain avoidance task [12]. The motivation for this study are the concerns and misconceptions about EID as mentioned in [9], where the authors of the research paper believe that risky behavior imposed by EID often occurs due to the fact that these designs are mostly focused on the physical rather than the intentional constraints [7], see also Figure 1. Aside from the intrinsic differences between the two types of constraints another difference is that intentional constraints are soft limits, meaning that they can be exceeded without catastrophic consequences. This is especially useful in unexpected situations, where the operator has to violate the intentional constraints while adhering to the physical constraints. As stated in the paper "only showing causal constraints can lead to boundary-seeking behavior. On the other hand, only showing intentional constraints would decrease the apparent solution space, which can result in situations where satisfactory solutions to difficult situations are not visible for consideration" [12].

Based on a previous experiment by Borst et. al [7], this experiment used the existing synthetic terrain display with a visualization of the aircraft's climb performance (physical constraints) and complemented this by the minimum safe altitude (intentional constraints), aimed to increase the minimum terrain clearance. The results show that by adding the intentional constraints to the display, pilots tend to keep a better ground clearance and thus violate the minimum clearance less frequently. Furthermore, it was shown that complementing the physical constraints by intentional constraints helps to keep the pilots above the minimum clearance limit, while significantly decreasing the spread compared to no intentional layer.

## 4.3 Automation Constraints

Within the space of possibilities defined by the intentional constraints lie the automation constraints, see Figure 1. The automation constraints are usually chosen to be more conservative than the intentional constraints in order to reduce the error with respect to a certain target value, in other words: to optimize the control task. Regarding the driving domain, previous studies have shown that the capabilities of driver assistance systems such as ACC are often misunderstood, resulting in reduced driver safety [47]. The reason for these control conflicts can be partly explained by the fact that only a limited level of information can be conveyed through the pedal position and/or force. When adding other feedback modalities such as visual and auditory feedback, it is believed that this will improve the development of a more accurate mental model of the underlying controller.

In this section it is described how EID can be applied to create a visual representation of ADAS behavior on the basis of a study on reflecting the operational envelope of ACC [45]. The aim of this study is to visualize the ACC limits in an intuitive manner to promote appropriate reliance and support effective transitions between manual and ACC control. The researchers used the principle of EID to reflect the automation constraints in relation to the physical constraints imposed by the lead vehicle and the ego-vehicle. Moreover, representing the status of the automation can improve situation awareness in unexpected scenarios and sensor failure, which in its turn could reduce human overreliance. The experiment has shown that by visualizing the ACC limits, the operators are able to develop an improved mental model of the automation behavior, which leads to a more effective attention allocation strategy. Additionally, by reflecting the operational envelope of the automation, the operators rely more appropriately on its capabilities, improving primary performance, automation reliance and secondary task performance.

## 4.4 Summary

It was shown that constraint based interfaces as discussed in this chapter can improve the mental model of the automation, allowing operators to develop a better understanding of the underlying controller, which can be used to decide whether or not to follow the automation's preference. On the other hand "ecological interfaces reveal all feasible control actions within the work domain constraints, thereby increasing the chance that people will disagree with automation advice that wants to push them into one specific direction" [11]. Therefore, the design of an EID-inspired interface is highly dependent on the balance between automation transparency and the reflection of the work domain constraints. Future research is required to understand the effects of this relationship (for example on user acceptance) and the possible consequences for the representation of automation systems.

## 5 Discussion

In this literature study, research was done on the current developments and possible improvements in the field of cooperative control in vehicle locomotion. At first, a description of the theoretical background of HSC and EID. In the subsequent chapters, experimental results and conclusions from the vehicle locomotion domain were used to address the main research question, defined as: *How can EID be used to reflect the operational envelope of HSC in assisted driving?* A full chapter was devoted on continuous HSC to describe the effect of haptic and visual-haptic feedback on primary and secondary task performance, supporting both skill- and rule-based behavior. In Chapter 4, the constraint-based approach of EID is explained on the basis of practical examples, indicating that EID can significantly increase task performance for routine as well as non-routine tasks, supporting skills-, rules- and knowledge based behavior. This chapter will discuss the results and findings of this literature survey according to the sub-questions as defined in section 1.

### A Benefits and risks of HSC

Compared to manual control, HSC has proven to enhance primary performance for control tasks such as lane keeping, curve negotiation, car following and collision avoidance, while also improving safety, comfort and control effort. Since there are also negative effects related to the implementation of HSC, the following sub-question was addressed: *What are the benefits and risks of the currently applied HSC models in car driving and how can these systems possibly be improved?*

Several methods have been proposed to solve the human factor issues associated with HSC, see section 3. In this section four of these methods will be discussed. The first way to solve control conflicts and other issues is to (1) personalize the controller to the driver's preferences [22, 38]. By measuring the human input during a control task the haptic guidance can be individualized, reducing control conflicts. However, since humans have a great capacity for adaptive behavior, the measurement of these varying control actions can be challenging. Therefore, many HSC applications today make use of adaptable instead of adaptive authority, where the operator decides what the level of haptic authority (LoHA) is, rather than the adaptive algorithm. Future improvements in driver modelling and action recognition will enable more use of adaptive control strategies. A second way to solve the human factor issues is by (2) changing the HSC structure, moving away from the optimization strategy. To achieve this a COFOR is used, ensuring that the reference model is compatible with the operator. Other parameters that can be altered are again the LoHA and the level, strength and strategy of the haptic feedback. A third solution is to (3) vary the LoHA such that guidance-as-needed can be provided to the operator. For example, it has been proven that decreasing the LoHA with increased user grip resulted in a significant reduction in control effort (steering force), especially when the guidance system was incorrect [46]. Given the fact that

this strategy resulted in comparable performance to the traditional systems, this method seems promising for future usage. The last method to eliminate the human factor issues is by (4) complementing HSC with the integration of different feedback modalities (sensor fusion). In section 3 it was shown that the visualization of the operational envelope of HSC can improve both primary and secondary task performance, by supporting both skill- and rule-based behavior. Furthermore, it was shown that visual-haptic feedback results in less control effort compared to haptic feedback only. However, these conclusions only hold for routine tasks, in which all control conditions are properly defined. Designing a robust support system which can also be used for non-routine scenarios requires a different approach that does not only consider the automation constraints, but rather considers the complete work domain.

## **B How can EID be applied to the driving domain?**

Several design principles have been introduced to improve human-machine interaction in support systems for complex control tasks. A promising method named EID has been researched in several domains such as process control, marine, aviation and even in the automotive domain. Therefore, the following sub-question was defined: *In what way have EID-inspired systems been applied to mitigate human factor issues in human-machine systems and to what end can these principles potentially be combined with HSC?*

In the driving domain EID has already successfully been applied to reflect the operational envelope of ACC with respect to the physical constraints. However, it has not yet been combined with haptic guidance systems such as HSC. It is believed that EID can complement HSC by reflecting the automation constraints with respect to all feasible trajectories in the work domain. Where haptic feedback mainly supports skill-based behavior in routine tasks, it was shown that visual feedback of the automation status can complement haptic support, such that rule-based behavior is supported at the same time. It is believed that the visualization of intentional and physical constraints on top of this can further enhance primary and secondary task performance, improving the robustness in unexpected time-critical events. By combining HSC and EID-inspired visual feedback, all cognitive levels of the SRK-taxonomy (including knowledge-based behavior) are supported, which could improve situation and automation awareness, improving performance and reducing control conflicts. Frequent control conflicts in HSC are given in [21], where it can be seen that the automation often behaves differently than expected by the operator. It is believed that some of these conflicts can be solved by representing the automation status based on EID. In this way an operator can for example anticipate better on the fact that the automation has not seen a lead car, since the visualization of the detection is not present, resulting in faster fallback response times, higher safety and better situation awareness, assuming that the driver is attentive. As indicated in section 4, care should be taken with the correct balance between automation transparency and the reflection of the work domain constraints, to prevent for the ignorance of automation suggestions. This can be explained by the fact that EID-inspired feedback reflects all possible control actions within the work domain, increasing the chance that people will disagree with certain automation suggestions in one specific direction. Other problems with EID could be that the visualization of work domain constraints could lead to an information overload, resulting in an increased rather than reduced work load.

## **C In what way can HSC and EID be applied practically?**

The aim of this study was to provide a review on the possibility of complementing HSC by the principle of EID. Thus far, this paper has not focused on the practical implementation of such a system, however this section will elaborate on suggestions for the application of HSC in combination with EID. Therefore, the following sub-question was defined: *In what way could the combination of HSC and visual EID be*

*applied practically and what are the potential problems of this application?* To answer this question, research was done on the practical implementation of visual cues in car driving. There are roughly three ways to provide visual information to the driver, being: through a Head-Up Display (HUD) in the focal field of view, a Head-Down Display (HDD) behind the steering wheel and a Multi-Function Display (MFD) placed centrally in the dashboard. The strengths and weaknesses of these types of displays are discussed in [25], where it can be seen that the benefits of a HUD are a fast response time, little physical movement and easy detection. The downsides of a HUD are the constrained space and visual interference. In the case of a HDD the advantages are medium physical movement and high familiarity, where the downsides are ignorance and crowded information. The pros and cons of the MFD are similar to the HDD, except for the fact that a MFD requires a high physical movement and thus leads to more distraction. The application of a HUD seems promising when compared to HDD and MFD, indicated by an improved performance and higher user acceptance [3].

Advancing on the idea of implementing visual feedback through a HUD, one visualization strategy named Augmented Reality (AR) has recently gained interest in several domains, including the driving domain [26, 32, 50, 24]. In brief, AR refers to the integration of real world and artificial stimuli, aimed at improving human performance. Typically, this is achieved by overlaying the real world cues with computer graphics that can reflect cues such as navigation, object detection and collision avoidance. Apart from the technical challenges, it is believed that a HUD based on AR can be used to reflect visual feedback as defined by the principle of EID [25]. To eliminate the problem of having a constrained space in a HUD, one can think of a HUD that uses the entire windscreen to project the visual cues. In this way the work domain constraints can be represented as an overlay on the driving scene. A negative side-effect of a HUD could be the visual interference caused by the computer graphics. This effect has also been found in a study on cognitive tunneling [49], defined as "the effect where observers tend to focus attention on information from specific areas of a display to the exclusion of information presented outside of these highly attended areas." To avoid these effects, the design of the visualizations should be carefully balanced to convey the right amount of information in an intuitive way, aimed to improve the situation awareness while not negatively influencing the workload.

## 6 Conclusions and Future Work

The main research question addressed in this literature review is: *How can Ecological Interface Design be used to reflect the operational envelope of Haptic Shared Control in assisted driving?* This question has been answered in segments through the elaboration of four sub-questions, as discussed in section 5. In this section the main research question will be answered, followed by recommendations on future work.

Human factors research has shown that the human operator remains a key element as long as full automation is not yet accomplished. Many forms of automation exist between manual control and full automation, often called human-machine systems. To avoid human factor issues in these systems, they should be designed such that the utilization of the automation capabilities is maximized, while automation awareness should be developed in order to compensate for the system limitations. As a form of cooperative control, HSC has been proven to improve both primary and secondary task performance in routine tasks by keeping the driver in-the-loop. This is achieved by providing the driver with haptic guidance, optimized for a certain target trajectory, aimed at reducing human variability and supporting skill-based behavior. Despite the improvements, some human factor issues remain prevalent, being overreliance, loss of skills, behavioral adaptation, reduced situation awareness and control conflicts.

The major improvements of the current HSC systems can be obtained by increasing the user acceptance through the improvement of the mental model of the automation, thus reducing control conflicts. In the domain of HSC, several methods have been proposed to achieve this, for example by personalizing the controller, changing the structure of the controller, varying the LoHA or by combining different feedback modalities. The last strategy has been found to be effective in studies applying visual-haptic feedback, reflecting the automation constraints of the controller, aimed at supporting skill- and rule-based behavior. Continuing on the idea of complementing HSC with visual feedback, the principle of EID has been proposed to further enhance performance by following a constraint-based approach. This means that not only the automation constraints are visualized, but also the other constraints imposed by the work domain. It is believed that by applying EID, more insight can be provided in terms of external and internal physical constraints, such that the consciousness of these entities is not only based on human perception and prior knowledge, but also on the actual physical constraints. The satisficing character of EID has been proven to improve performance, reliance and acceptance in both routine and non-routine tasks, by reflecting the automation status with respect to the available trajectories to reach a certain target, supporting all cognitive levels of the SRK-taxonomy.

Further experimental research is required to determine the effects of complementing HSC with EID on driving performance, reliance, behavioral adaptation, situation awareness, workload, control conflicts and the overall user acceptance. In this paper it was proposed to implement the EID-inspired visual feedback into a HUD based in the form of AR, such that the visual interference and workload is kept to a minimum. To narrow down the scope of such an experiment, one specific nested control loop should be considered, focusing on one particular time scale. Care should be taken to avoid other human factor issues such as cognitive tunneling, information overload and automation ignorance.

## References

- [1] David A. Abbink, Erwin R. Boer, and Mark Mulder. "Motivation for continuous haptic gas pedal feedback to support car following". In: *2008 IEEE Intelligent Vehicles Symposium*. IEEE, June 2008. DOI: 10.1109/ivs.2008.4621325. URL: <https://doi.org/10.1109/ivs.2008.4621325>.
- [2] David A Abbink, Mark Mulder, and Erwin R Boer. "Haptic shared control: smoothly shifting control authority?" In: *Cognition, Technology & Work* 14.1 (2012), pp. 19–28.
- [3] Markus Ablameier et al. "Eye gaze studies comparing head-up and head-down displays in vehicles". In: *Multimedia and Expo, 2007 IEEE International Conference on*. IEEE, 2007, pp. 2250–2252.
- [4] Avinash Balachandran et al. "Predictive haptic feedback for obstacle avoidance based on model predictive control". In: *IEEE Transactions on Automation Science and Engineering* 13.1 (2016), pp. 26–31.
- [5] D Beefink et al. "Increasing Task-Sharing Performance by Haptically Assisting a Tunnel-in-the-Sky Approach". In: *submitted to IEEE* (2018). DOI: [uid:e5f509a2-755b-4ba9-b8bb-30b1ba2cbea8](https://doi.org/10.1109/ivs.2018.8453588).
- [6] Rolf Boink et al. "Understanding and reducing conflicts between driver and haptic shared control". In: *Systems, Man and Cybernetics (SMC), 2014 IEEE International Conference on*. IEEE, 2014, pp. 1510–1515.
- [7] C Borst, M Mulder, and MM Van Paassen. "Design and simulator evaluation of an ecological synthetic vision display". In: *Journal of Guidance, Control and Dynamics* 33.5 (2010), pp. 1577–1591.
- [8] Clark Borst. "Ecological approach to pilot terrain awareness". In: (2009).
- [9] Clark Borst, John M Flach, and Joost Ellerbroek. "Beyond ecological interface design: Lessons from concerns and misconceptions". In: *IEEE Transactions on Human-Machine Systems* 45.2 (2015), pp. 164–175.
- [10] Clark Borst et al. "Ecological interface design for terrain awareness". In: *The International Journal of Aviation Psychology* 16.4 (2006), pp. 375–400.
- [11] Clark Borst et al. "Ecological interface design: supporting fault diagnosis of automated advice in a supervisory air traffic control task". In: *Cognition, Technology & Work* 19.4 (2017), pp. 545–560.
- [12] Jan Comans et al. "Risk perception in ecological information systems". In: *Advances in Aviation Psychology* (2014), pp. 121–138.
- [13] Nick Dinadis and Kim J Vicente. "Designing functional visualizations for aircraft systems status displays". In: *The international journal of aviation psychology* 9.3 (1999), pp. 241–269.
- [14] Mario Enriquez and Karon E MacLean. "Impact of haptic warning signal reliability in a time-and-safety-critical task". In: *Haptic Interfaces for Virtual Environment and Teleoperator Systems, 2004. HAPTICS'04. Proceedings. 12th International Symposium on*. IEEE, 2004, pp. 407–414.
- [15] ROBERT E Fenton. "An improved man-machine interface for the driver-vehicle system". In: *IEEE Transactions on Human Factors in Electronics* 4 (1966), pp. 150–157.
- [16] Frank Flemisch et al. "Automation spectrum, inner/outer compatibility and other potentially useful human factors concepts for assistance and automation". In: *Human Factors for assistance and automation* (2008).
- [17] Frank Flemisch et al. "Cooperative control and active interfaces for vehicle assistance and automation". In: (2008).
- [18] Benjamin AC Forsyth and Karon E MacLean. "Predictive haptic guidance: Intelligent user assistance for the control of dynamic tasks". In: *IEEE transactions on visualization and computer graphics* 12.1 (2006), pp. 103–113.
- [19] Paul G Griffiths and R Brent Gillespie. "Sharing control between humans and automation using haptic interface: primary and secondary task performance benefits". In: *Human factors* 47.3 (2005), pp. 574–590.
- [20] Daniel S Hall, Lawrence G Shattuck, and Kevin B Bennett. "Evaluation of an ecological interface design for military command and control". In: *Journal of Cognitive Engineering and Decision Making* 6.2 (2012), pp. 165–193.
- [21] Makoto Itoh, Frank Flemisch, and David Abbink. "A hierarchical framework to analyze shared control conflicts between human and machine". In: *IFAC-PapersOnLine* 49.19 (2016), pp. 96–101.
- [22] Arnold W de Jonge et al. "The effect of trial-by-trial adaptation on conflicts in haptic shared control for free-air teleoperation tasks". In: *IEEE transactions on haptics* 9.1 (2016), pp. 111–120.
- [23] D Katzourakis et al. "Shared control for road departure prevention". In: *Systems, Man, and Cybernetics (SMC), 2011 IEEE International Conference on*. IEEE, 2011, pp. 1037–1043.
- [24] Hyungil Kim et al. "Exploring head-up augmented reality interfaces for crash warning systems". In: *Proceedings of the 5th International Conference on Automotive User Interfaces and Interactive Vehicular Applications*. ACM, 2013, pp. 224–227.
- [25] Sang Ho Kim, Jose Fernando Sabando, and Woo Hyun Kim. "An Ecological Interface Design Approach for Developing Integrated and Advanced In-Vehicle Information System". In: *Indian Journal of Science and Technology* 9.16 (2016).
- [26] SeungJun Kim and Anind K Dey. "Simulated augmented reality windshield display as a cognitive mapping aid for elder driver navigation". In: *Proceedings of the SIGCHI Conference on Human Factors in Computing Systems*. ACM, 2009, pp. 133–142.
- [27] JD Lee et al. "Application of ecological interface design to driver support systems". In: *Proceedings of IEA 2006: 16th World Congress on Ergonomics*. 2006.

- [28] Monica N Lees et al. "Cross-modal warnings for orienting attention in older drivers with and without attention impairments". In: *Applied ergonomics* 43.4 (2012), pp. 768–776.
- [29] Jani Lylykangas et al. "Responses to visual, tactile and visual–tactile forward collision warnings while gaze on and off the road". In: *Transportation research part F: traffic psychology and behaviour* 40 (2016), pp. 68–77.
- [30] Marieke Hendrikje Martens and Arie P van den Beukel. "The road to automated driving: Dual mode and human factors considerations". In: *Intelligent Transportation Systems-(ITSC), 2013 16th International IEEE Conference on*. IEEE. 2013, pp. 2262–2267.
- [31] Timothy R McEwen, John M Flach, and Nancy C Elder. "Interfaces to medical information systems: Supporting evidenced based practice". In: *Systems, Man and Cybernetics (SMC), 2014 IEEE International Conference on*. IEEE. 2014, pp. 335–340.
- [32] Zeljko Medenica et al. "Augmented reality vs. street views: a driving simulator study comparing two emerging navigation aids". In: *Proceedings of the 13th International Conference on Human Computer Interaction with Mobile Devices and Services*. ACM. 2011, pp. 265–274.
- [33] Mark Mulder, David A Abbink, and Erwin R Boer. "Sharing control with haptics: Seamless driver support from manual to automatic control". In: *Human factors* 54.5 (2012), pp. 786–798.
- [34] Mark Mulder, David A Abbink, and Erwin R Boer. "The effect of haptic guidance on curve negotiation behavior of young, experienced drivers". In: *Systems, Man and Cybernetics, 2008. SMC 2008. IEEE International Conference on*. IEEE. 2008, pp. 804–809.
- [35] Mark Mulder et al. "Car-following support with haptic gas pedal feedback". In: *Proceedings of IFAC Symposium on Analysis, Design, and Evaluation of Human-Machine Systems*. 2004.
- [36] Mark Mulder et al. "Haptic gas pedal support during visually distracted car following". In: *IFAC Proceedings Volumes* 43.13 (2010), pp. 322–327.
- [37] Marie-Christin Ostendorp, Jan Charles Lenk, and Andreas Lüdtke. "Smart glasses to support maritime pilots in harbor maneuvers". In: *Procedia Manufacturing* 3 (2015), pp. 2840–2847.
- [38] Sjors Oudshoorn. "Design of Criticality-Based Haptic Steering Guidance for Human Like Adaptation to Different Lane Keeping Tasks". In: *Master Thesis* (2017). DOI: [f83ccd61-aa5e-44cc-a478-14d5d878d798](https://doi.org/10.1016/j.ijhcs.2006.10.001).
- [39] Raja Parasuraman and Victor Riley. "Humans and automation: Use, misuse, disuse, abuse". In: *Human factors* 39.2 (1997), pp. 230–253.
- [40] Sebastiaan M Petermeijer, David A Abbink, and Joost CF de Winter. "Should drivers be operating within an automation-free bandwidth? Evaluating haptic steering support systems with different levels of authority". In: *Human factors* 57.1 (2015), pp. 5–20.
- [41] Sebastiaan M Petermeijer et al. "The effect of haptic support systems on driver performance: A literature survey". In: *IEEE transactions on haptics* 8.4 (2015), pp. 467–479.
- [42] Jens Rasmussen. "Skills, rules, and knowledge; signals, signs, and symbols, and other distinctions in human performance models". In: *IEEE transactions on systems, man, and cybernetics* 3 (1983), pp. 257–266.
- [43] Jens Rasmussen and Kim J Vicente. "Coping with human errors through system design: implications for ecological interface design". In: *International Journal of Man-Machine Studies* 31.5 (1989), pp. 517–534.
- [44] Matteo Razzanelli et al. "A Visual-Haptic Display for Human and Autonomous Systems Integration". In: *International Workshop on Modelling and Simulation for Autonomous Systems*. Springer. 2016, pp. 64–80.
- [45] Bobbie D. Seppelt and John D. Lee. "Making adaptive cruise control (ACC) limits visible". In: *International Journal of Human-Computer Studies* 65.3 (Mar. 2007), pp. 192–205. DOI: [10.1016/j.ijhcs.2006.10.001](https://doi.org/10.1016/j.ijhcs.2006.10.001). URL: <https://doi.org/10.1016/j.ijhcs.2006.10.001>.
- [46] Jan Smisek et al. "Adapting haptic guidance authority based on user grip". In: *Systems, Man and Cybernetics (SMC), 2014 IEEE International Conference on*. IEEE. 2014, pp. 1516–1521.
- [47] Neville A Stanton and Philip Marsden. "From fly-by-wire to drive-by-wire: safety implications of automation in vehicles". In: *Safety Science* 24.1 (1996), pp. 35–49.
- [48] Heather A Stoner, Emily E Wiese, and John D Lee. "Applying ecological interface design to the driving domain: the results of an abstraction hierarchy analysis". In: *Proceedings of the Human Factors and Ergonomics Society Annual Meeting*. Vol. 47. 3. SAGE Publications Sage CA: Los Angeles, CA. 2003, pp. 444–448.
- [49] Lisa C Thomas and Christopher D Wickens. "Visual displays and cognitive tunneling: Frames of reference effects on spatial judgments and change detection". In: *Proceedings of the Human Factors and Ergonomics Society Annual Meeting*. Vol. 45. 4. SAGE Publications Sage CA: Los Angeles, CA. 2001, pp. 336–340.
- [50] Cuong Tran, Karlin Bark, and Victor Ng-Thow-Hing. "A left-turn driving aid using projected oncoming vehicle paths with augmented reality". In: *Proceedings of the 5th International Conference on Automotive User Interfaces and Interactive Vehicular Applications*. ACM. 2013, pp. 300–307.
- [51] Kakin K Tsoi, Mark Mulder, and David A Abbink. "Balancing safety and support: Changing lanes with a haptic lane-keeping support system". In: *Systems Man and Cybernetics (SMC), 2010 IEEE International Conference on*. IEEE. 2010, pp. 1236–1243.
- [52] Stijn BJ Van Dam, Max Mulder, and MM Van Paassen. "Ecological interface design of a tactical airborne separation assistance tool". In: *IEEE Transactions on Systems, Man, and Cybernetics-Part A: Systems and Humans* 38.6 (2008), pp. 1221–1233.
- [53] Marinus M Van Paassen et al. "For design choices for haptic shared control". In: *Doctoral thesis* (2017).
- [54] Kim J Vicente. *Cognitive work analysis: Toward safe, productive, and healthy computer-based work*. CRC Press, 1999.

- [55] Kim J Vicente, Klaus Christoffersen, and Alex Pereklita. "Supporting operator problem solving through ecological interface design". In: *IEEE transactions on systems, man, and cybernetics* 25.4 (1995), pp. 529–545.
- [56] Guy H Walker, Neville A Stanton, and Mark S Young. "The ironies of vehicle feedback in car design". In: *Ergonomics* 49.2 (2006), pp. 161–179.
- [57] Carl Westin, Clark Borst, and Brian Hilburn. "Strategic conformance: Overcoming acceptance issues of decision aiding automation?" In: *IEEE Transactions on Human-Machine Systems* 46.1 (2016), pp. 41–52.
- [58] Joost CF de Winter and Dimitra Dodou. "Preparing drivers for dangerous situations: A critical reflection on continuous shared control". In: *Systems, Man, and Cybernetics (SMC), 2011 IEEE International Conference on*. IEEE. 2011, pp. 1050–1056.

## B Haptic Feedback Design

Haptic Shared Control has proven to be a successful alternative to automation systems such as traded control. The main advantage of shared control is the fact that during a driving task the automation and driver are jointly operating the vehicle, for example by exerting torque on the steering wheel. This can increase performance, while decreasing the control activity. The main disadvantage of shared control arises when there is a misalignment between the driver and automation, resulting in control conflicts. These conflicts are most prevalent in non-critical control tasks, where the operator is able to develop a well-founded strategy. In contrast, time critical situations do not allow for elaborate decision-making, meaning that assistive automation is often desired and not considered as conflicting.

### Four-Design-Choice Controller

In previous research it was shown that the personalization of haptic shared control through a human compatible reference (HCR) can significantly reduce control conflicts in terms of human steering wheel torque [2], compared to a shared controller which only uses feedback based on the road center reference. In Figure 1 an overview is given of the applied FDC controller, showing the relationship between (1) the HCR, (2) strength of the Haptic Feedback (SoHF), (3) Level of Haptic Support (LoHS) and (4) the Level of Haptic Authority (LoHA). In the overview it can also be seen that apart from position ( $X_R, Y_R$ ) and heading ( $\Psi_R$ ) feedback, the steering wheel input ( $\delta_R$ ) is used as a feed-forward signal, improving the 'feeling' of the provided haptic torque.

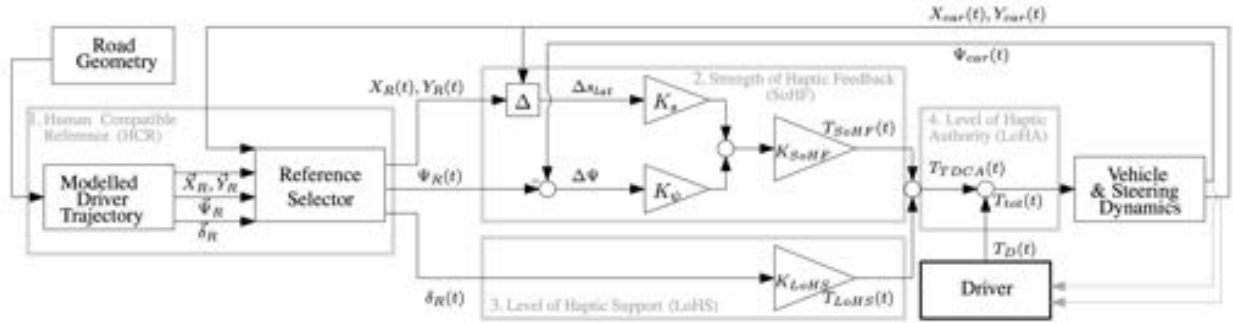


Figure 1: The implemented Four-Design-Choice (FDC) Haptic Shared Controller from [2].

### Human Compatible Reference

For this study, it was chosen to implement the HCR by recording several manual trails of the final experiment, which on their turn are used to create a generic reference of which the behavior should be similar for all obstacle conditions (critical and non-critical). In Figure 1 it can be seen that the required inputs for the FDC controller are position ( $X_R, Y_R$ ), vehicle heading ( $\Psi_R$ ) and steering wheel input ( $\delta_R$ ). Since the evasive manoeuvres are only present on the straight sections of the trajectory, all other parts of the HCR can be based on the position and heading as defined by the generated road trajectory, used in the DUECA simulation. This means that the evasive sections in the HCR can be constructed by replacing the road trajectory data with the generic inputs for the evasive manoeuvre in terms of  $X_R, Y_R$  and  $\Psi_R$ .

In Figure 2 an example is given of the recorded heading during a manual experimental run. It can be seen that the road heading has a constant profile, where the car heading shows several peaks during the obstacle avoidance. Note that large peaks (5 in total) represent a critical obstacle avoidance and small peaks (5 in total) a non-critical avoidance. For the construction of the HCR, these 10 sections were replaced by a generic avoidance trajectory  $\Psi_R$ , by averaging and smoothing the recorded manoeuvres.

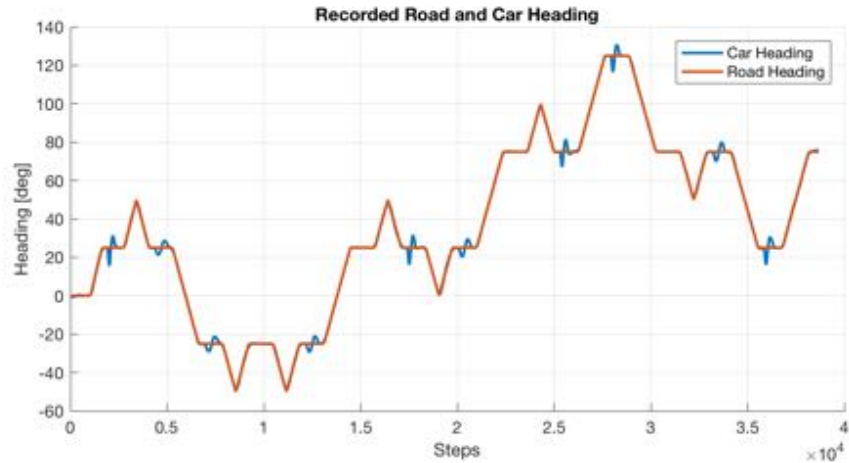


Figure 2: Example of recorded heading during manual experimental run.

A more detailed overview of the recorded car heading sections is depicted in Figure 3, where the headings are split into both critical and non-critical obstacle manoeuvres. Note that all recorded vectors were converted such that they would start with a heading of zero degrees. Additionally, the origin of the x-axis corresponds to the moment when the obstacle appears on the road. All sections (left) were used to create two generic heading profiles (right) which were later used to replace the straight parts of the original simulation trajectory, at the locations where the obstacles would occur. Note that the amount of steps (x-axis) is different for the recorded data compared to the obtained generic headings. This can be explained by the difference between the logging rate of the simulator (100 Hz) and the step size of the simulation trajectory (0.2 m). This difference was taken into account for the creation of the HCR, avoiding timing errors during the simulation.

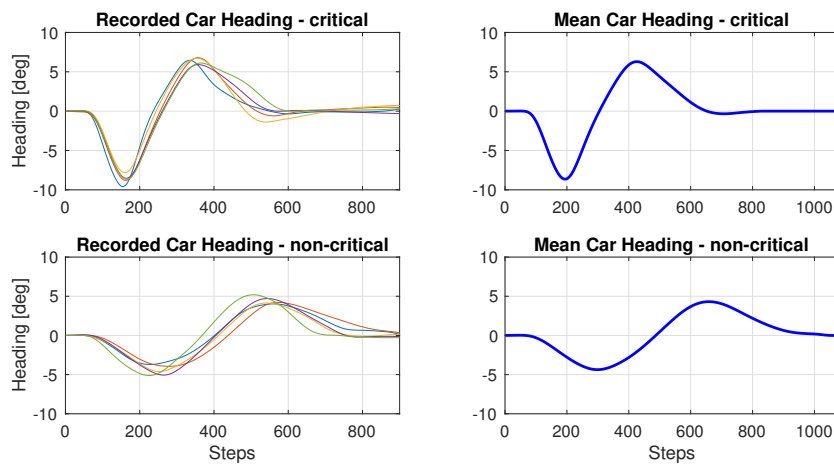


Figure 3: Recorded (colored) and generic car headings (blue) for critical and non-critical manoeuvres.

In terms of  $X_R$  and  $Y_R$ , the evasive sections were cut from the recorded data, after which they had to be rotated back to a zero degree heading, in order to average out the trajectories. Afterwards, all sections were converted to start at zero in lateral direction. The resulting generic trajectories can be seen below in Figure 4. These generic trajectories were subsequently used to overwrite the straight parts of the original simulation trajectory. This was done by rotating them back to the required road heading, while replacing the straight trajectory.

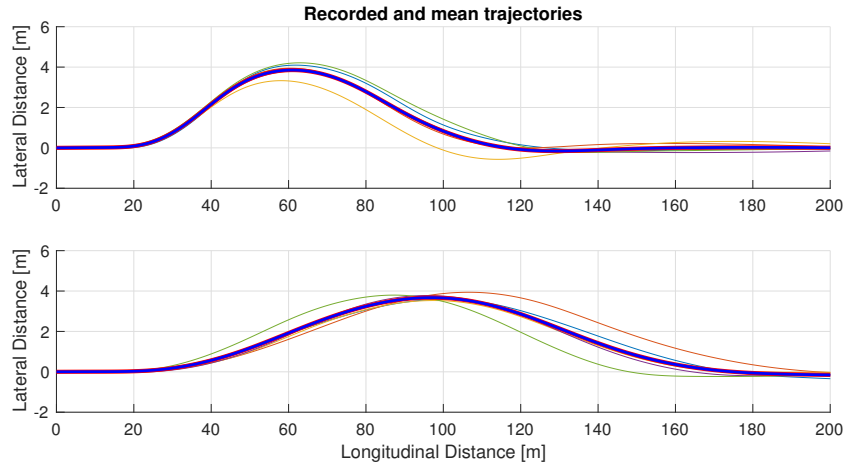


Figure 4: Recorded (colored) and generic trajectory (blue) for critical and non-critical manoeuvres.

The approach for the steering wheel input  $\delta_R$  is comparable to the strategy used in the previous parts, meaning that again the recorded steering wheel input was used to create a generic steering profile, visible in Figure 5. However, where the basis of the  $X_R$ ,  $Y_R$  and  $\Psi_R$  were obtainable from the simulation trajectory, the human-dependent steering wheel input  $\delta_R$  was not known a priori. This means that for this case all other parts of the trajectory (including curves) had to be generated manually.

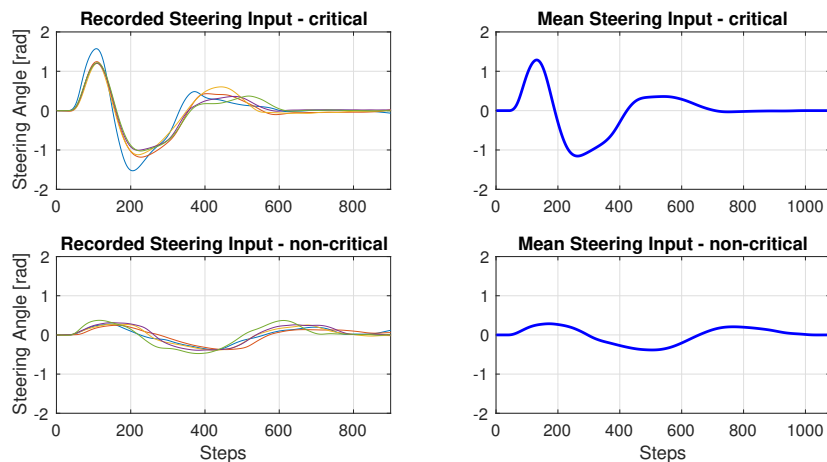


Figure 5: Recorded (colored) and generic steering (blue) for critical and non-critical manoeuvres.

The manual creation of the steering wheel input reference was done in three steps, being (1) smoothing of the total signal, (2) assigning zero steering on straight sections and (3) replacing the straight sections by the generic steering profile of Figure 5. See Figure 6 and Figure 7 for an overview of the approach.

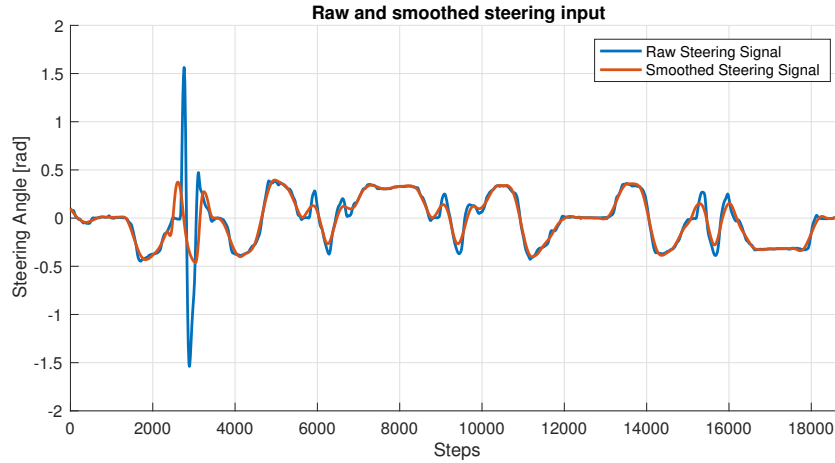


Figure 6: Step 1: smoothing the raw steering signal, only to be used for the curves and straight sections. The evasive manoeuvres are obtained from the generic steering profile.

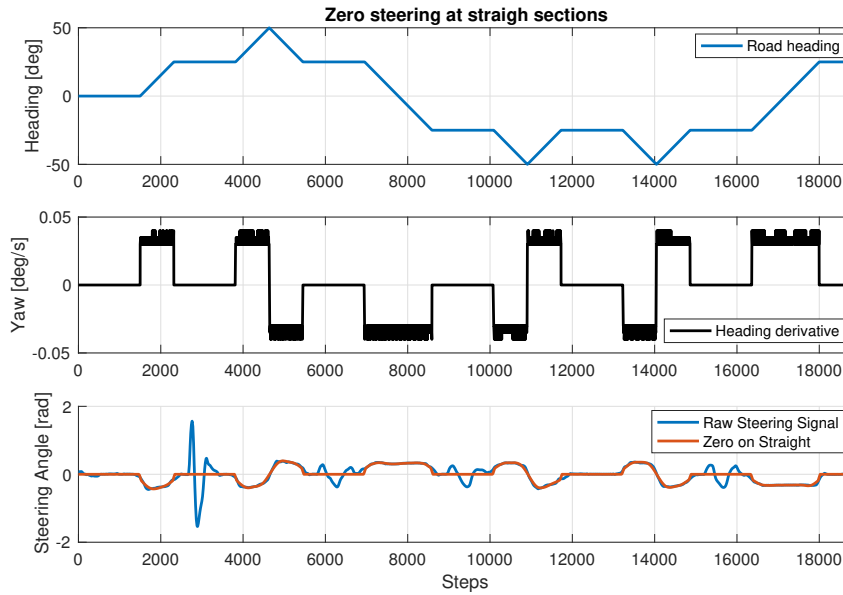


Figure 7: Step 2: using the road heading derivative to assign zero steering to straight sections, later to be replaced by the generic steering input profile.

The final step to be taken in order to create the HCR in terms of  $X_R$ ,  $Y_R$ ,  $\Psi_R$  and  $\delta_R$  is to replace all straight sections by the generic profiles as previewed above. In Figure 8 a close-up of the final trajectory is given, in which an example of a critical manoeuvre is depicted. In this image, the vehicle drives from the top left corner to the bottom right corner. Note how the generic trajectory has a quicker response time than the recorded trajectory. This can be explained by the fact the the human response time (from the recorded data) was eliminated by shifting the generic profiles by approximately 0.34 s, improving obstacle avoidance performance.

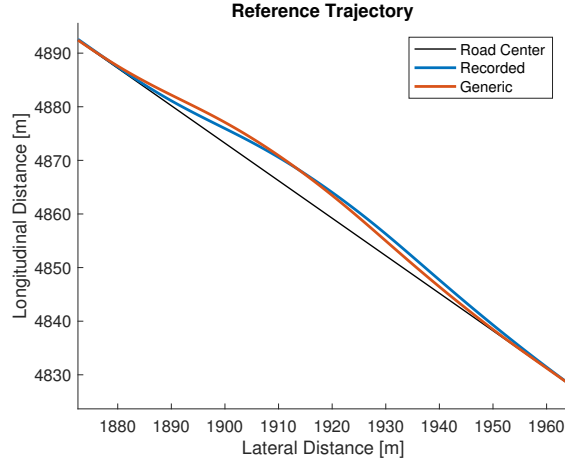


Figure 8: Detailed view of the final HCR trajectory compared to the road center and recorded data.

In Figure 9 an overview is given of the final HCR in terms of  $\Psi_R$  and  $\delta_R$ . It can be seen that the generic reference show a much more consistent behavior than the recorded human input. Furthermore, a close-up is depicted in which the elimination of the human reaction time is visible. The generic profiles were shifted by 40 steps, which corresponds to a time of 0.34 seconds, based on a step size of 0.2 m and a vehicle speed of 23.82 m/s.

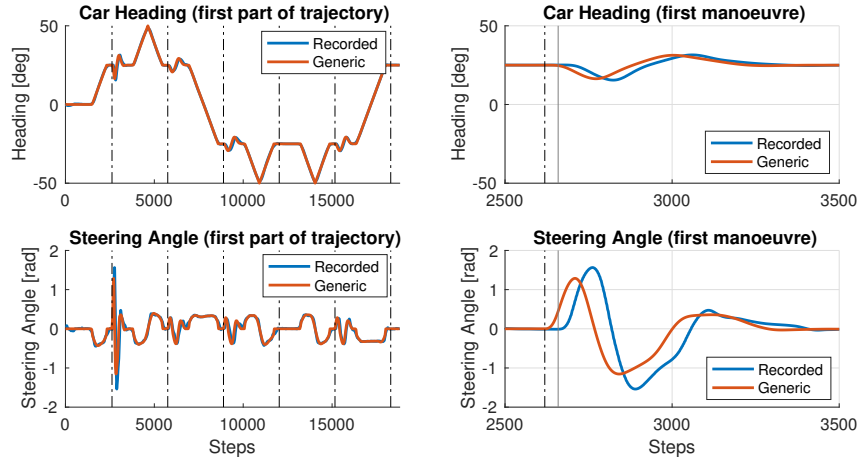


Figure 9: Overview of the final HCR in terms of heading and steering compared to the recorded data. The dashed lines indicate the moment at which the obstacle appears. Note the shift of the generic signals with respect to the recorded data.

## Haptic Settings DUECA

After the implementation of the HCR, the parameters of the Haptic Shared Controller had to be defined. These settings were chosen similar to previous research with the FDC, see the table below from [2].

Gain	TDCA-HSC	Gain	M-HSC
$K_s$	0.05 [N]	$D$	0.08 [N]
$K_\Psi$	0.03 [Nm/deg]	$P$	0.9 [Nm/deg]
$K_{S_oHF}$	1.5 [-]	$K_f$	2.0 [-]
$K_{L_oHS}$	0.45 [Nm/rad]	$t_{LH}$	0.7 [s]



## C Visual Ecological Feedback Design

### Abstraction Hierarchy

Central to the ecological approach is the abstraction hierarchy, a functional model to examine the work domain following a top-down approach. This means that rather than starting with the end user, it is analyzed from the work domain which functional purpose is desired and what other underlying functions are required to fulfill this. Therefore, it is explicitly not specified how the task is to be performed or by whom. For this study an abstraction hierarchy considering obstacle avoidance in car driving was made, see Figure 10.

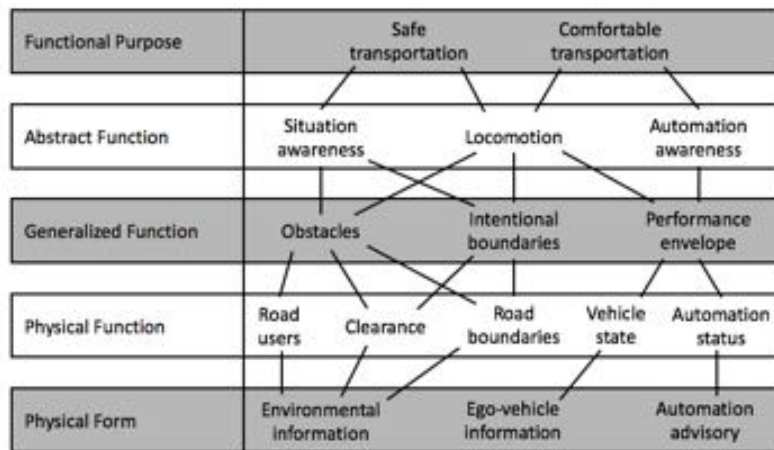


Figure 10: Abstraction hierarchy, with means-ends relationships for obstacle avoidance in cars.

From the abstraction hierarchy it can be seen how the physical functions and corresponding forms are deduced from the functional purpose. Note that the physical forms are roughly subdivided between environmental information, ego-vehicle information and automation advisory. In the simulator study, the work domain constraints were implemented by several types of visual ecological feedback.



## D Implementation

### MATLAB Simulation

The basic foundation of the experimental simulation was developed in the initial design phase of the thesis work. For this phase it was chosen to create a MATLAB simulation based on the linear bicycle model in order to rapidly provide a working concept. The bicycle model is based on the following assumptions, being (1) that the wheels of one axle are lumped in a single wheel, (2) heave, roll and pitch motions are neglected (no load transfer present on the wheels), (3) lateral dynamics are negligible, (4) the vehicle moves forward with a constant speed on a flat road and (5) it is assumed that there is a linear relation between the tire slip angle and the lateral tire force. As previously derived in [1], the transfer functions from steering wheel input to global lateral position and yaw angle are:

$$\frac{\psi_g}{\theta_{wheel}}(s) = \frac{V_x LC}{V_x I_z s^2 + 2L^2 C s} \quad (1)$$

$$\frac{y_g}{\theta_{wheel}} = \frac{V_x^2 LC}{V_x I_z s^3 + 2L^2 C s^2} \quad (2)$$

The bicycle model and its corresponding transfer functions were implemented in a Simulink model (see Figure 11) to obtain the lateral position, speed, acceleration and the yaw angle, rate and acceleration. The input of the Simulink model consists of a predetermined sinusoidal steering wheel pattern, simulating a double lane change at a constant longitudinal speed, see Figure 12. The data of the double lane change is logged such that an animation can be created, showing the trajectory of the vehicle complemented by the ecological feedback. The overall goal of this simulation was to get an idea of the possible options for the ecological interface design.

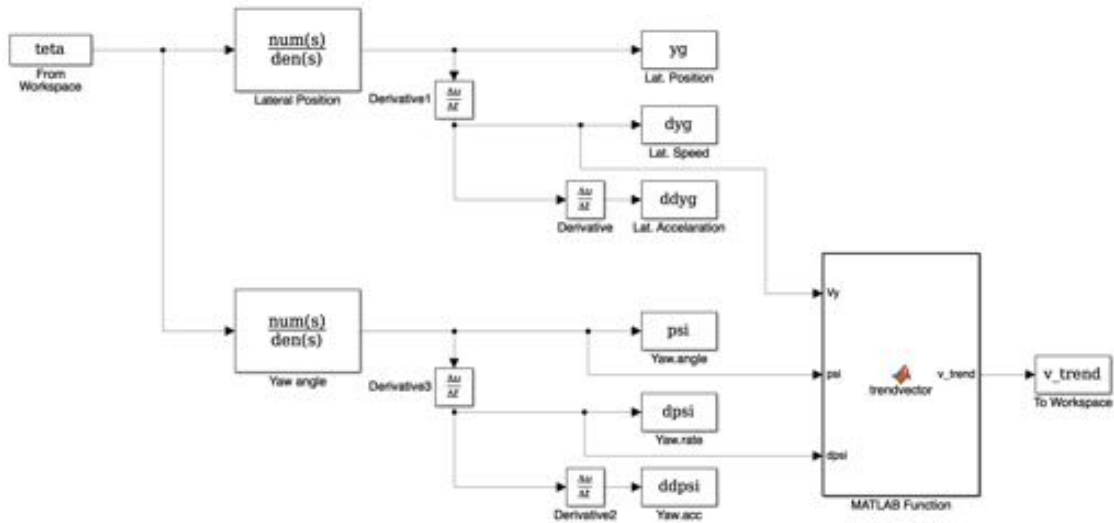


Figure 11: MATLAB Simulink Flow Diagram

In the MATLAB simulation, the trajectory of the lane change and thus the trajectory of the Haptic Shared Controller is displayed on a two lane road, including a simplification of the obstacle, see Figure 13. The static lines of the performance envelope are calculated once, after which they can be animated by translating and rotating the lines according to the predetermined path. Since the trend vector requires real time updating, it was chosen to use a MATLAB function to calculate the shape of the dynamic curve

at every time step. During the simulation the trend line is continuously updated to indicate the future heading for the given steering wheel angle. As a whole the curves form a cone-shaped area that is fixed to the vehicle. To indicate the intentional constraints it is checked in the simulation whether the chosen points on the curves are exceeding the boundaries such that the colouring can be altered.

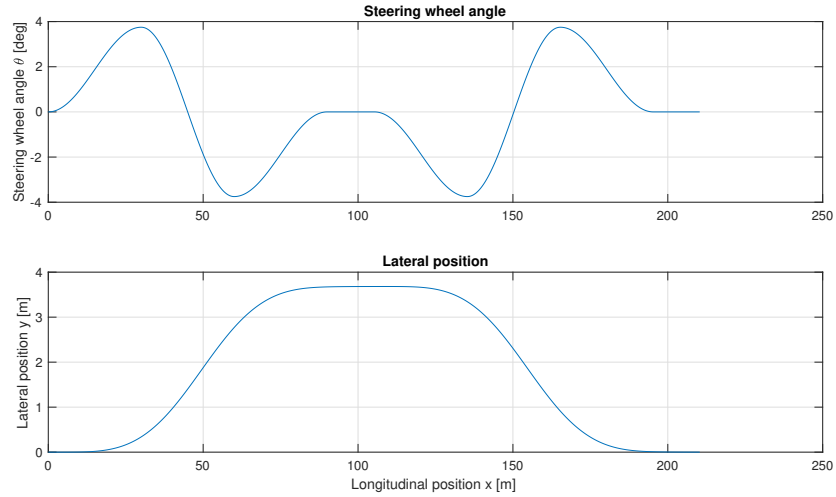


Figure 12: Steering Input Used For Double Lane Change, Including The Resulting Translation

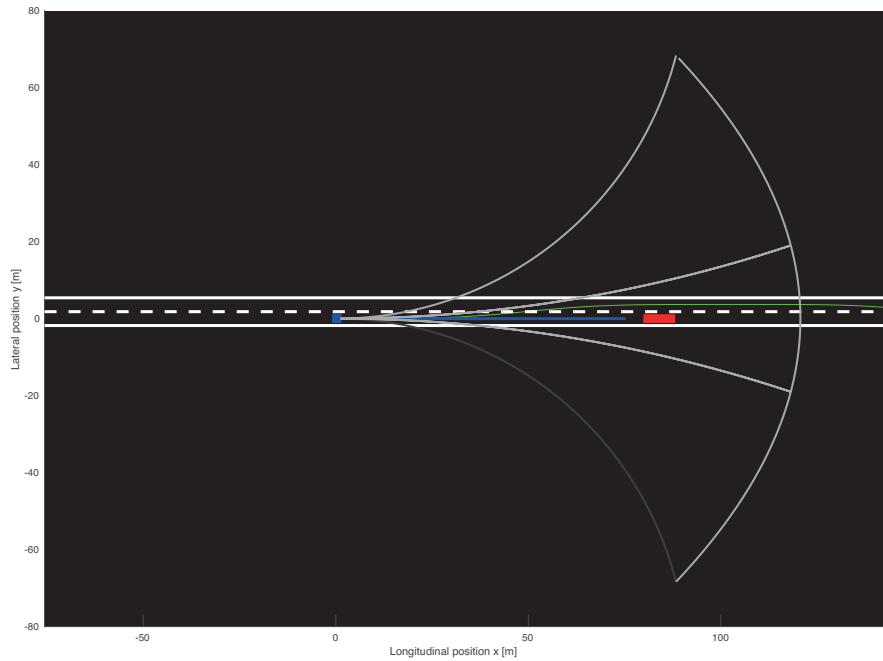


Figure 13: MATLAB Simulation Snapshot. Blue indicates the vehicle position including the trend vector, red is the obstacle, green shows the optimal path of the haptic shared controller and the grey lines represent the performance envelope. Curves can be toggled on and off by the lane boundaries, in the figure indicated by the rightmost dark grey curve.

## DUECA Simulation

From the concept study in Matlab, the design strategy was implemented in the driving simulator at the HMI Lab of Delft University of Technology. The basis of the experiment was based on previous driving simulator experiments. The overall software package for the implementation of the simulation was DUECA, which stands for Delft University Environment for Communication and Activation. A flow diagram indicating the modules of the simulator is depicted in Figure 16.

For the experimental study, a trajectory had to be defined. The idea behind the trajectory was to incorporate 14 straight sections, alternated by curves having the same radius, for simplicity. Since the main focus of this experiment concerns the straight road sections, the trajectory was chosen similar for all participants during all conditions. During the main trails, obstacles had to be avoided, of which 5 critical and 5 non-critical, resulting in 4 empty sections per run. The straight sections all have a length of 300 m, which corresponds to approximately 12 seconds at a speed of 24 m/s. The trajectory was made by assigning the curvature of the road at different instances. The curvature profile is depicted in Figure 14.

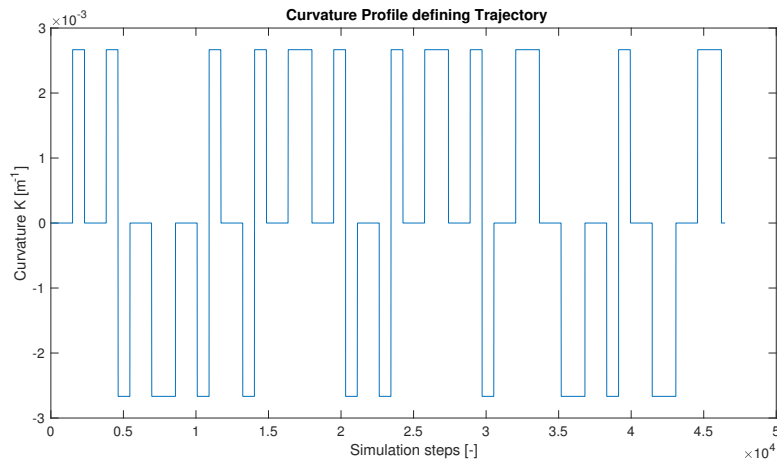


Figure 14: Curvature profile used to define the simulation trajectory. note that all curves have the same radius for simplicity.

After the end of a curve, an initial distance of 60 metres was applied before the obstacle appeared on the road, such that the participants had some time to stabilize their position in the right lane. Obstacles appeared with two different TTC's, meaning that the distance from the vehicle to the obstacle at appearance was altered throughout the simulation. The final trajectory and the order of the obstacles can be seen in Figure 15. During the training, the obstacle order was similar for all conditions, while during the main trails the obstacle order was altered between 1 and 2 among the four driving conditions.

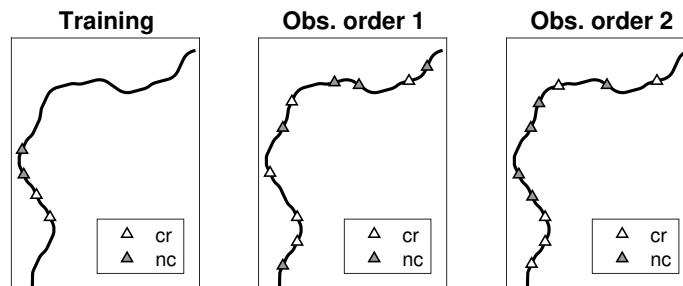


Figure 15: Trajectory and applied obstacle orders for training and main trails.



## **E Experiment Forms**



# DRIVING SIMULATOR RESEARCH PARTICIPATION CONSENT

## Obstacle avoidance performance study

**Introduction:** This is an invitation to participate in the research study of MSc student Wilco Vreugdenhil. Before agreeing to participate in this study, it is important that the following explanation of the proposed procedures are read and understood properly. This document describes the purpose, procedures, benefits, risks and possible discomforts of the study. It also discloses the right to withdraw from the study at any time.

**Purpose of the study:** The purpose of this driving simulator study is to investigate driving behaviour, control effort, subjective experience and acceptance of three different driving feedback systems. During the experiment you will experience either (1) no feedback, (2) visual feedback, (3) haptic feedback in the form of a steering wheel torque or (4) a combination of both. You will be one of the 20 participants taking part in this study. The results of this experiment will be statistically analysed and anonymously published in a Master's thesis and possibly in a scientific publication.

**Procedure:** The total participation in this study will take approximately 1.5 hours. Before the simulation is started, you will be asked to fill out a questionnaire regarding your driving habits and previous driving experience. Next, you will be seated in the driving simulator (a fixed-base simulator with a wide-angle view). In the first phase of the experiment you will get 15 minutes of training to get used to the simulator and the different feedback systems. During the experiment, the car speed is held constant at 85 km/h by a cruise control system. Therefore, you will be only able to change the vehicle heading via the steering wheel, all other controls (like the gas pedal) are inactive. You will be asked to place your hands in a ten-to-two position on the steering wheel.

In the second phase, you will drive four trails of 7 minutes each, where you will experience the feedback systems in a random order. Your task in this experiment will be to stay in the middle of the right lane on a curvy two-lane road, while avoiding objects that randomly appear on the road. After the obstacle is avoided, you should turn back to the right lane at your own pace. After each of the four trails you will have a short break of 5 minutes (outside the simulator) in which you are asked to answer a questionnaire to assess your subjective experience and acceptance of the driven feedback system.

**Risks and discomforts:** During this experiment there is a risk of simulator sickness, with symptoms like nausea, drowsiness, fatigue or headache. These symptoms are similar to motion sickness. After each condition you will be asked whether you are experiencing any form of discomfort. If you feel uncomfortable, you have the right to stop participating at any time without any negative consequences.

**Confidentiality:** All data collected in this study will be kept confidential and will be used for research purposes only. Throughout the study you will only be identified by a participant number.

**Right to refuse or withdraw:** Your participation is strictly voluntary and you may refuse to participate, or discontinue your participation at any time, without negative consequences.

**Contact details:** For more information or concerns about this experiment, please feel free to contact:  
Wilco Vreugdenhil  
Faculty of Mechanical Engineering, TU Delft - Mekelweg 2, 2628 CD Delft  
Phone: +316 54767927 - E-mail: w.vreugdenhil-1@student.tudelft.nl

**I acknowledge that I completely understand this consent and I agree to participate in this study.**

Signature of participant \_\_\_\_\_

Date \_\_\_\_\_



# Driving condition 1 - questionnaire B

Please tick a dot on every line and look carefully at the order

Q1: I find the feedback system \*

Useful (+2)      +1      0      -1      (-2) Useless

1                       

Q2: I find the feedback system \*

Pleasant (+2)      +1      0      -1      (-2) Unpleasant

2                       

Q3: I find the feedback system \*

Bad (-2)      -1      0      +1      (+2) Good

3                       

Q4: I find the feedback system \*

Nice (+2)      +1      0      -1      (-2) Annoying

4                       

Q5: I find the feedback system \*

Effective (+2)      +1      0      -1      (-2) Superfluous

5                       

Q6: I find the feedback system \*

Irritating (-2)      -1      0      +1      (+2) Likeable

6                       

Q7: I find the feedback system \*

Assisting (+2)      +1      0      -1      (-2) Worthless

7                       

Q8: I find the feedback system \*

Undesirable (-2)      -1      0      +1      (+2) Desirable

8                       

Q9: I find the feedback system \*

Raising alertness...      +1      0      -1      (-2) Sleep-inducing

9



## F Conflict Torque Analysis

The occurrence and amount of conflicts were evaluated by determining whether the human and HSC torque were in opposite direction during the straight sections in which obstacles were avoided. Conflicts in other situations during the trails were not in the scope of this study. In case of a conflict, the time-instance was flagged as 1, where a flag of 0 indicated that the HSC torque supported the driver intentions. The occurrence and absolute difference between human and HSC torque was used to determine the *mean conflicting rotational work*  $W_{con}$ , *mean conflict peak torque*  $T_{con,p}$  and the *mean percentage of time in conflict*.

In Figure 17 an example is given of the measured steering wheel torques during a critical obstacle avoidance. Both human torque as well as controller torque were measured during the simulation. Based on these two vectors, it was determined whether the torques were in opposing direction and thus whether conflicts were present. In the figure it can be seen that there is a number of times for which conflicts occur.

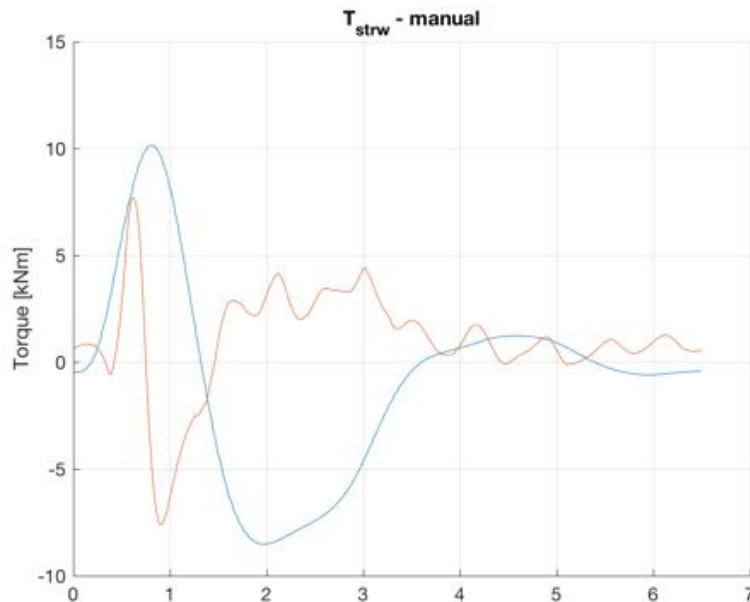


Figure 17: Example of measured steering wheel torques for a critical manoeuvre. Controller torque in blue, human torque in orange.

Subsequently, a script was written detecting the occurrence of conflicts and determining the absolute conflicting torque during the manoeuvre. The data of the conflicting torque (yellow) was used to determine the conflicting rotational work, mean conflict peak torque (maximum value) and the mean percentage of time in conflict. The latter value was determined by summing the time of conflict by the total time of the obstacle avoidance.

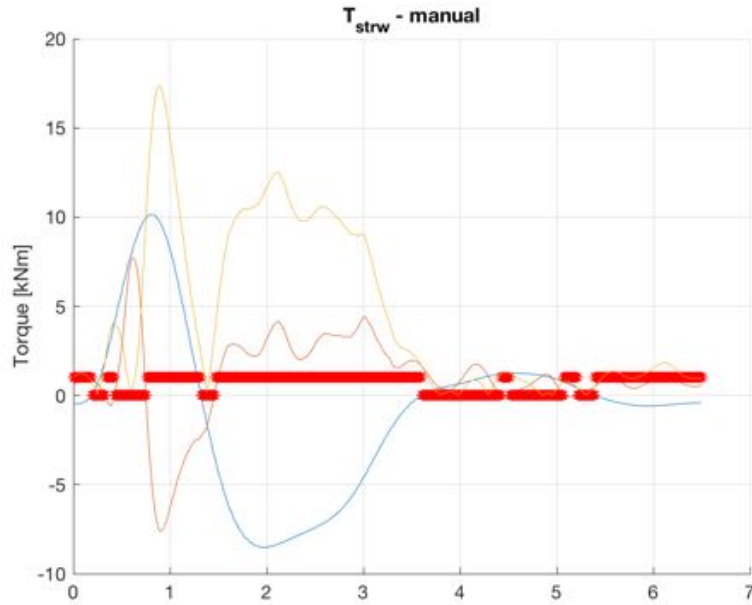


Figure 18: Example of conflict detection (red) and conflicting torque (yellow).

Lastly the profile of the calculated conflicting torque was compared to the lateral error of the vehicle with respect to the Human compatible Reference, as depicted in Figure 19. The figure shows the standard deviation of all participants in terms of trajectory, HCR error and absolute conflicting torque for both critical and non-critical sections, for HSC and Combi. The largest conflicts were present for critical obstacles, showing visible correlation between HCR error and conflicting torque.

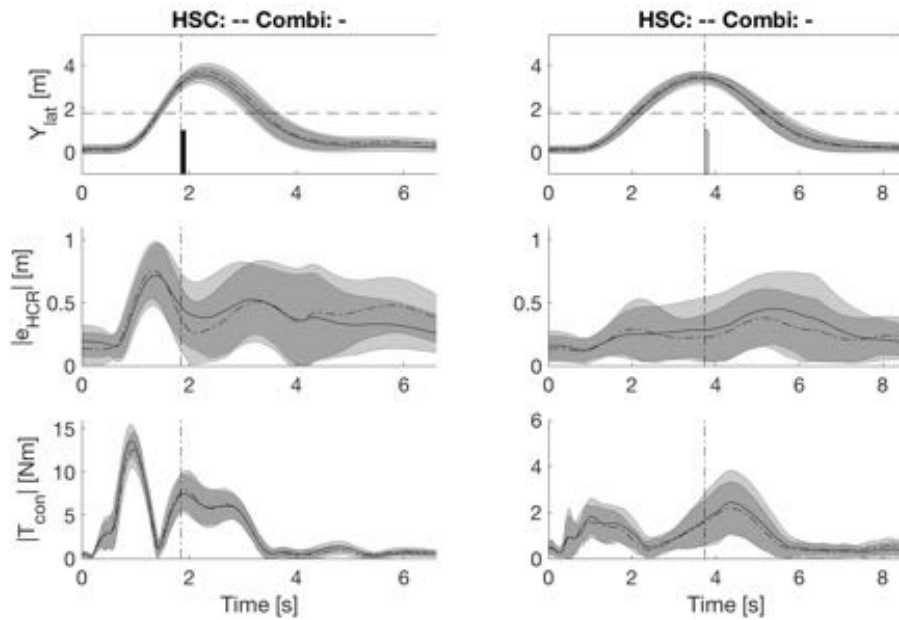


Figure 19: Error bars showing standard deviation of all participants for HSC and Combi during critical and non-critical obstacles.

## G Experimental Results

In this appendix an overview is given of the data obtained for the obstacle avoidance manoeuvres, including a description of the presented figures. The data is subdivided between pilot study and experimental study.

### Pilot Study

In Figure 20 the trajectories driven during the pilot study are depicted for all conditions. For each condition, 5 critical and 5 non critical obstacles were present, resulting in a similar number of trajectories. The trajectories were obtained by selecting parts of the vehicle trajectory corresponding to obstacle avoidance. The moment of obstacle appearance was chosen as the origin for all time traces, see horizontal axis Figure 20. For the HSC and Combi condition, an orange and green line is depicted, indicating the Human Compatible Reference.

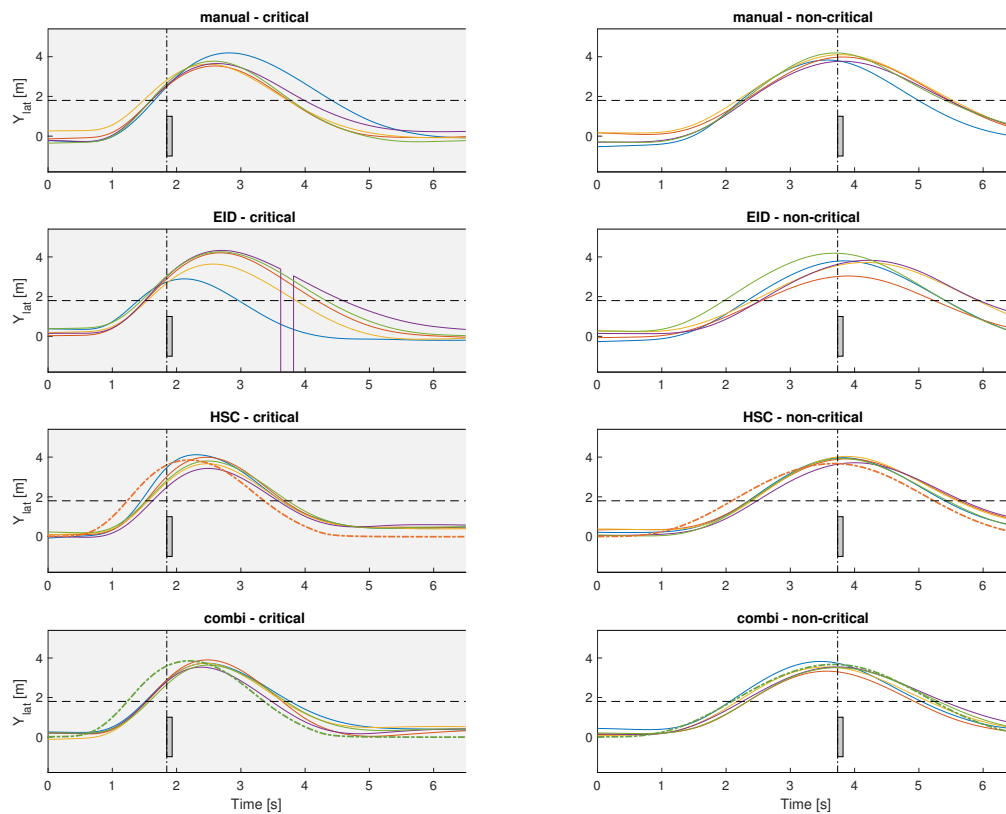


Figure 20: Driven trajectories during the experiment, for both critical (left) and non-critical (right) obstacles. Obstacle is indicated by the grey rectangle. The TTC of the obstacle is depicted by the dashed line.

The pilot results show visible differences between the conditions, with for example an increase of intra-subject variability between Manual-EID. The trajectories are used to determine several dependent measures to describe task execution. The only difference between the pilot study and the final experiments is the optimization of the timing of the Haptic Shared Controller, see Appendix B.

During the pilot, steering wheel torques were measured applied by either (1) the human operator or (2) the Haptic Shared Controller. In Figure 21 all measured torques during obstacle avoidance are shown per condition, for critical tasks only. A decrease of human torque was seen for HSC and Combi, indicating that the controller was able to reduce the required human input. Furthermore, the graphs of the controller torque (middle) show the characteristic torque that was applied during critical obstacle avoidance. On the right side a summation of the torques is presented, showing the combined torque of human and machine.

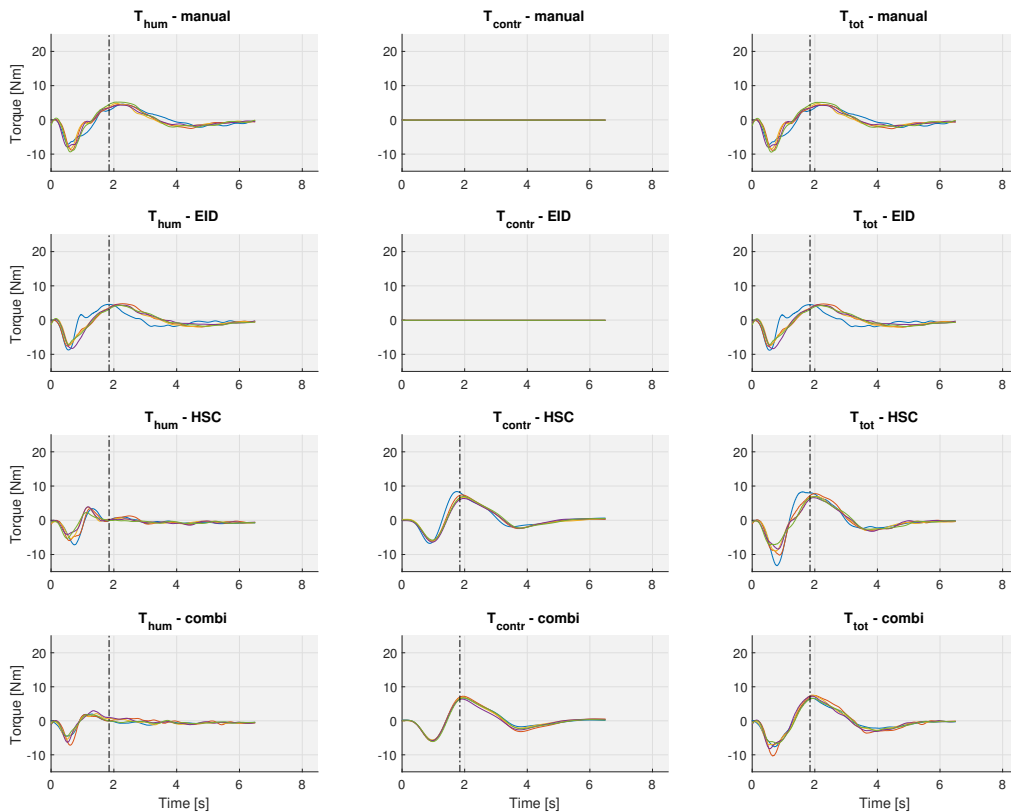


Figure 21: Measured torques during the experiment, for critical obstacles. Human torque on the left, controller torque in the middle and summation of torques on the right. The TTC of the obstacle is depicted by the dashed line.

Similar plots were generated for the non-critical obstacles, see Figure 22. Again, note the characteristic torque profile of the controller in the graphs depicted in the middle. It can be seen that the required torque for non-critical obstacles is severely lower, but more spread out than the critical obstacles.

One of the resulting dependent measures *mean lateral obstacle margin*, is shown in Figure 23. Already during the pilot, the characteristic behavior of reduced lateral obstacle margin was visible, indicating a noticeable effect of the implemented visuals for non-critical tasks. The results for non-critical tasks were still inconclusive.

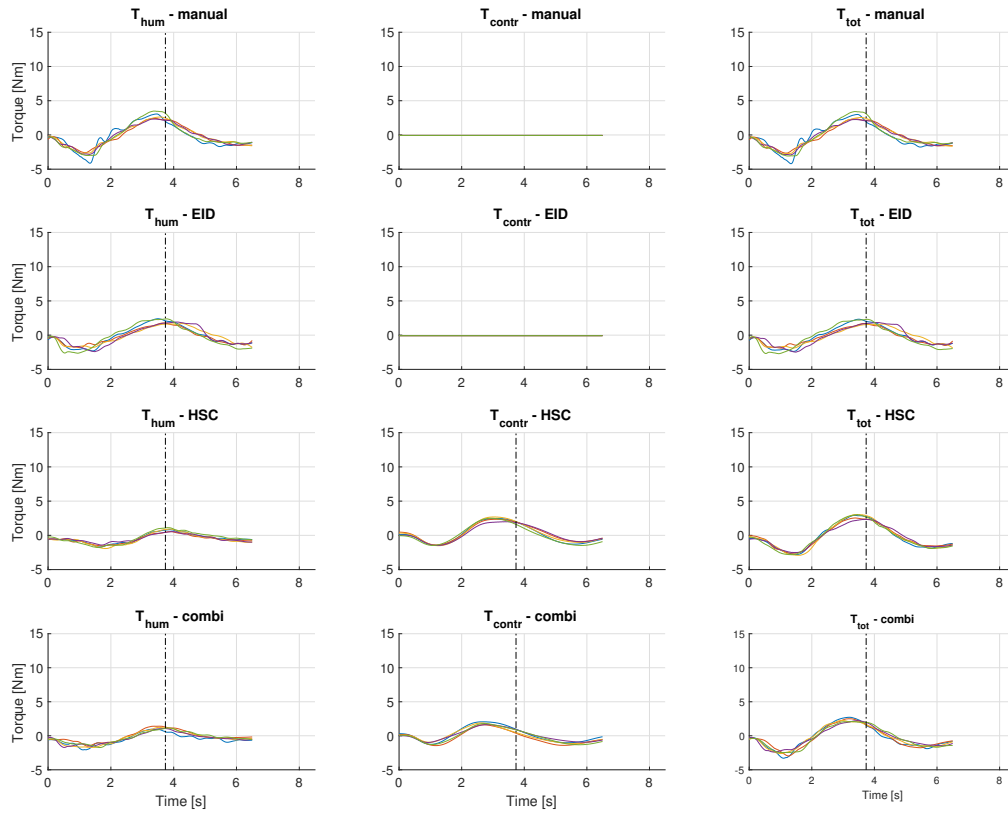


Figure 22: Measured torques during the experiment, for non-critical obstacles. Human torque on the left, controller torque in the middle and summation of torques on the right. The TTC of the obstacle is depicted by the dashed line.

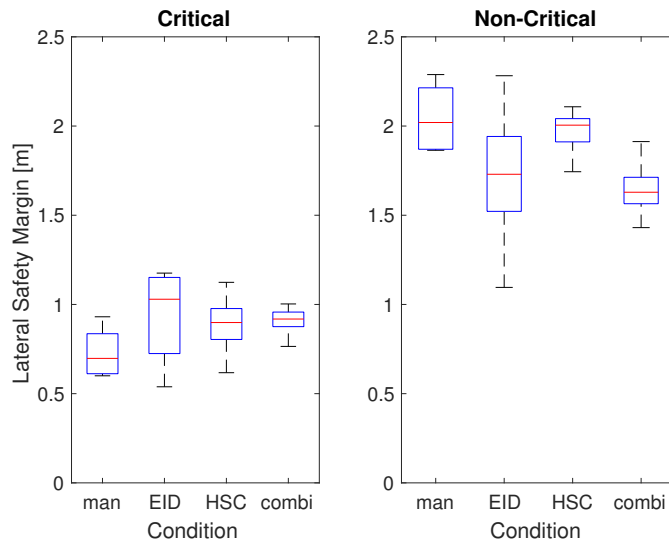


Figure 23: Box-plots of intra-subject variability of mean lateral obstacle margin (here called safety margin) during the pilot study.

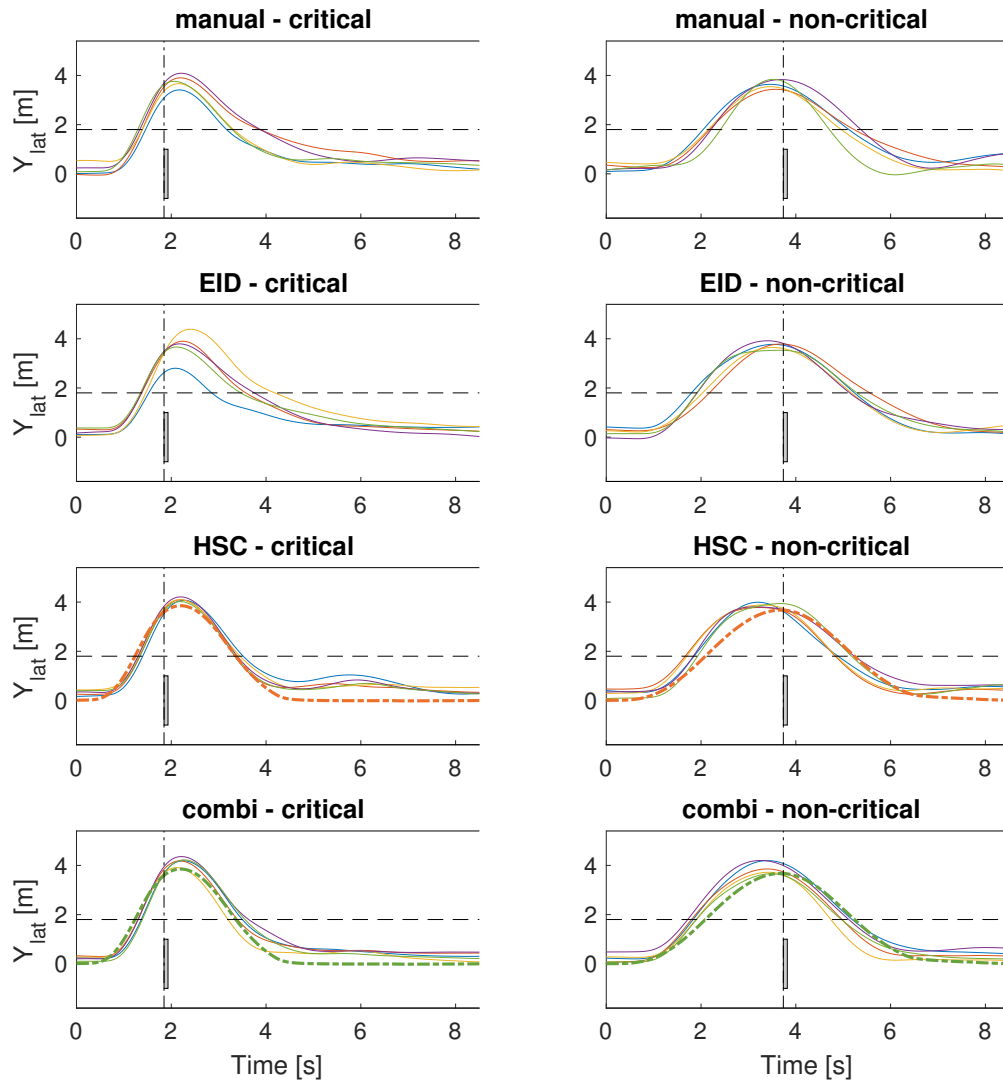


## Experimental Study

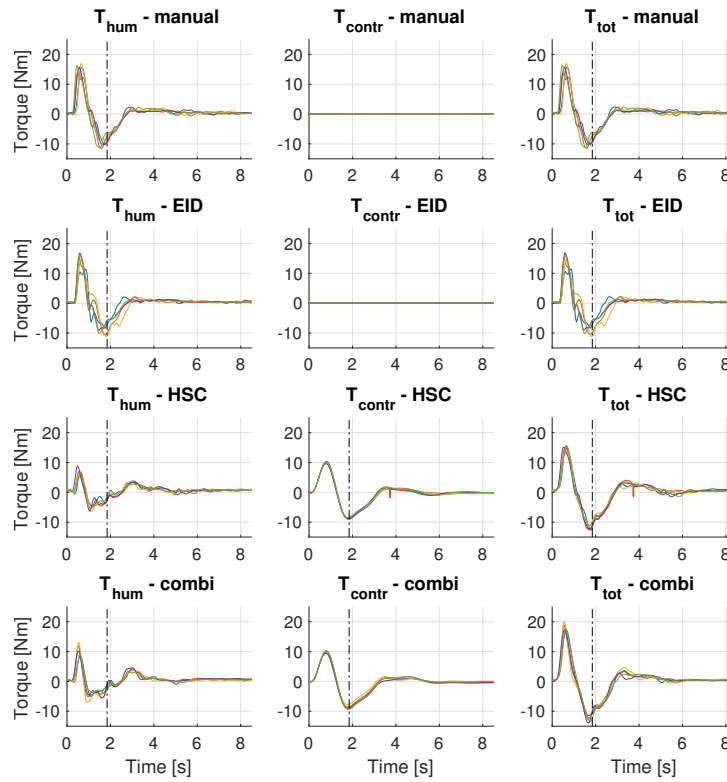
In this section the raw data of all participants is shown for the obstacle avoidance sections. A more detailed explanation of the graphs can be found in the previous section about the pilot study results. In general, three figures are presented per participant: (1) trajectories, (2) steering wheel torques - critical and (3) steering wheel torques - non-critical.

### P01 - Raw data results

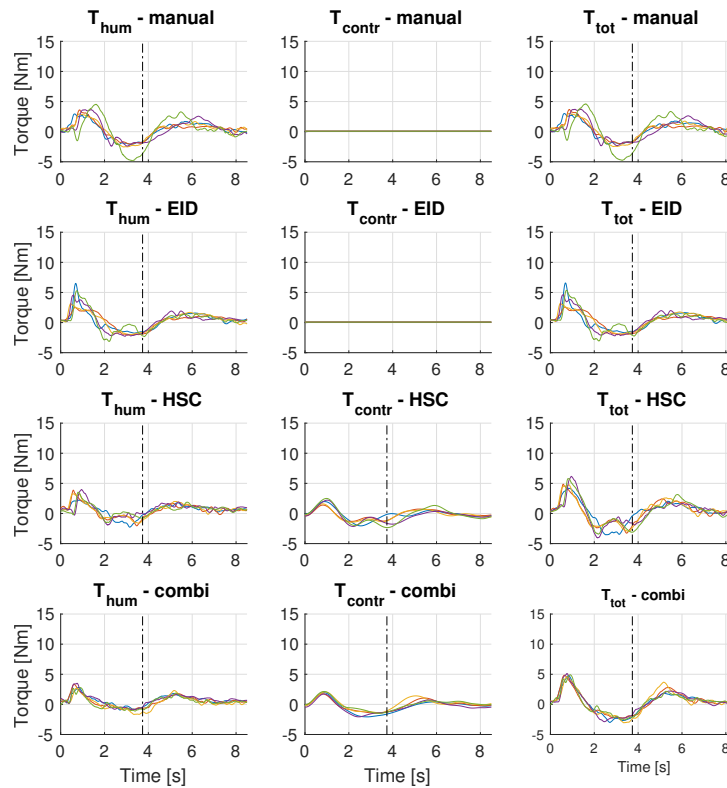
#### Trajectories



## Steering Wheel Torques - Critical

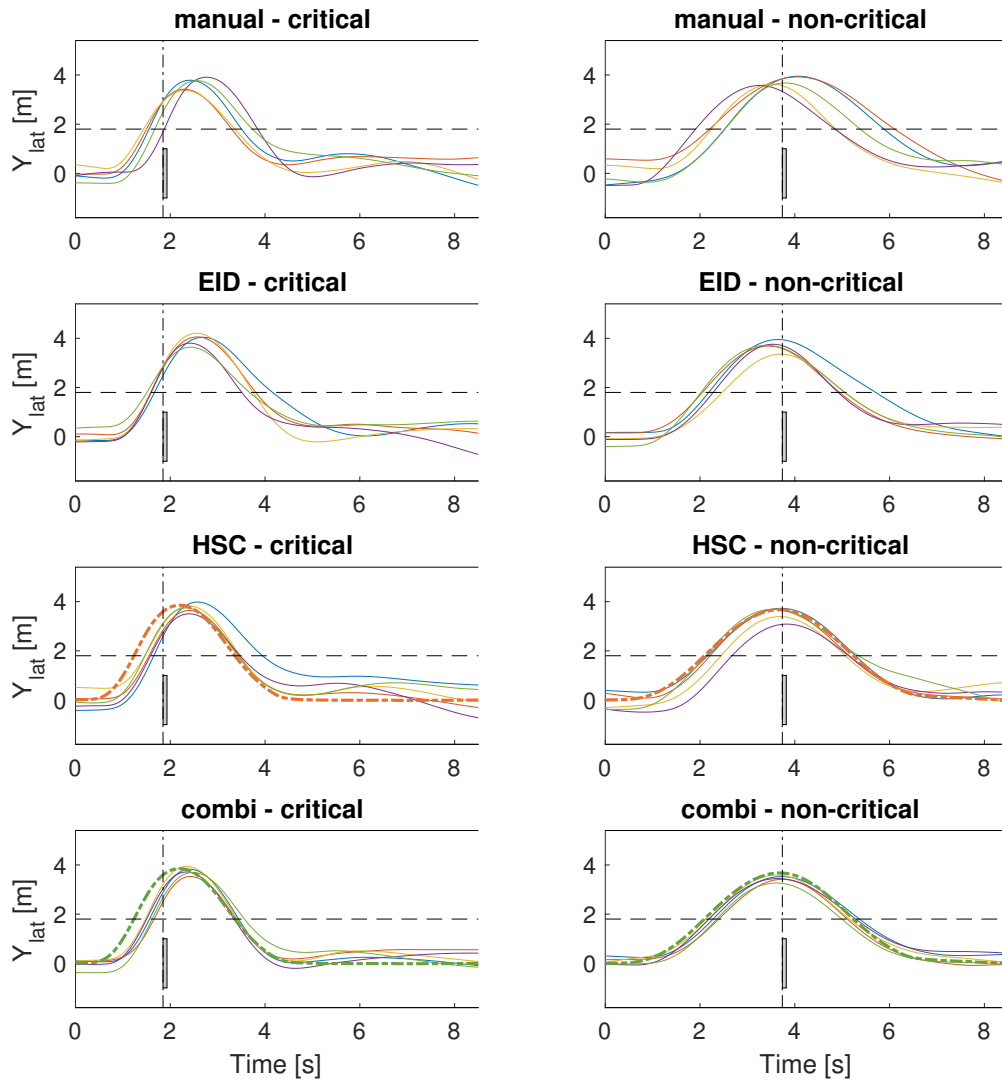


## Steering Wheel Torques - Non-Critical

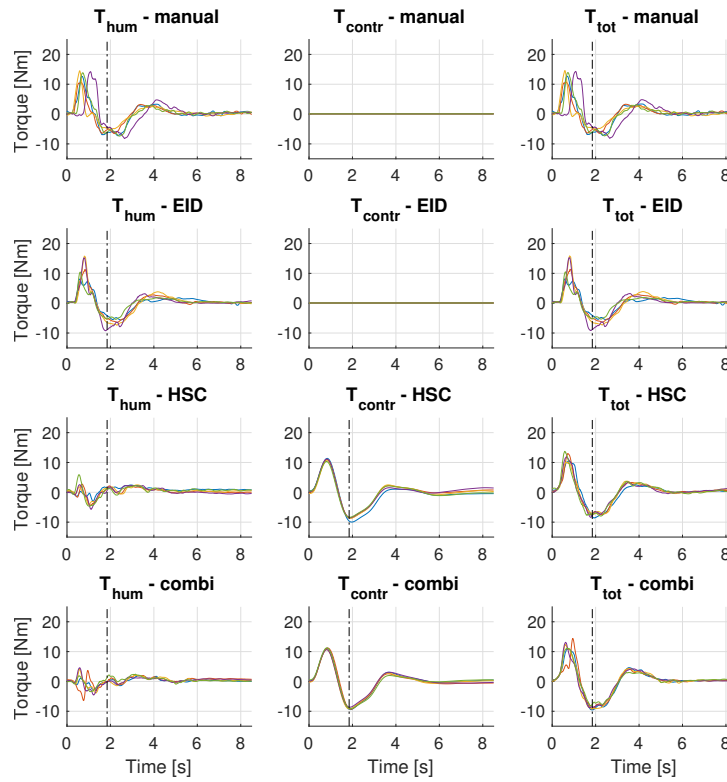


## P02 - Raw data results

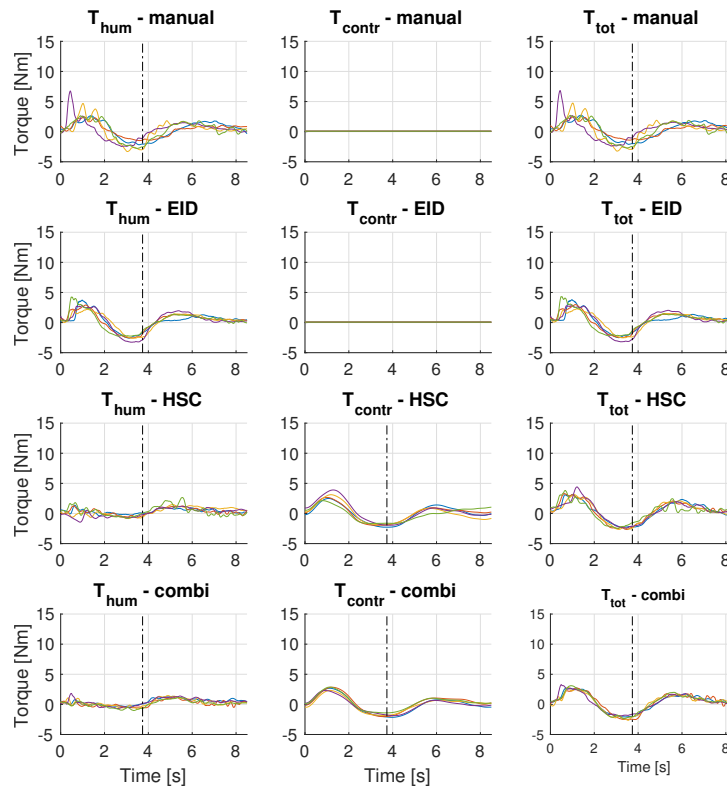
### Trajectories



## Steering Wheel Torques - Critical

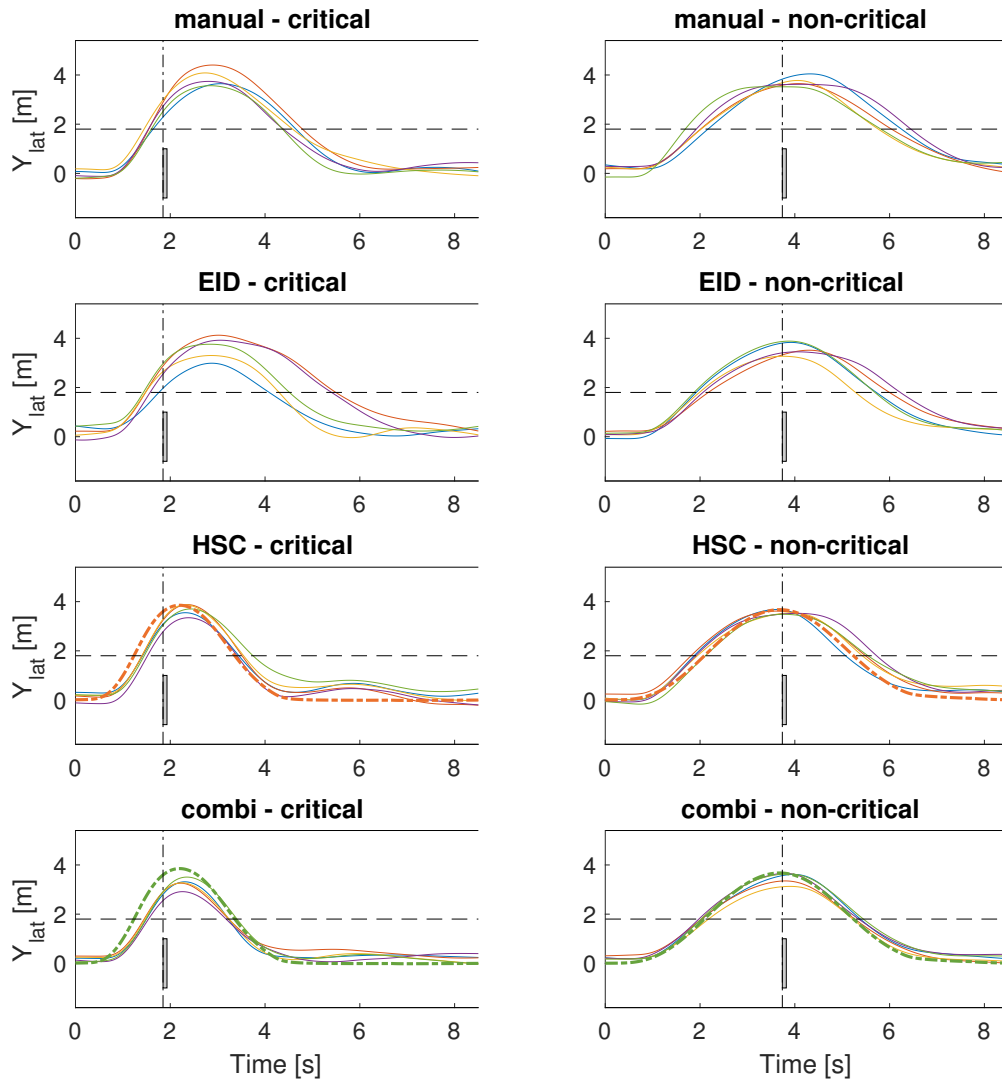


## Steering Wheel Torques - Non-Critical

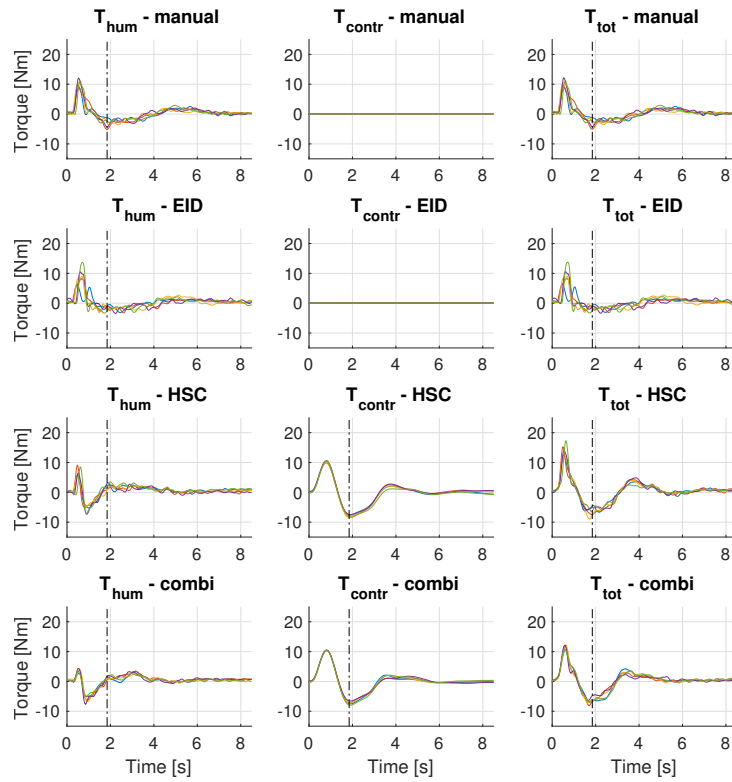


## P03 - Raw data results

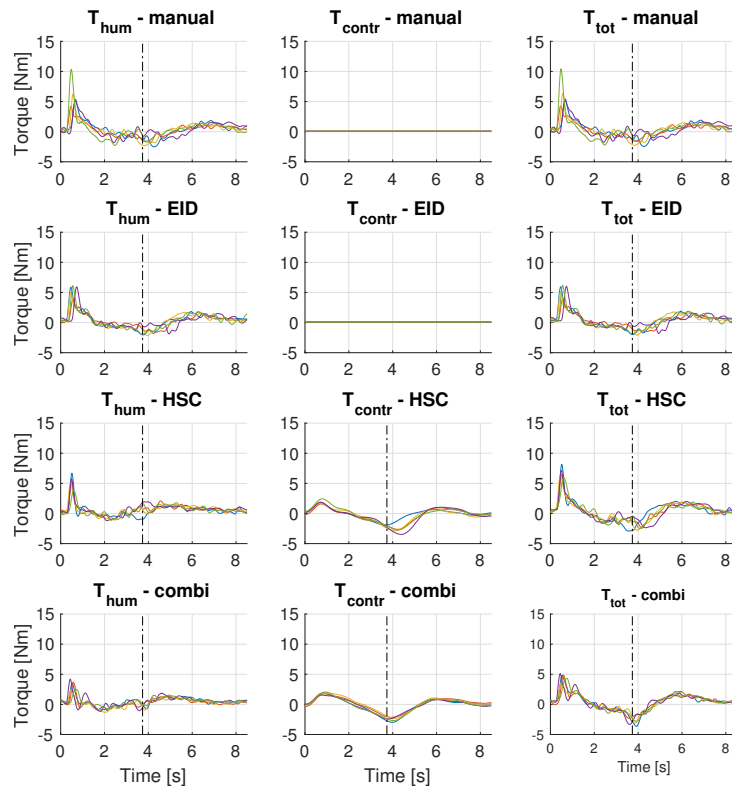
### Trajectories



## Steering Wheel Torques - Critical

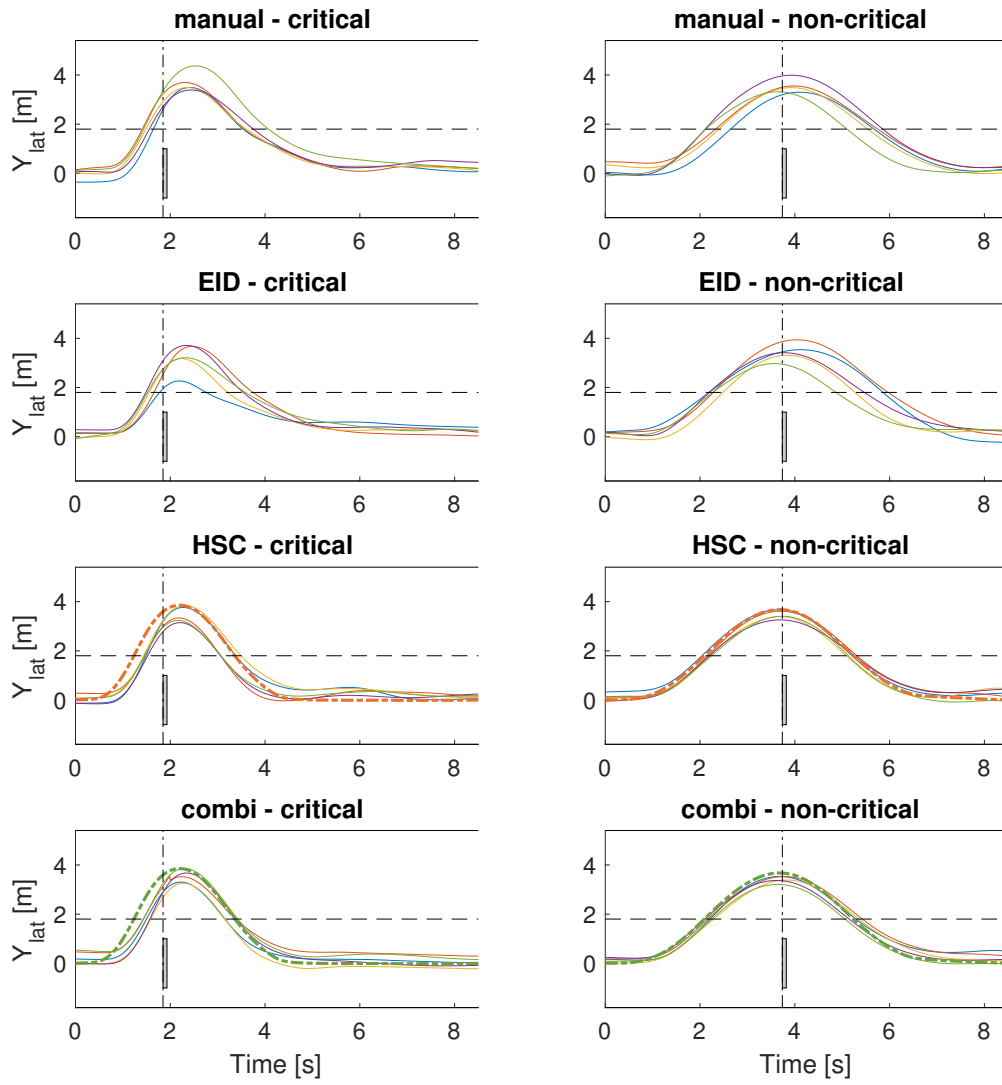


## Steering Wheel Torques - Non-Critical

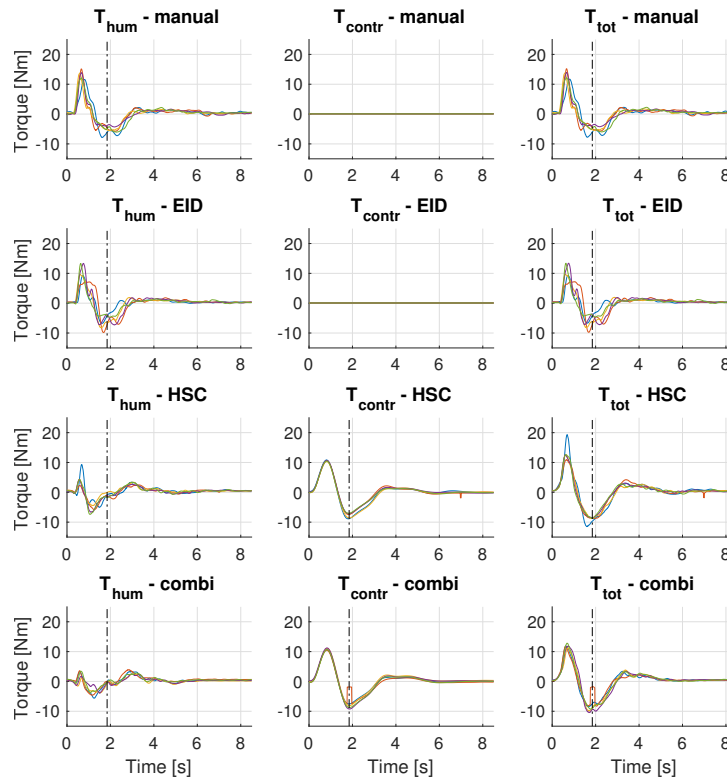


## P04 - Raw data results

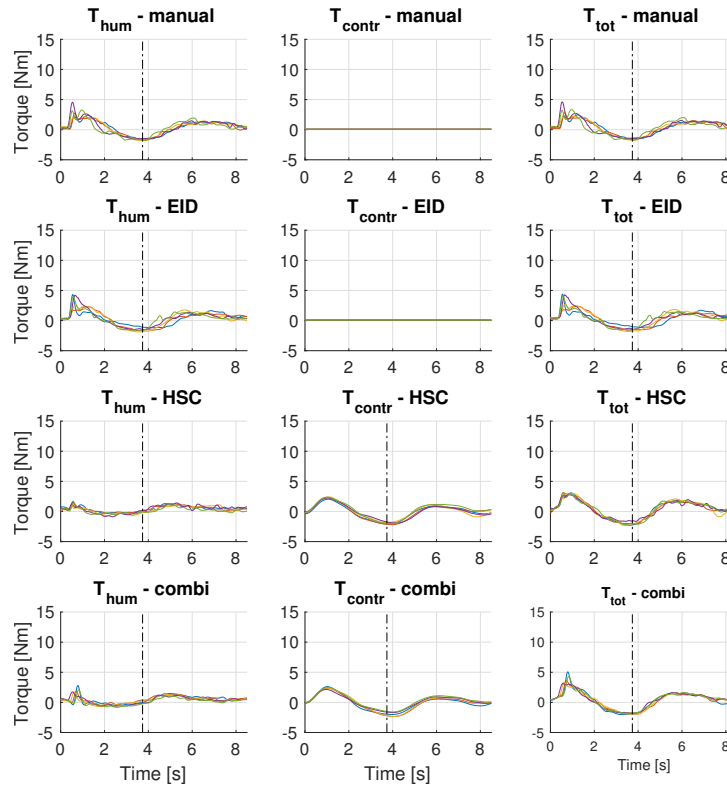
### Trajectories



## Steering Wheel Torques - Critical

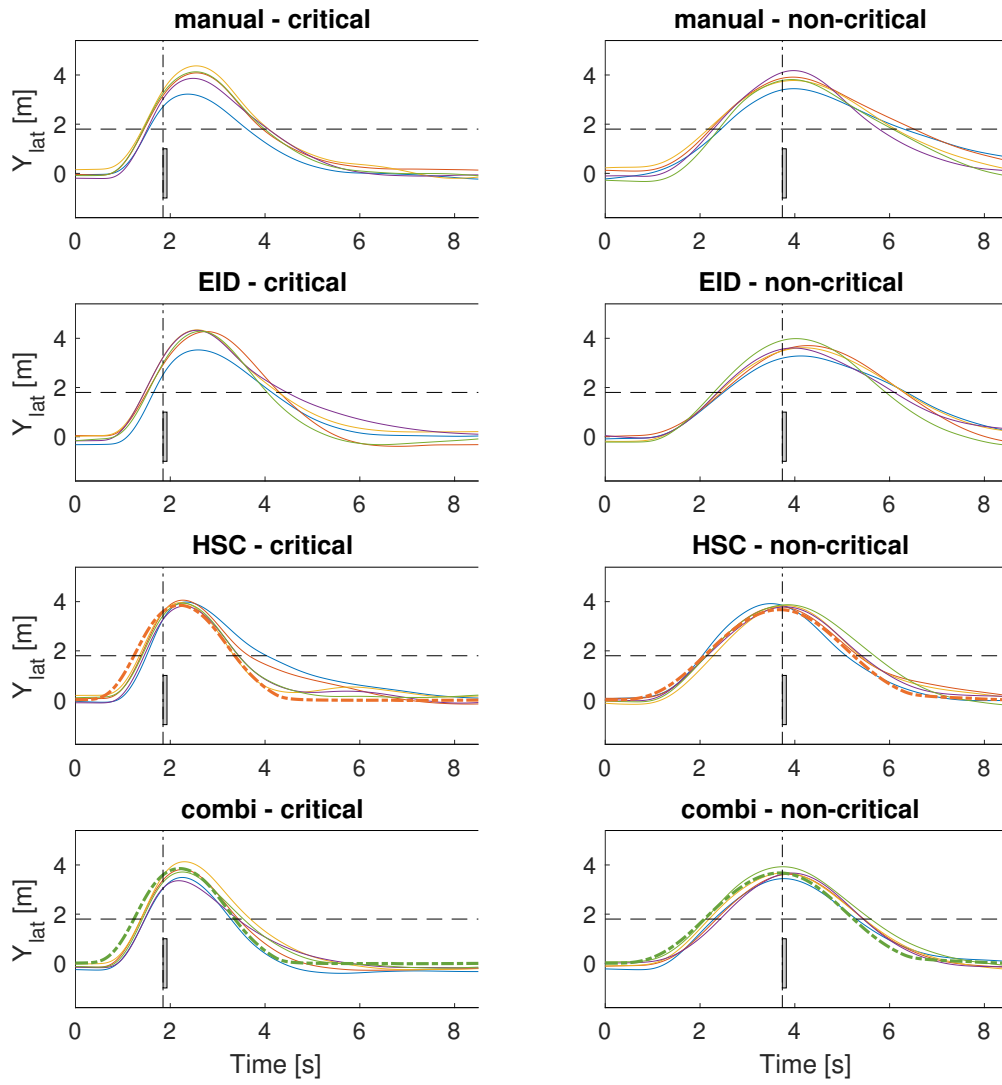


## Steering Wheel Torques - Non-Critical

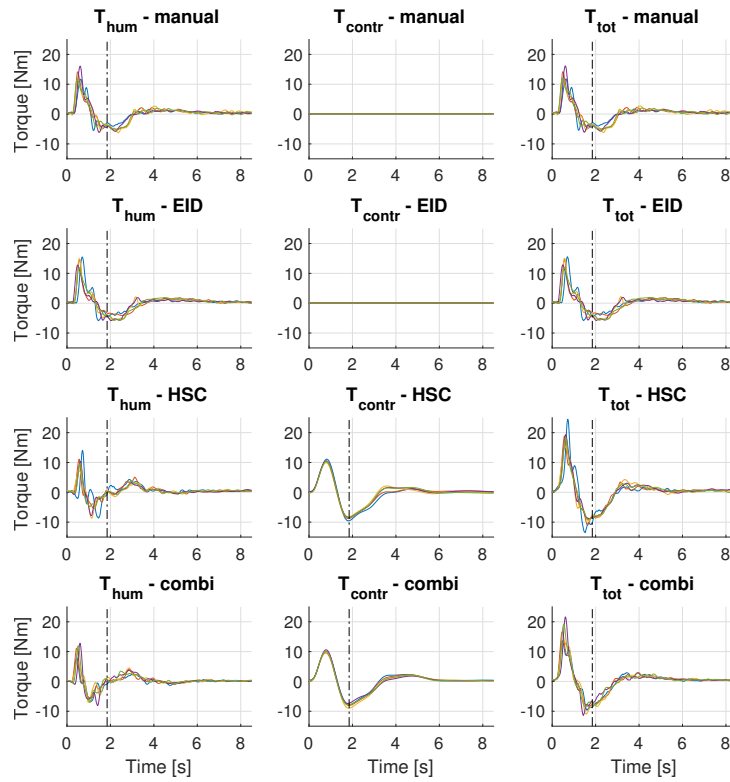


## P05 - Raw data results

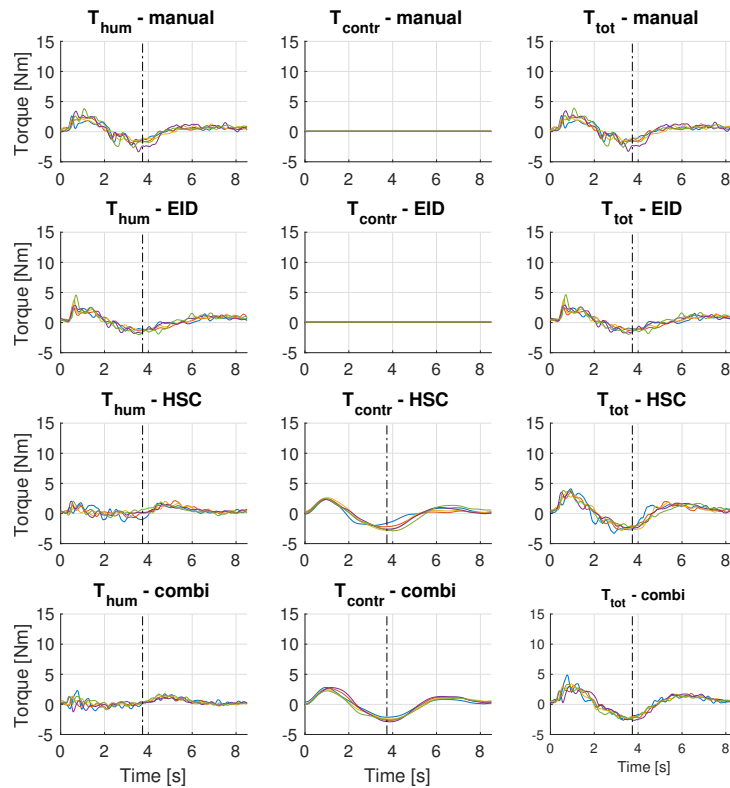
### Trajectories



## Steering Wheel Torques - Critical

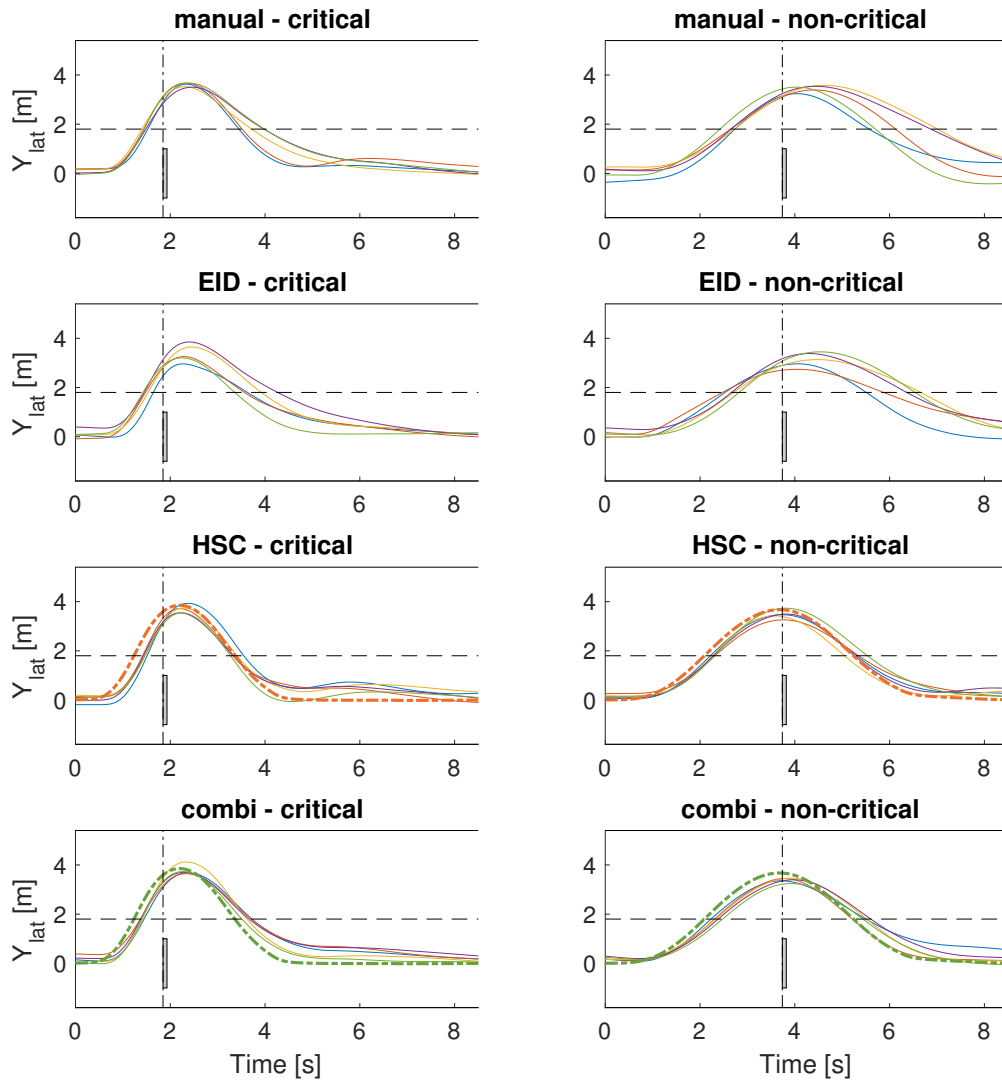


## Steering Wheel Torques - Non-Critical

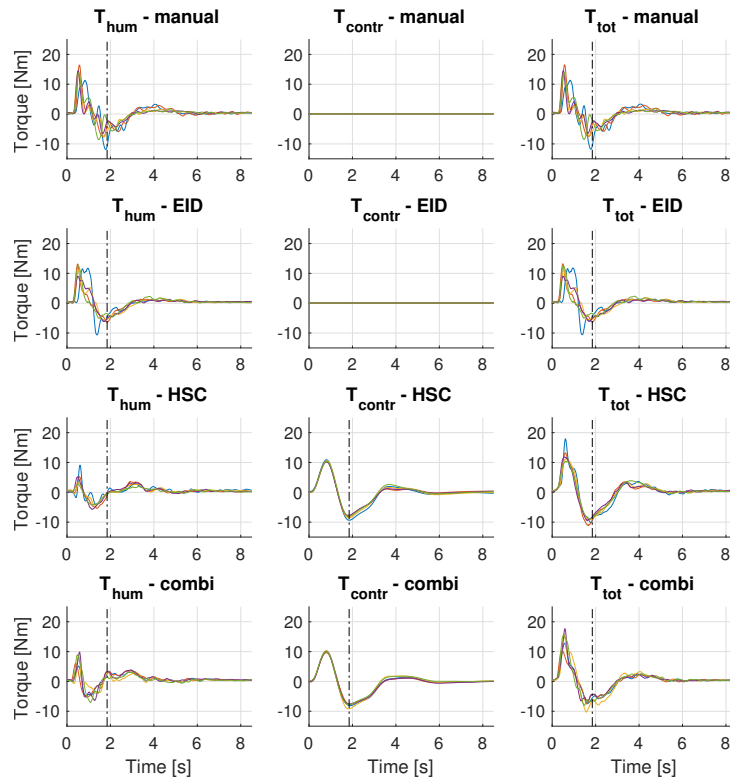


## P06 - Raw data results

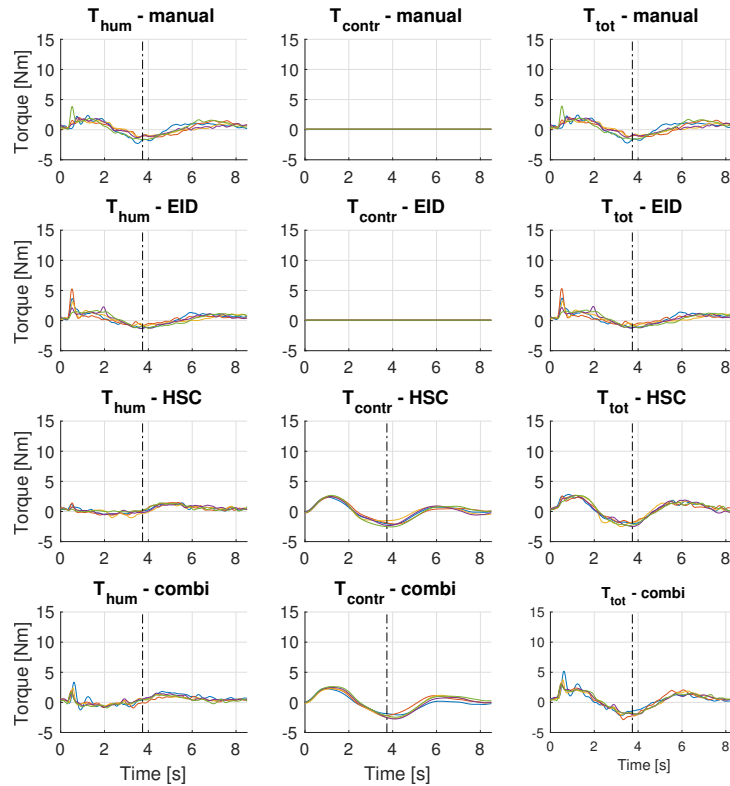
### Trajectories



## Steering Wheel Torques - Critical

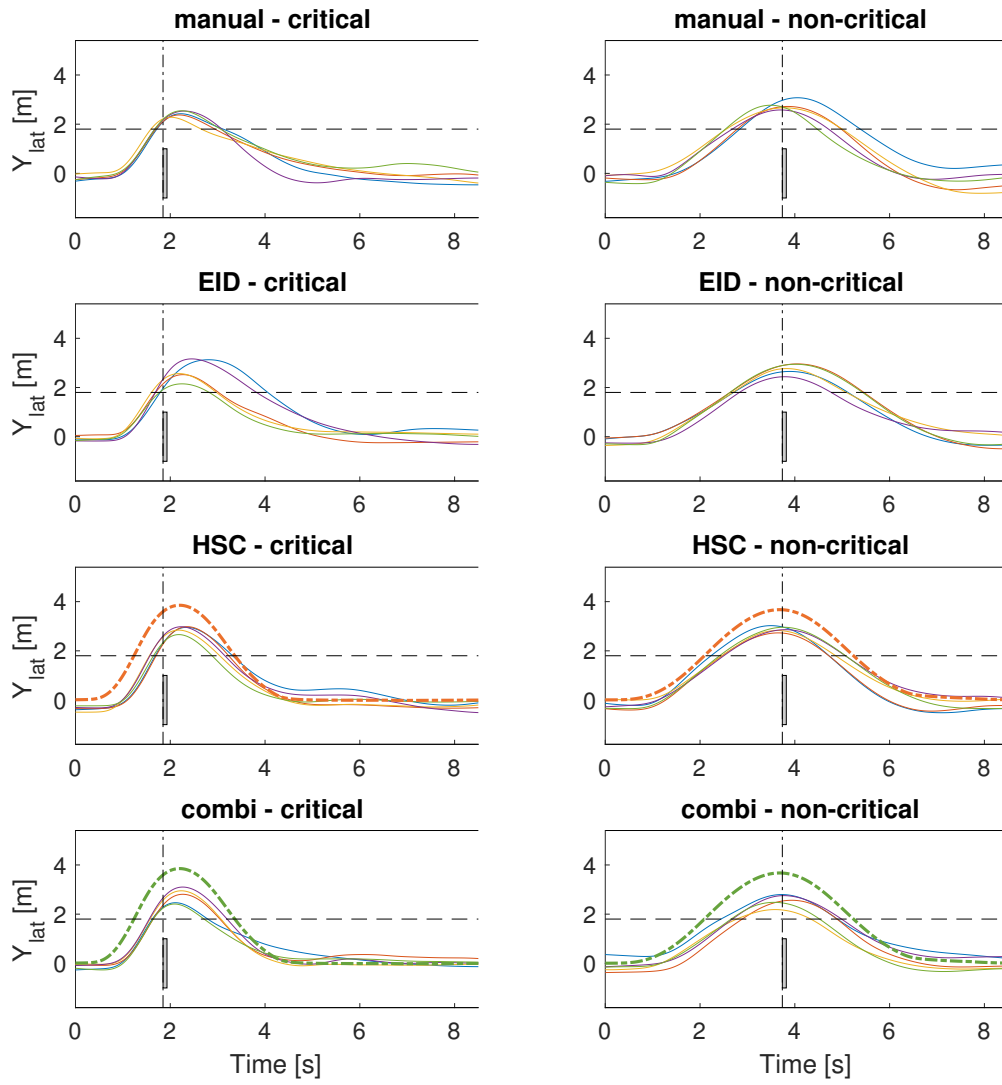


## Steering Wheel Torques - Non-Critical

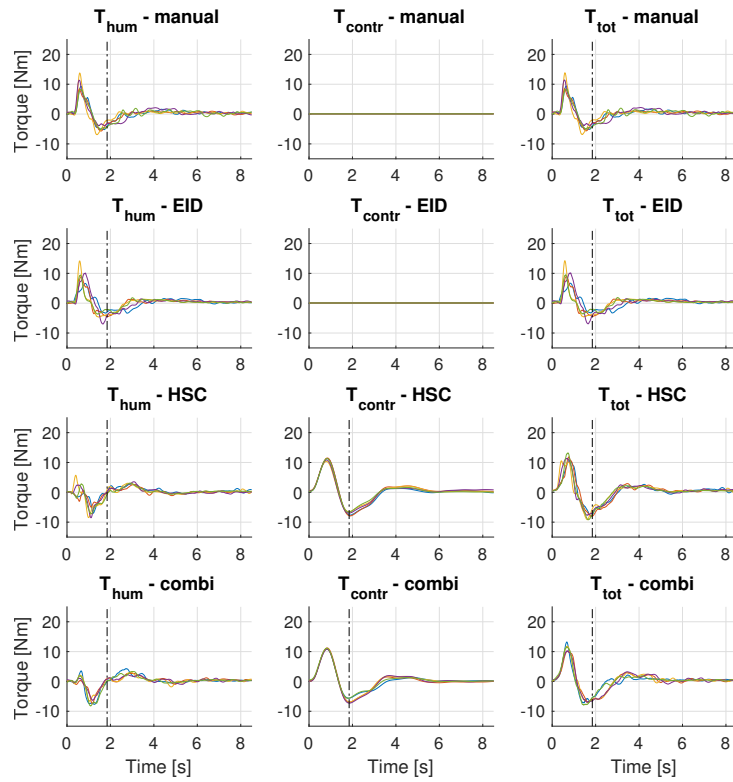


# P07 - Raw data results

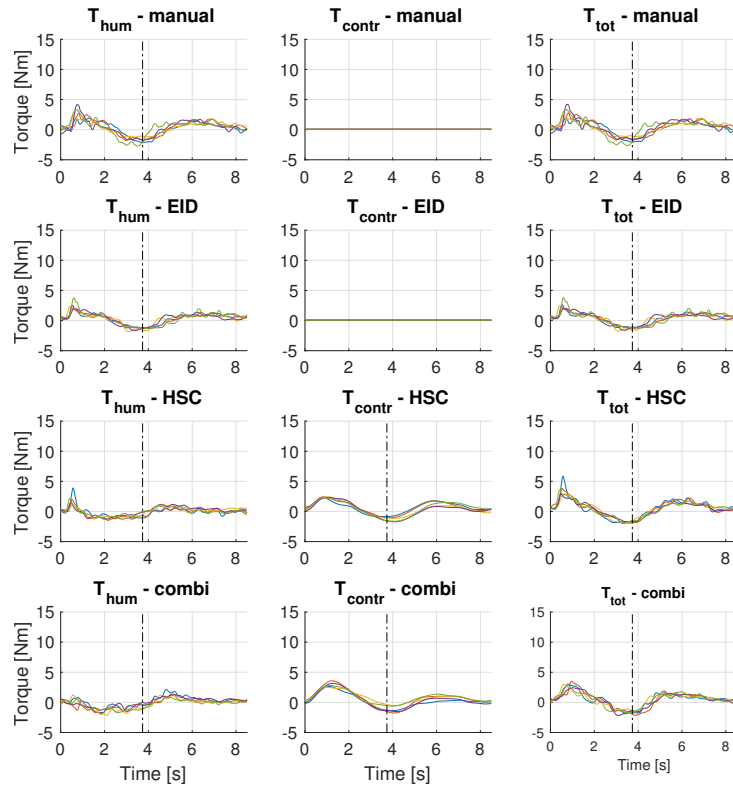
## Trajectories



## Steering Wheel Torques - Critical

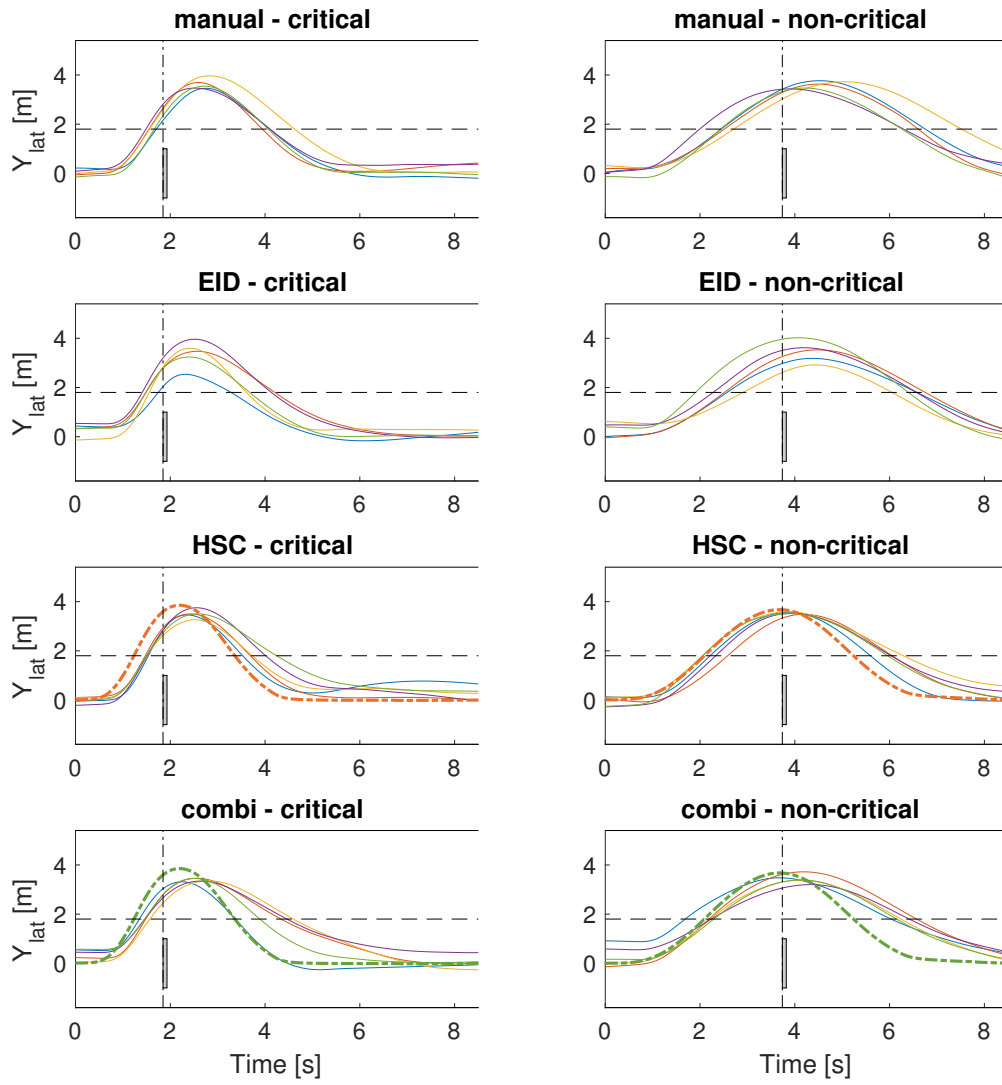


## Steering Wheel Torques - Non-Critical

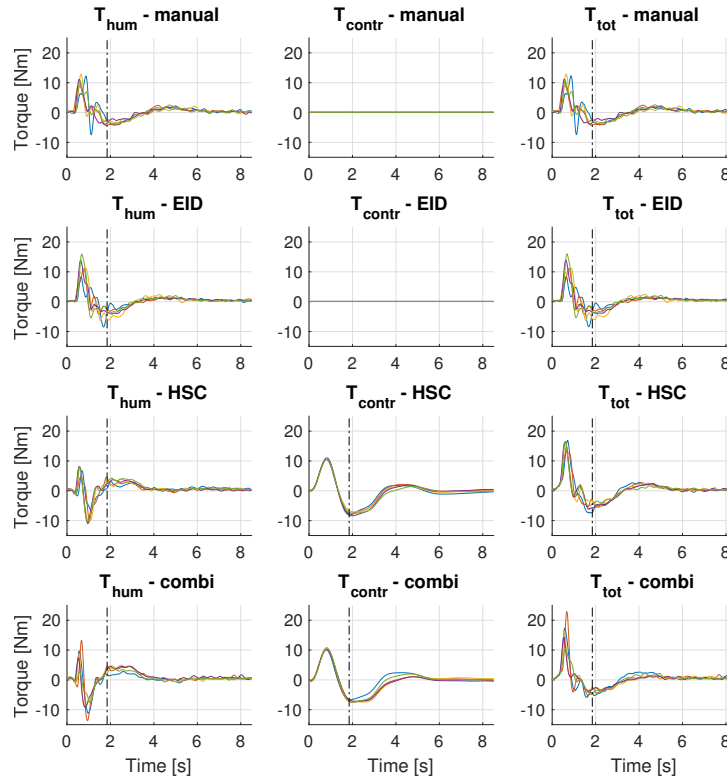


## P08 - Raw data results

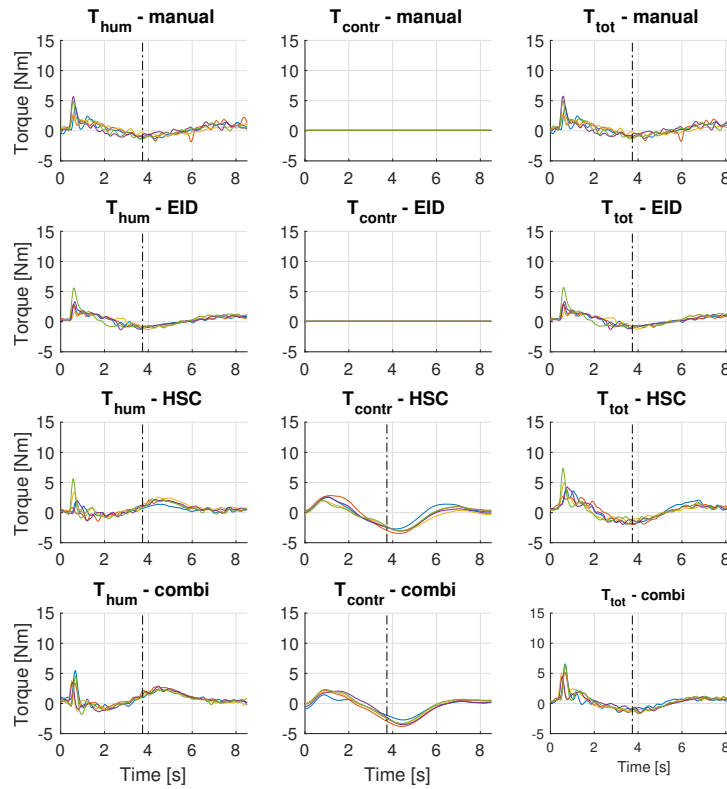
### Trajectories



## Steering Wheel Torques - Critical

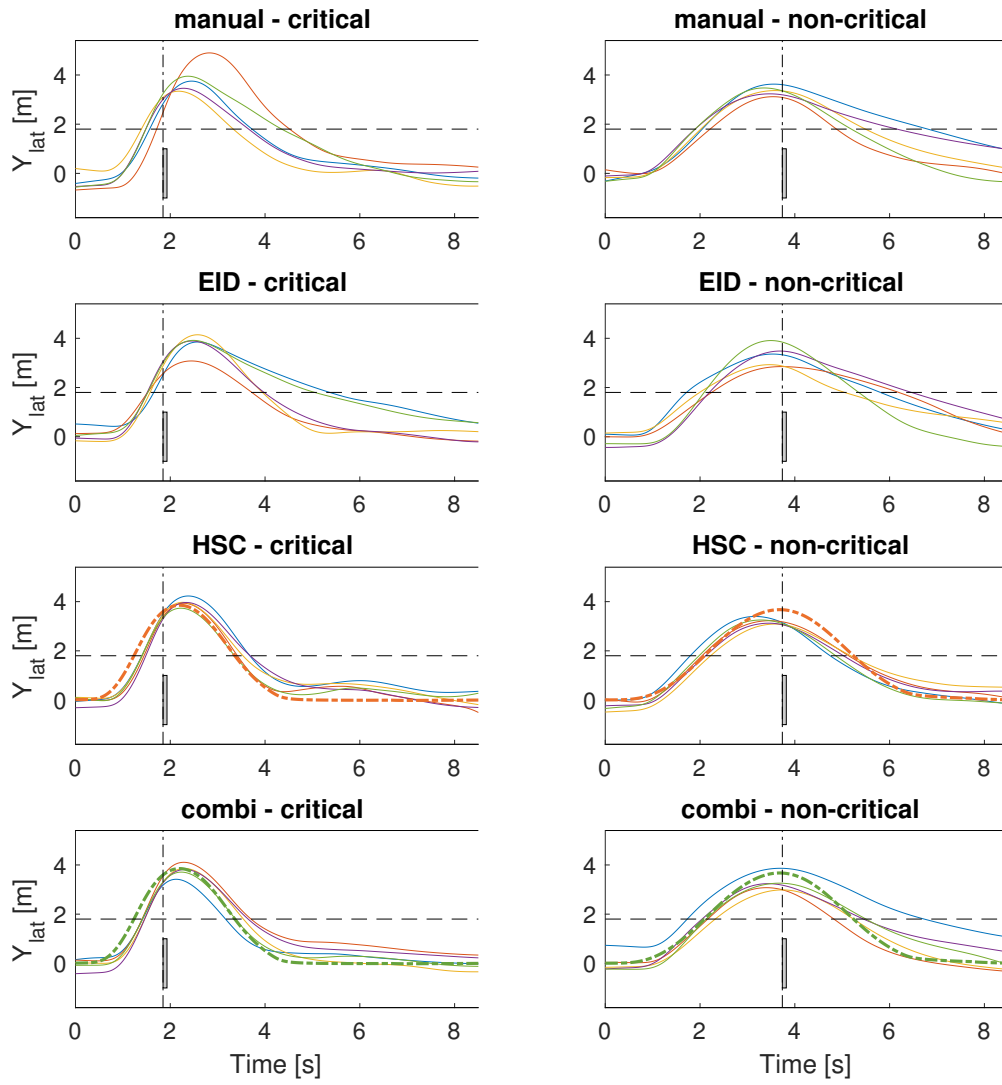


## Steering Wheel Torques - Non-Critical

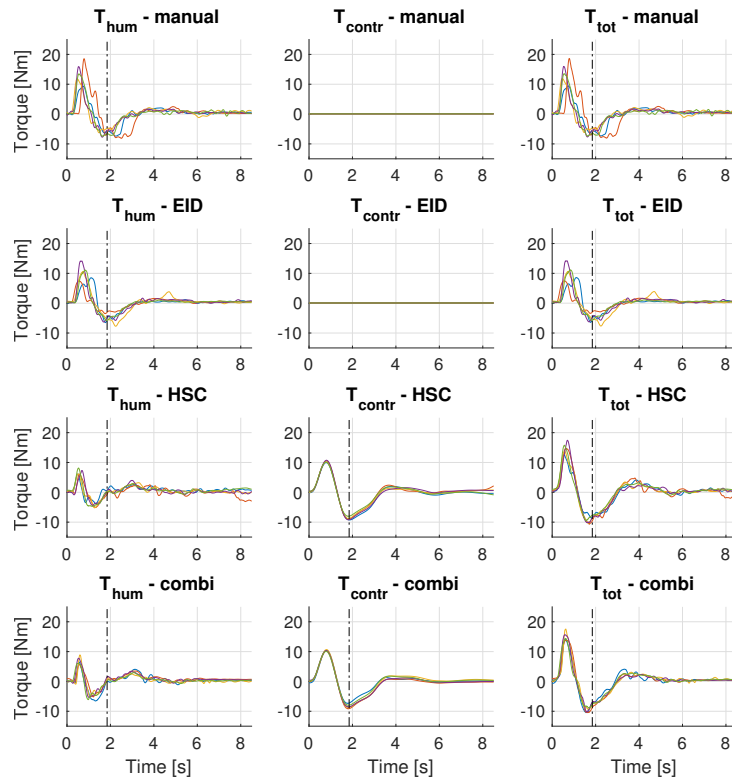


# P09 - Raw data results

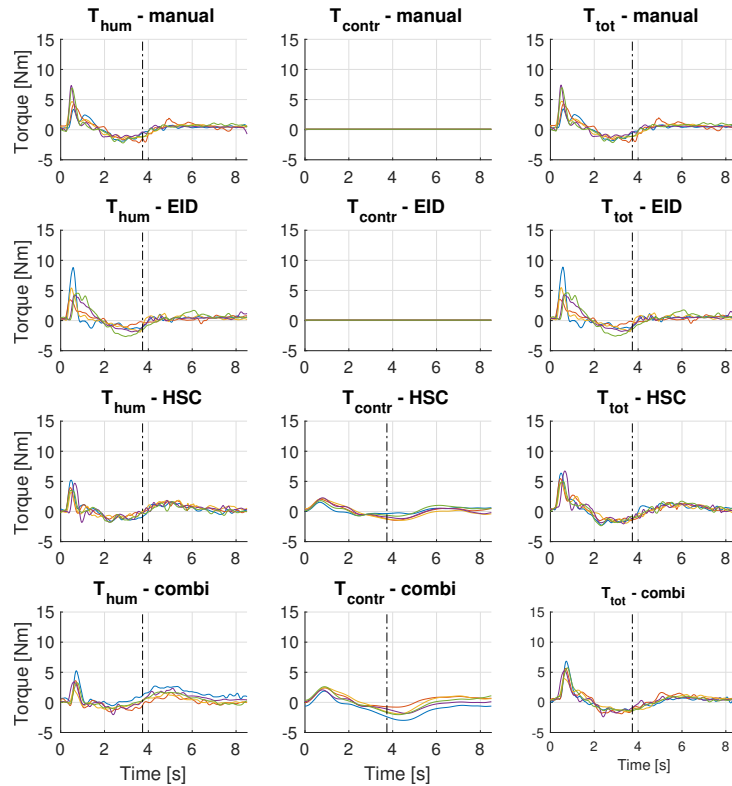
## Trajectories



## Steering Wheel Torques - Critical

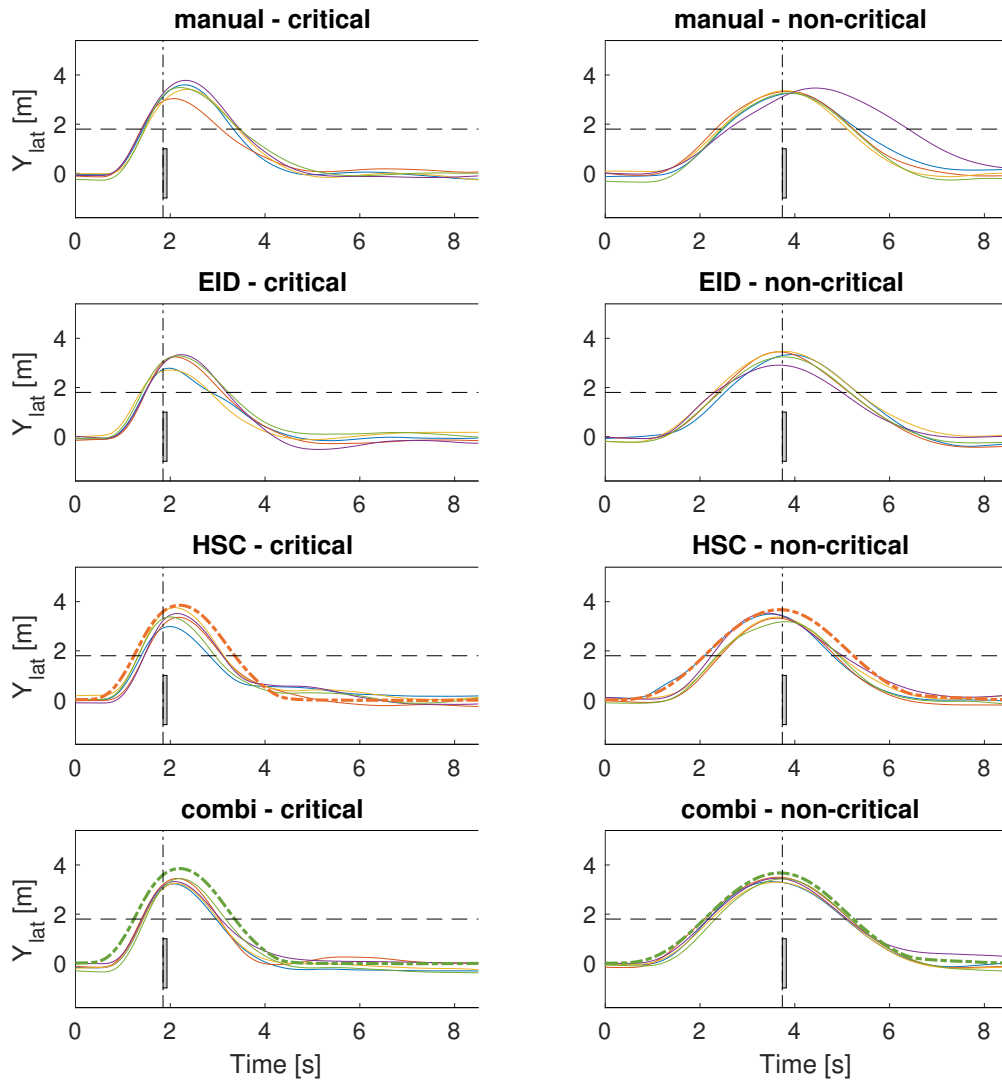


## Steering Wheel Torques - Non-Critical

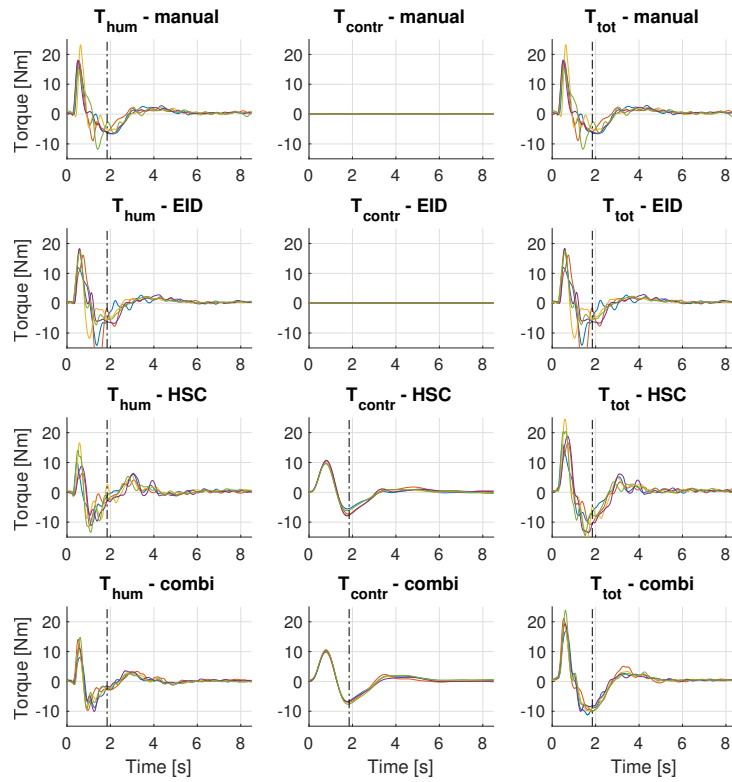


# P10 - Raw data results

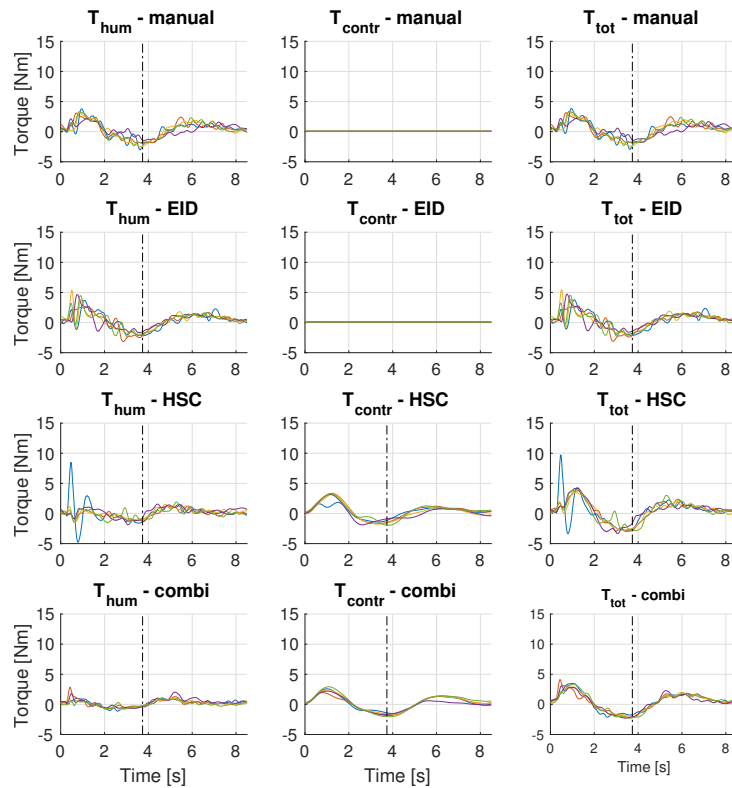
## Trajectories



## Steering Wheel Torques - Critical

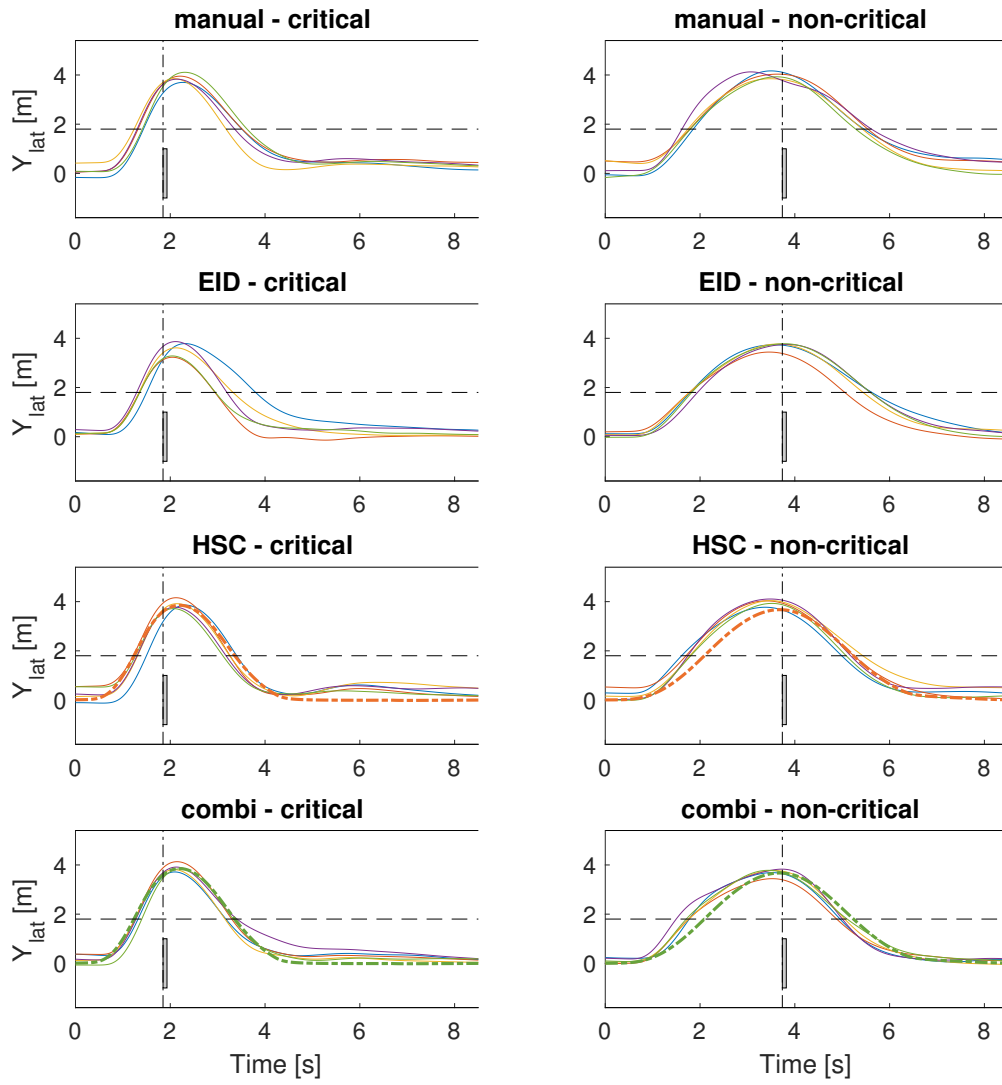


## Steering Wheel Torques - Non-Critical

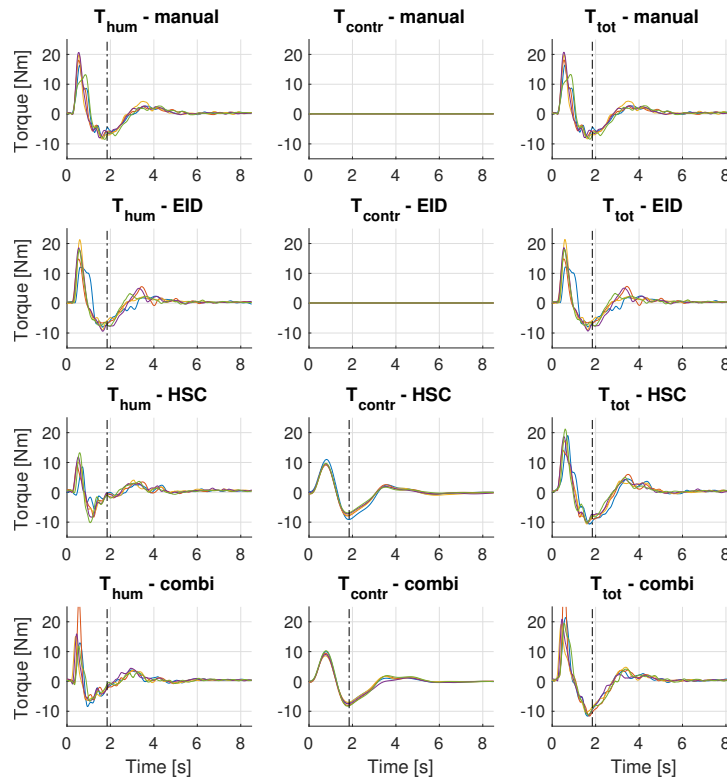


# P11 - Raw data results

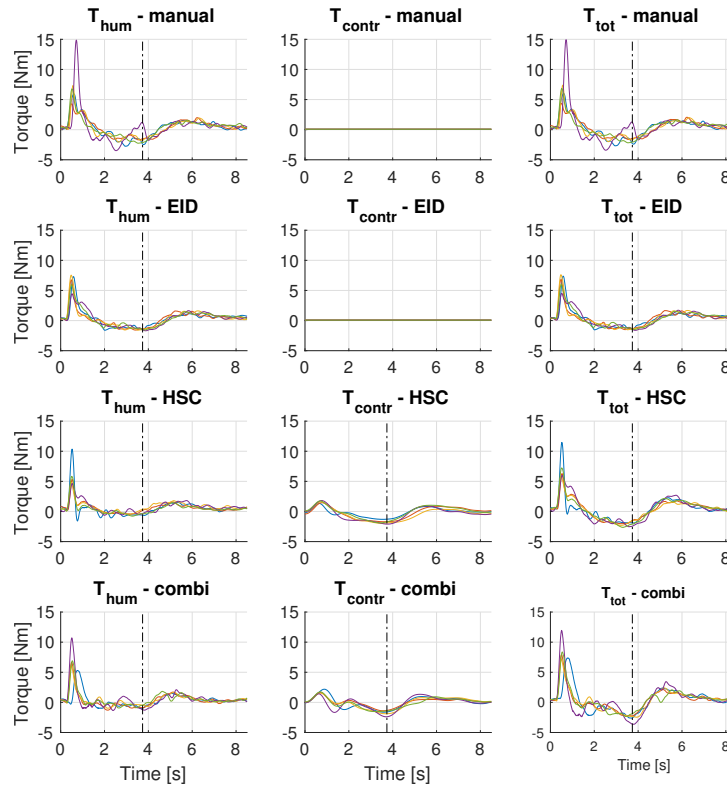
## Trajectories



## Steering Wheel Torques - Critical

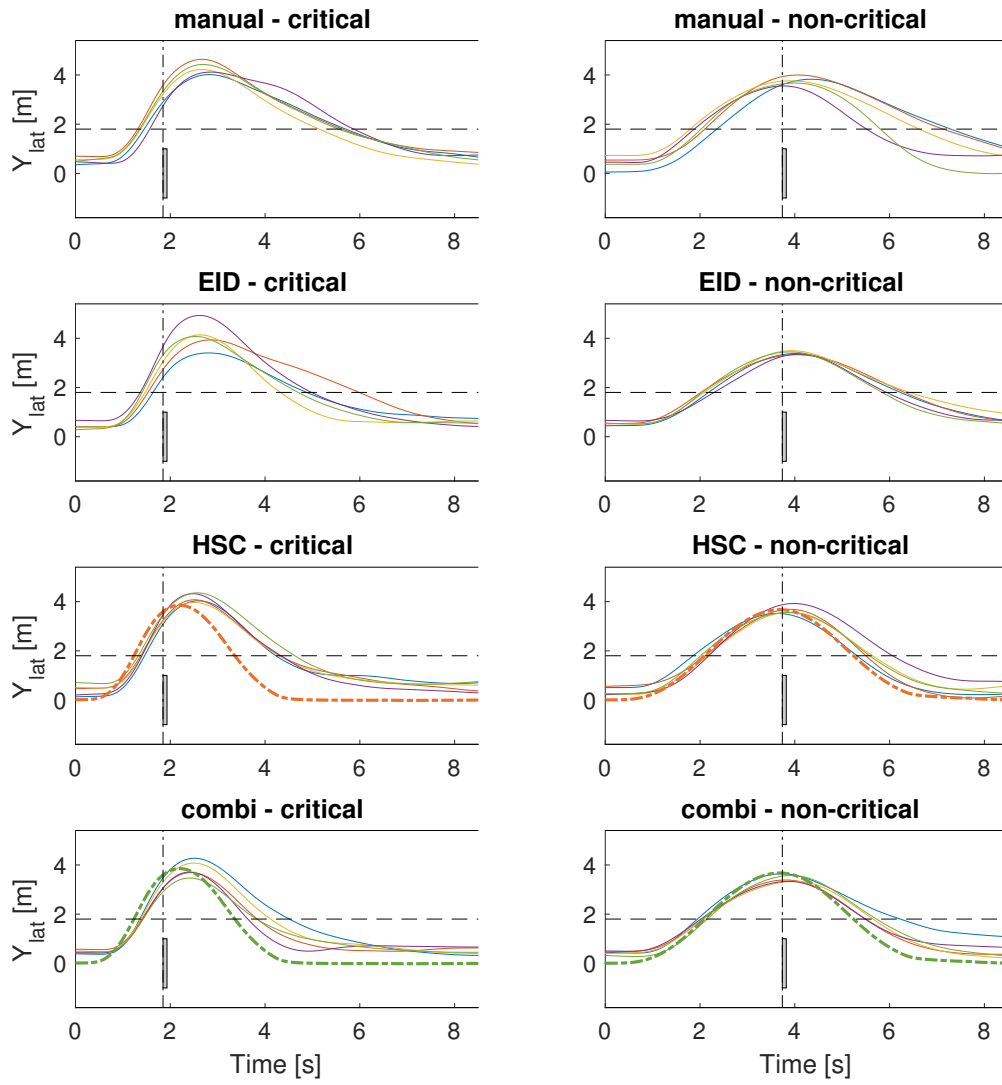


## Steering Wheel Torques - Non-Critical

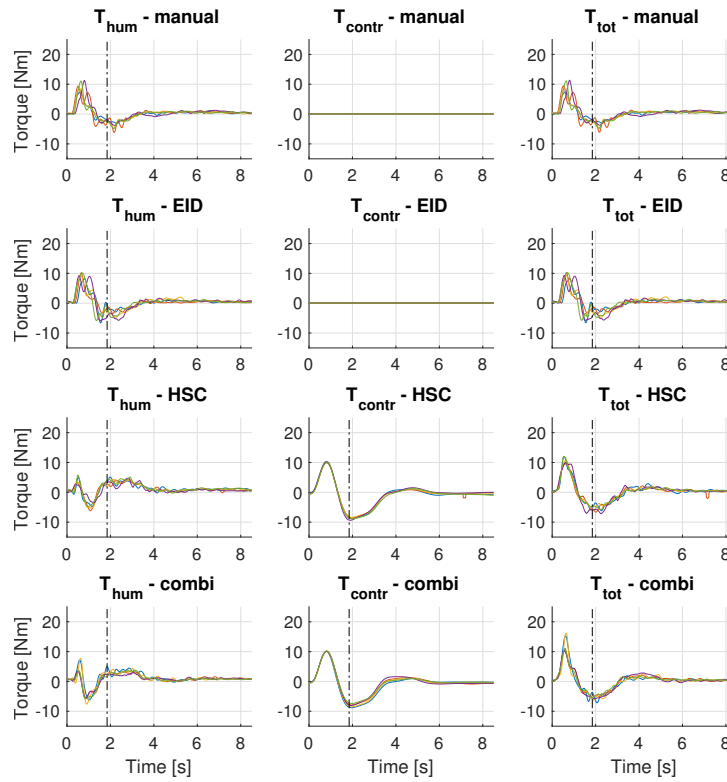


## P12 - Raw data results

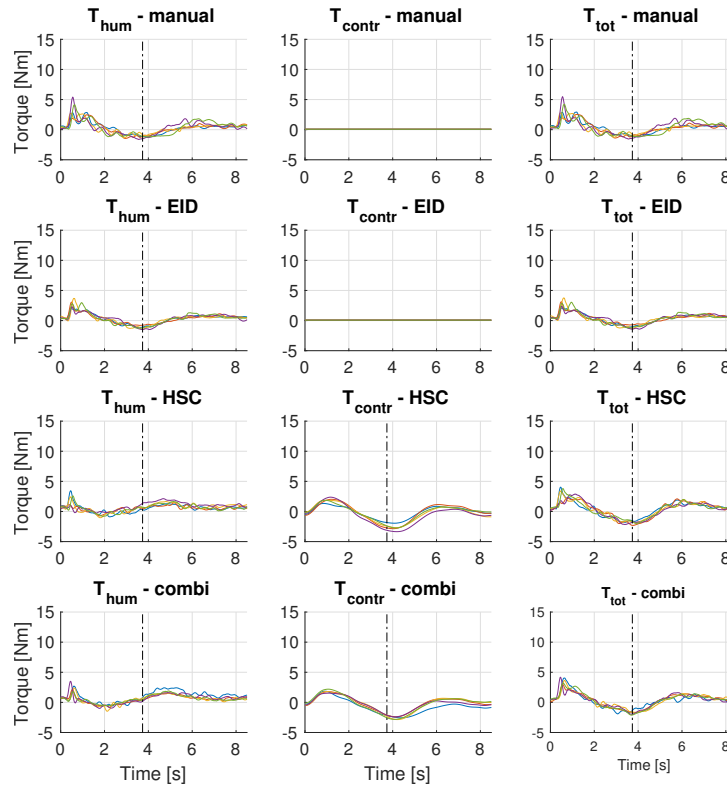
### Trajectories



## Steering Wheel Torques - Critical

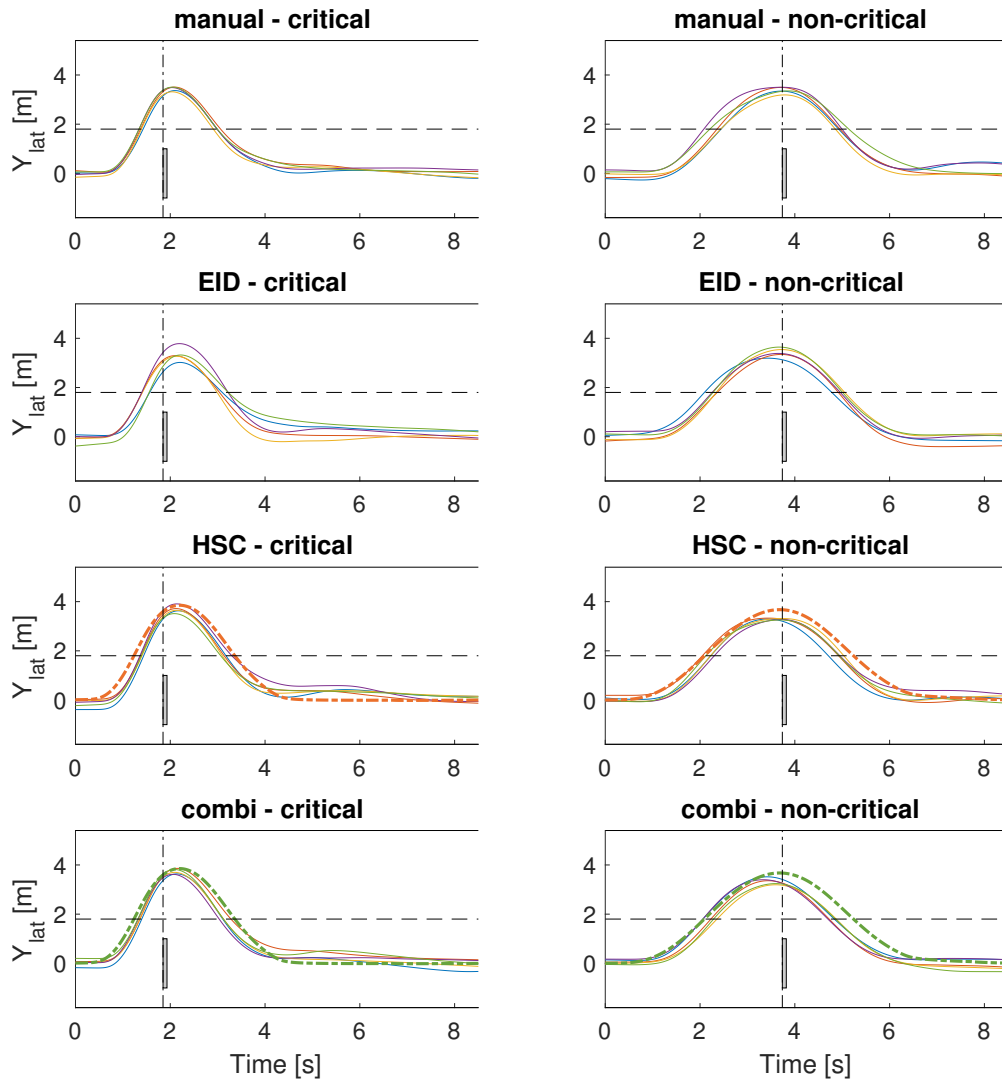


## Steering Wheel Torques - Non-Critical

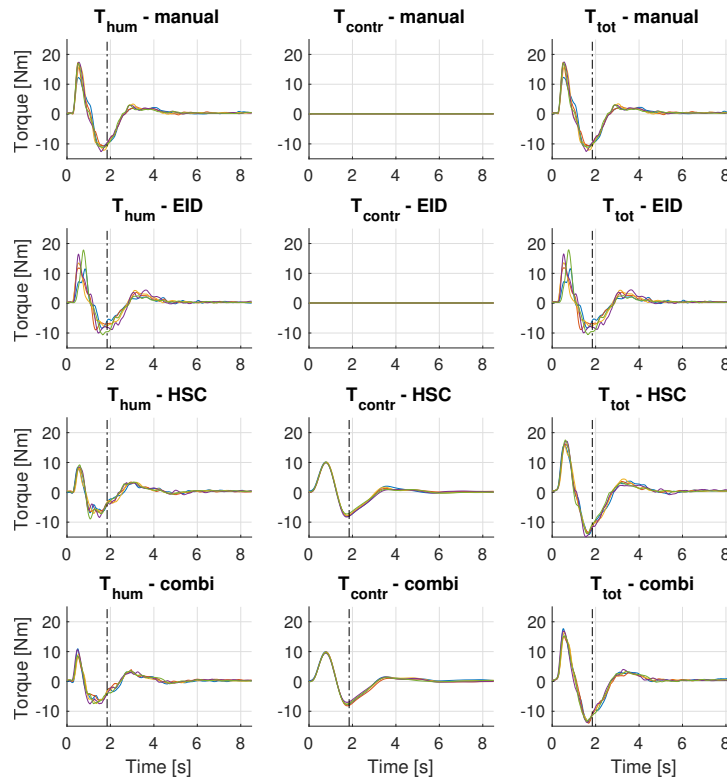


# P13 - Raw data results

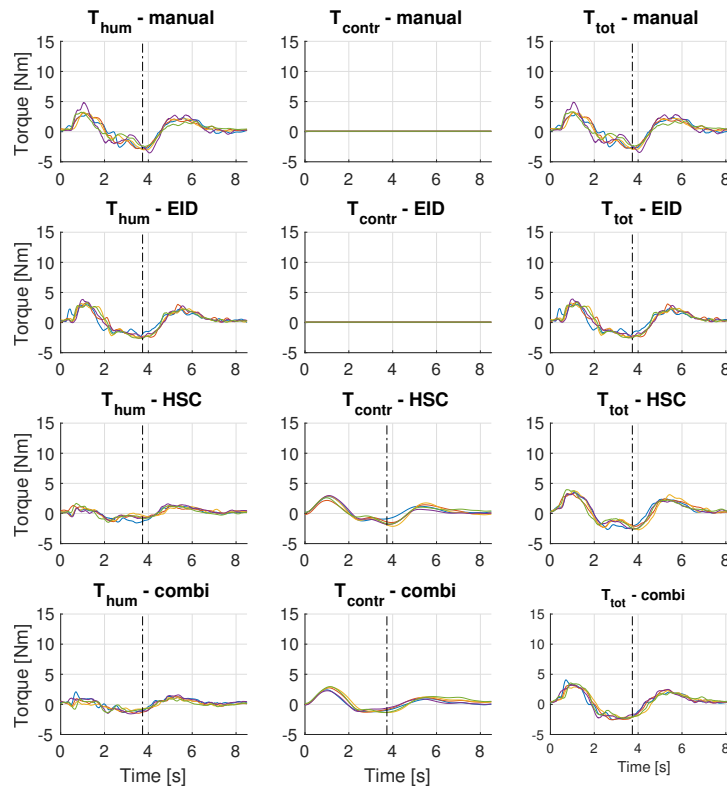
## Trajectories



## Steering Wheel Torques - Critical

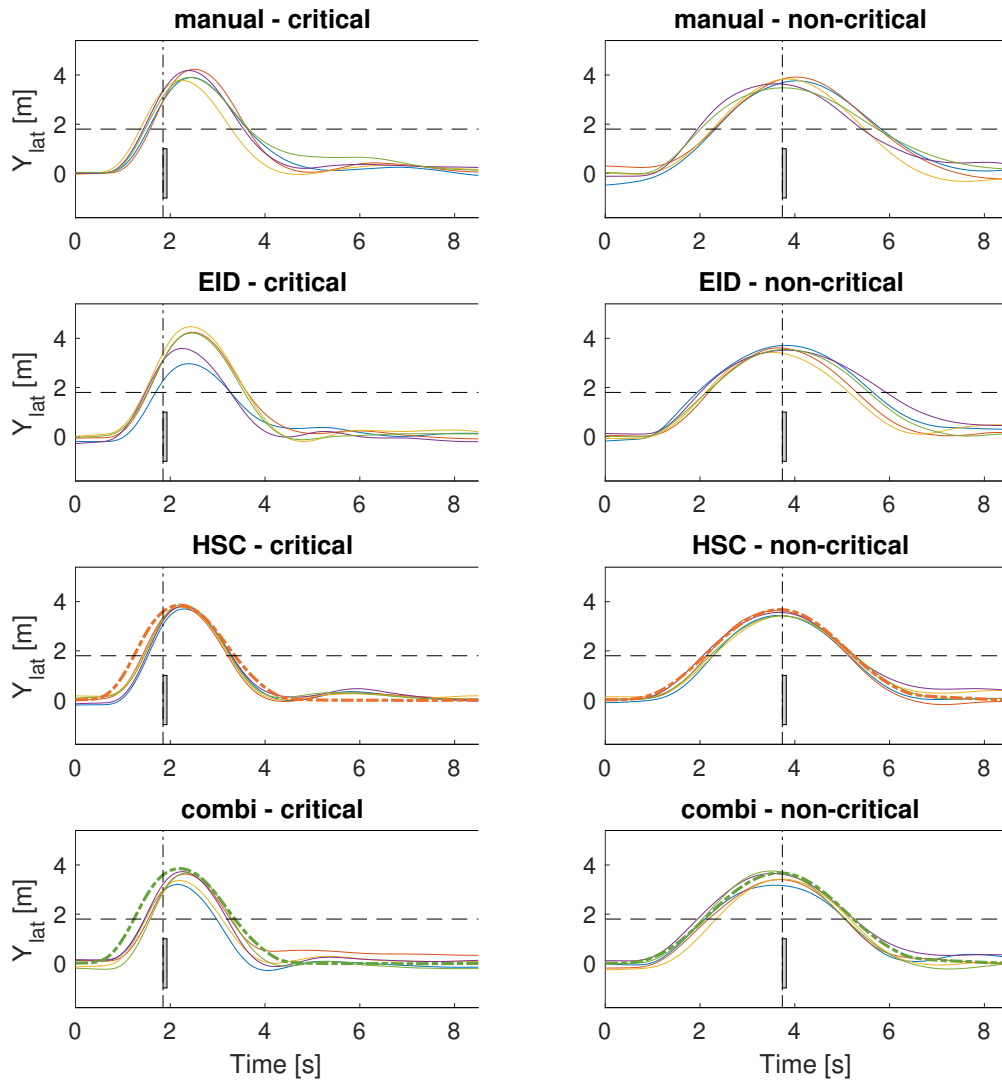


## Steering Wheel Torques - Non-Critical

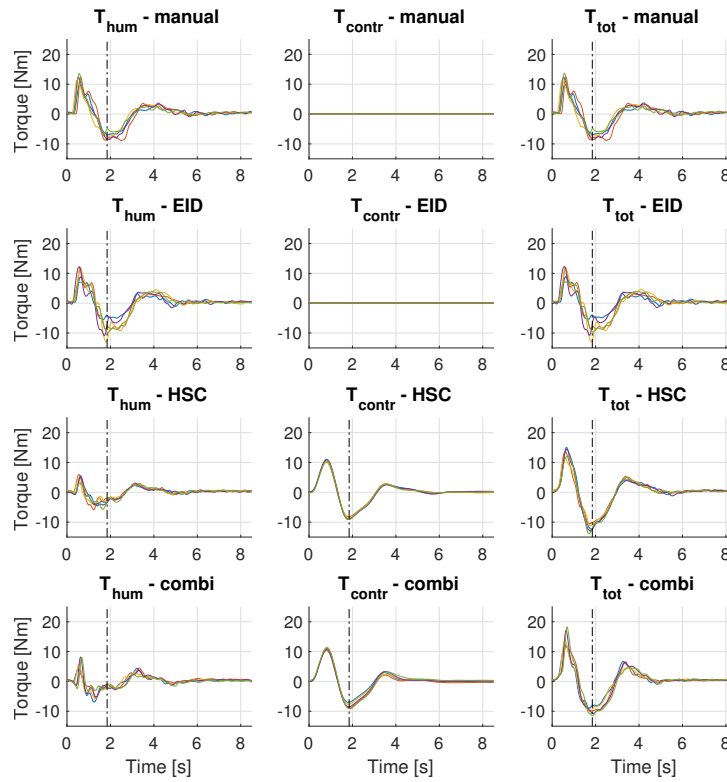


# P14 - Raw data results

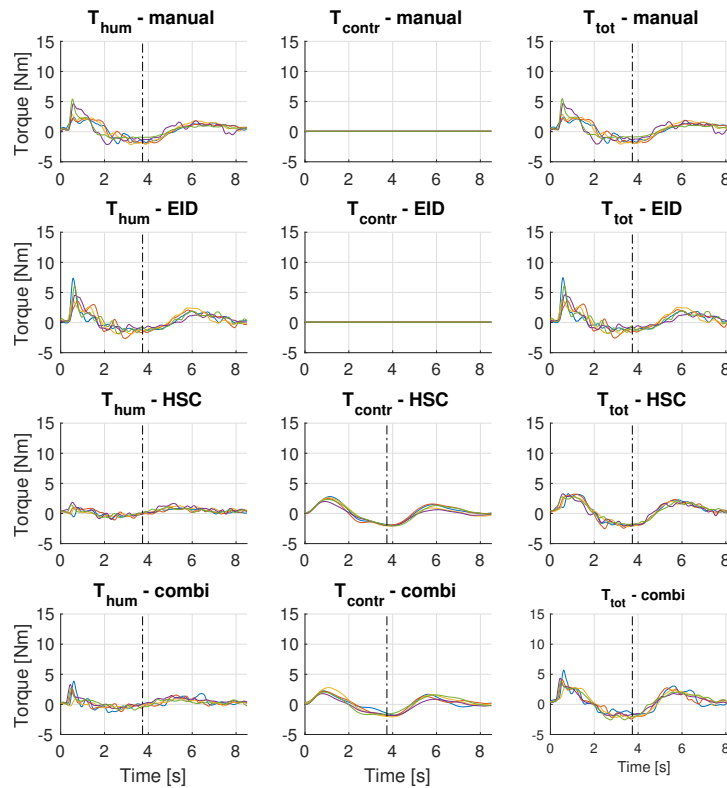
## Trajectories



## Steering Wheel Torques - Critical

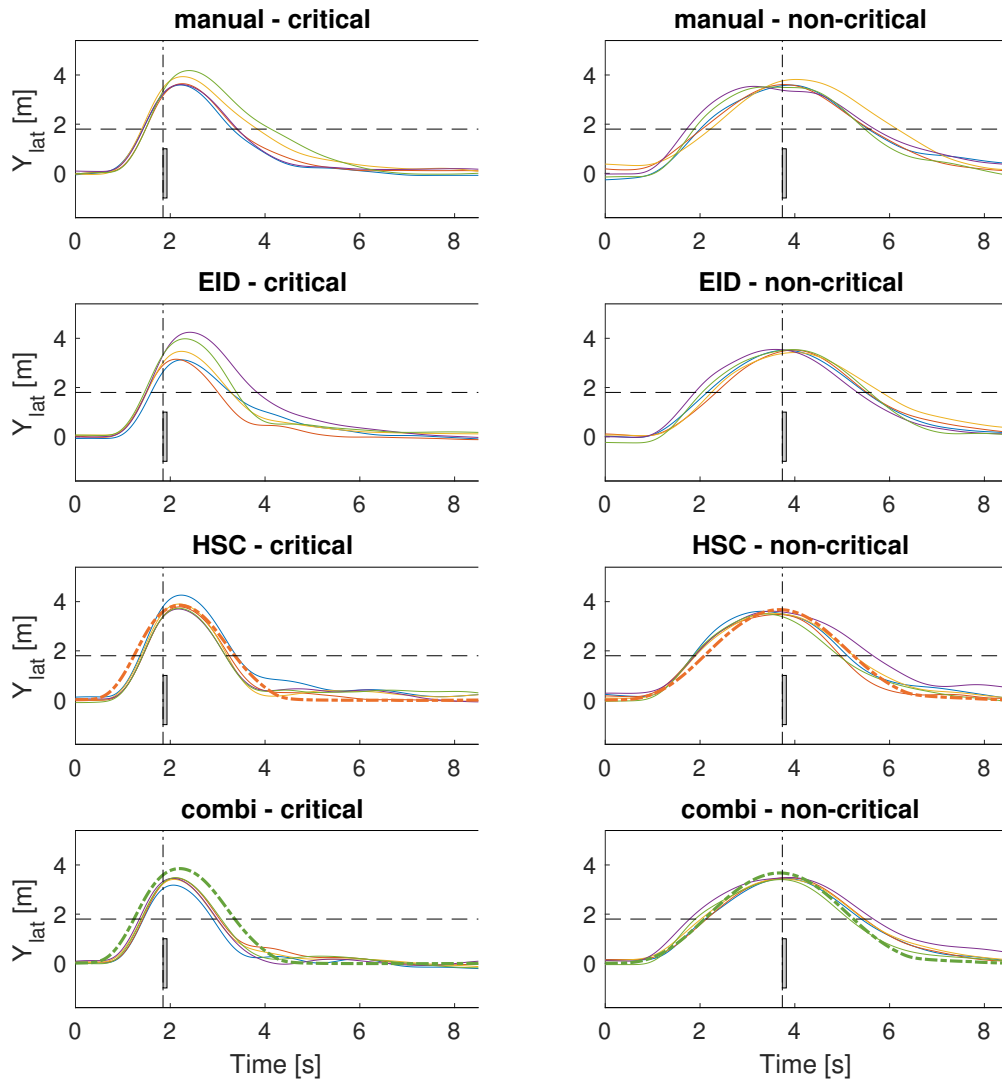


## Steering Wheel Torques - Non-Critical

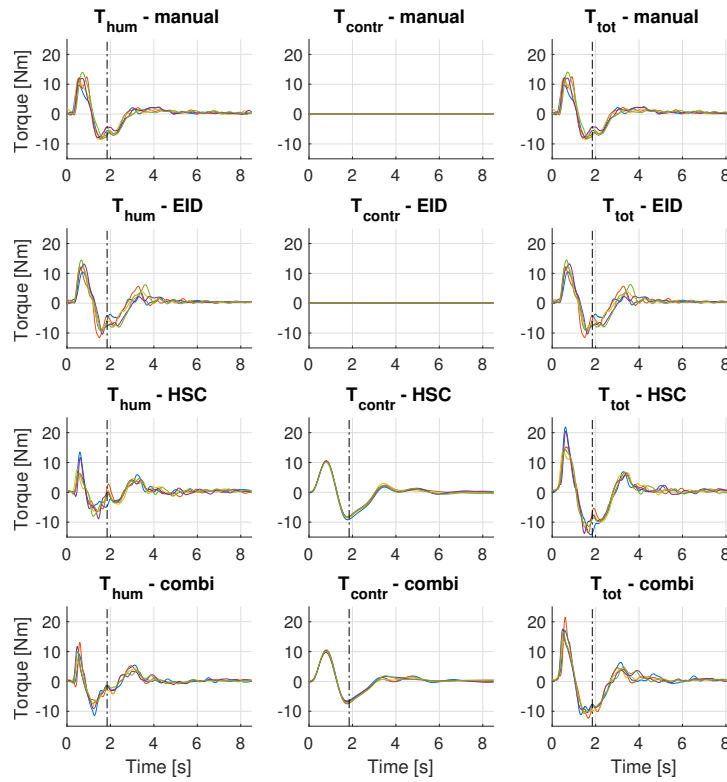


# P15 - Raw data results

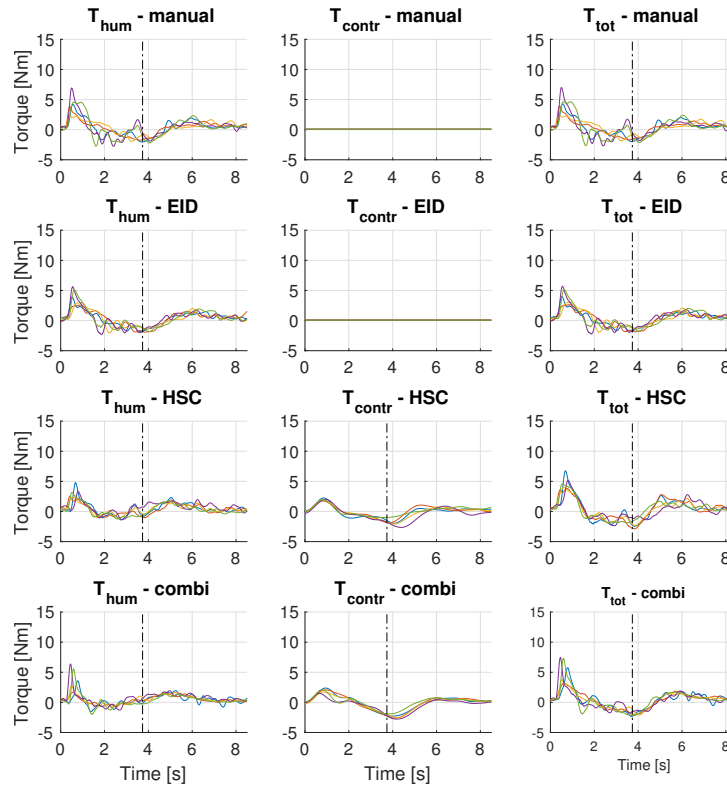
## Trajectories



## Steering Wheel Torques - Critical

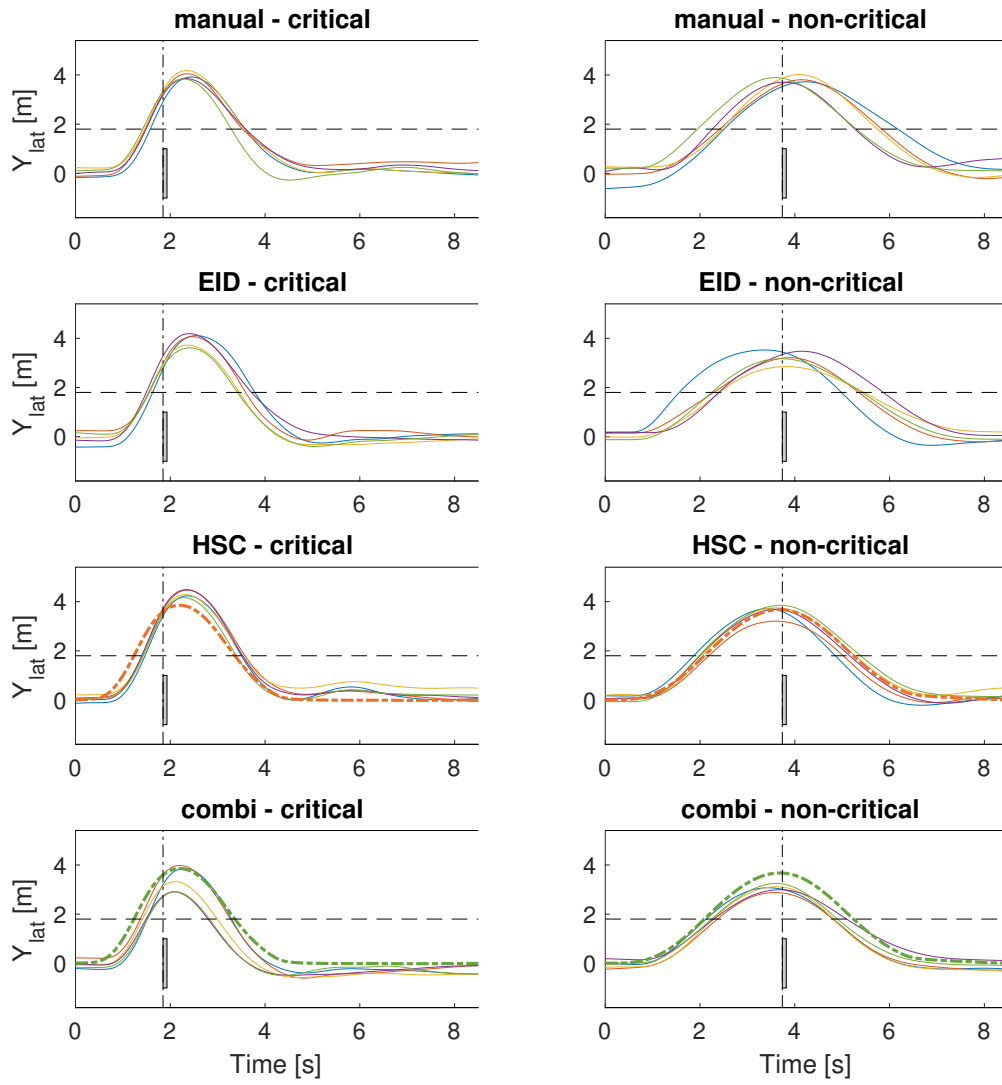


## Steering Wheel Torques - Non-Critical

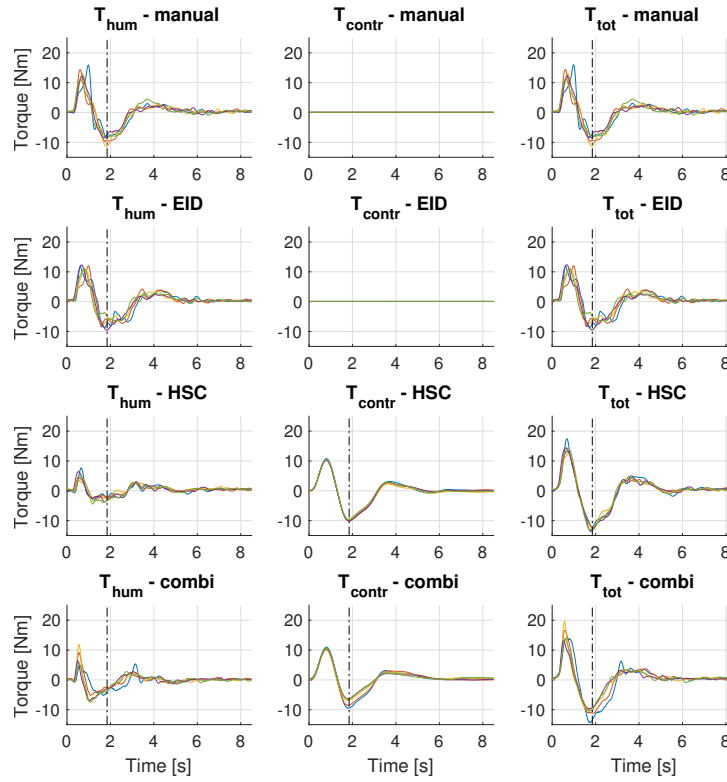


# P16 - Raw data results

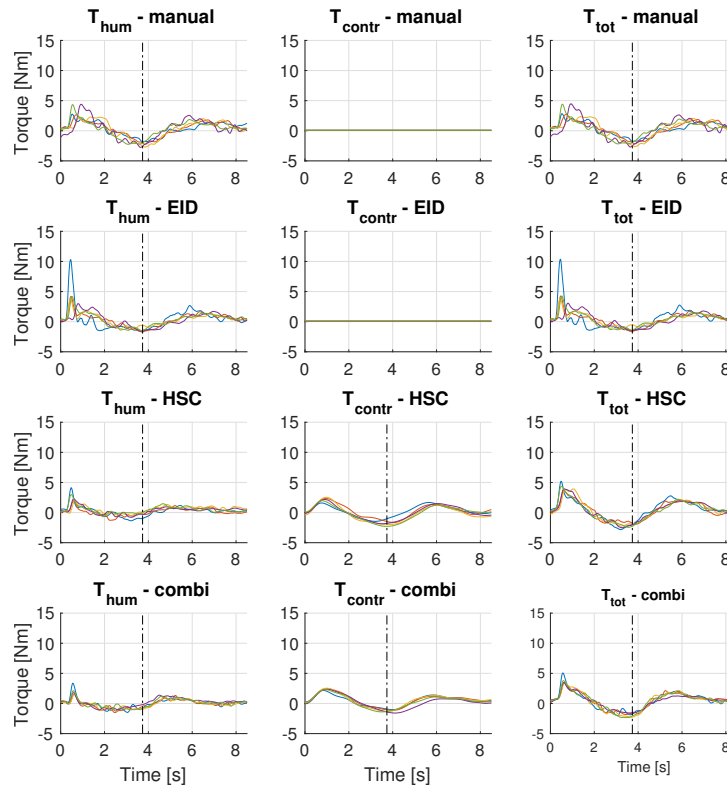
## Trajectories



## Steering Wheel Torques - Critical

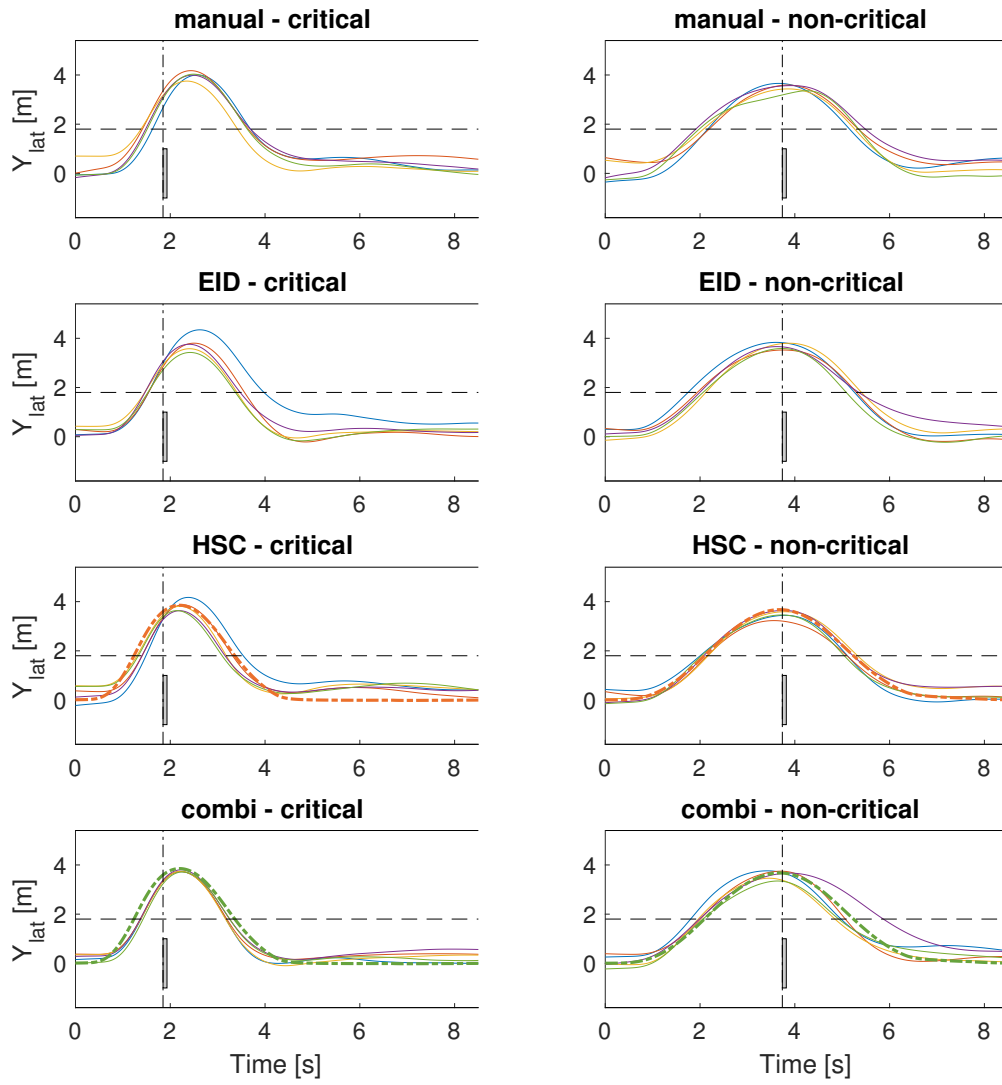


## Steering Wheel Torques - Non-Critical

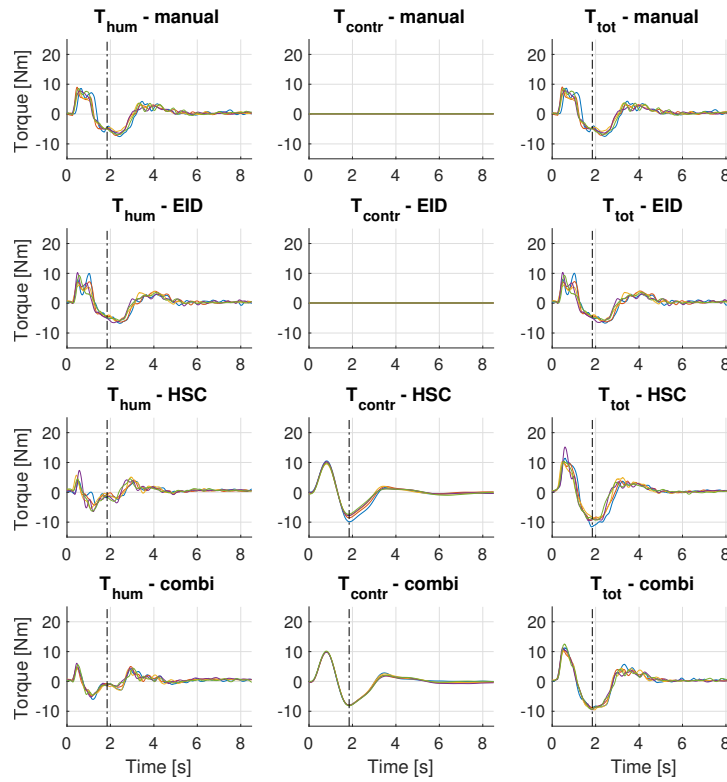


# P17 - Raw data results

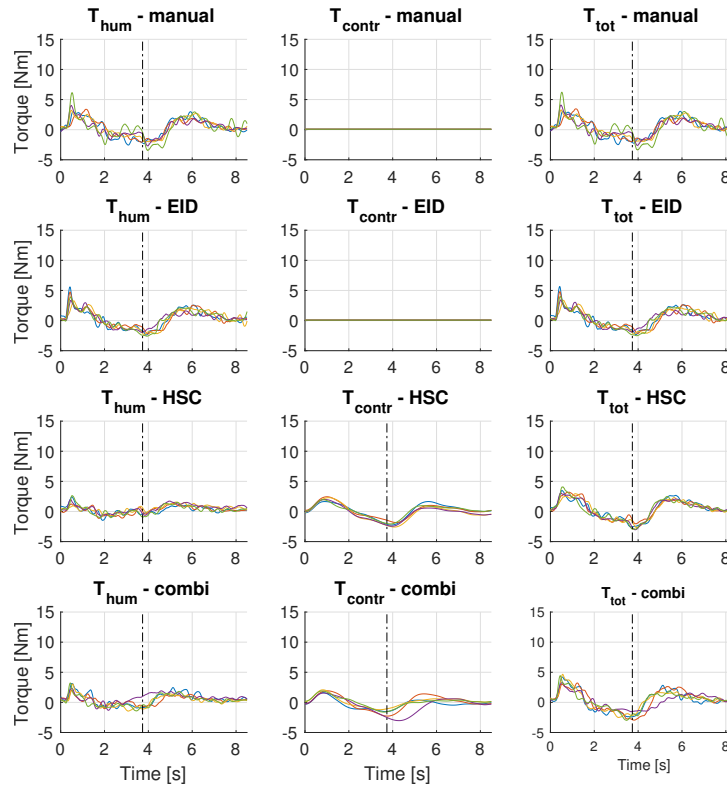
## Trajectories



## Steering Wheel Torques - Critical

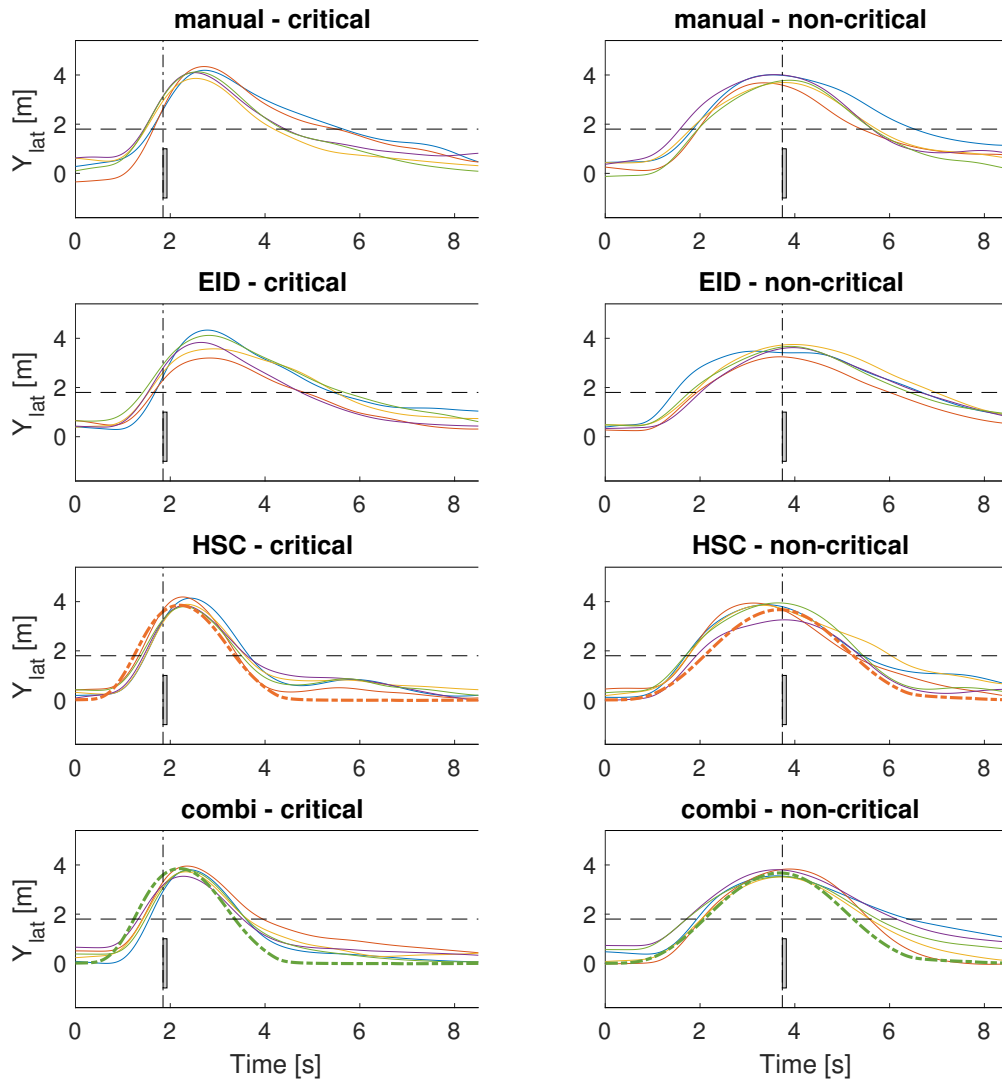


## Steering Wheel Torques - Non-Critical

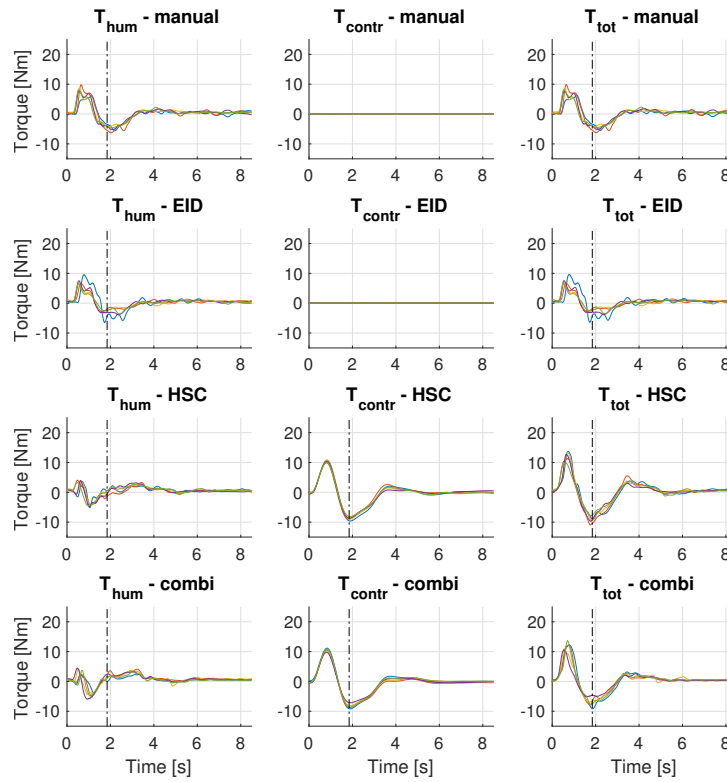


# P18 - Raw data results

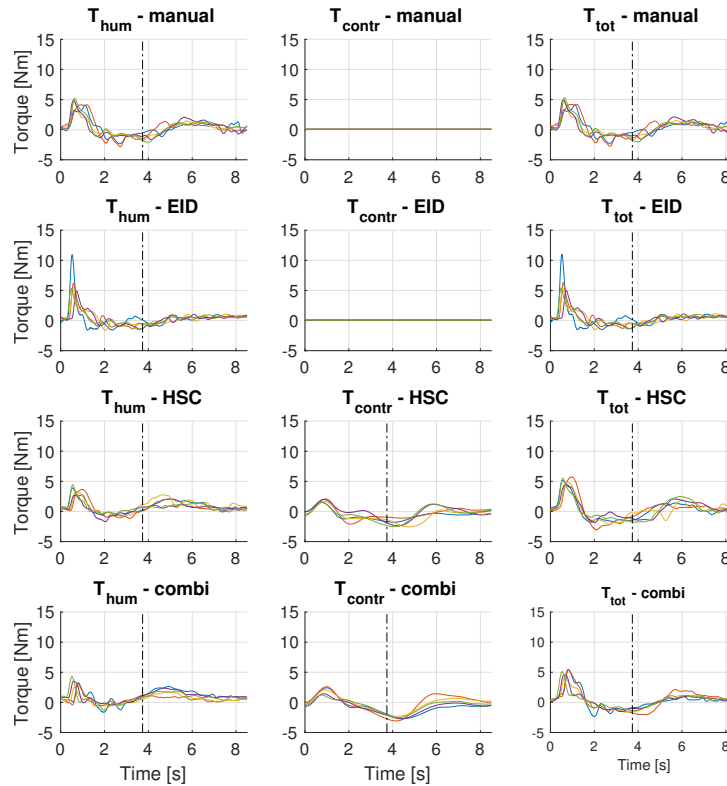
## Trajectories



## Steering Wheel Torques - Critical

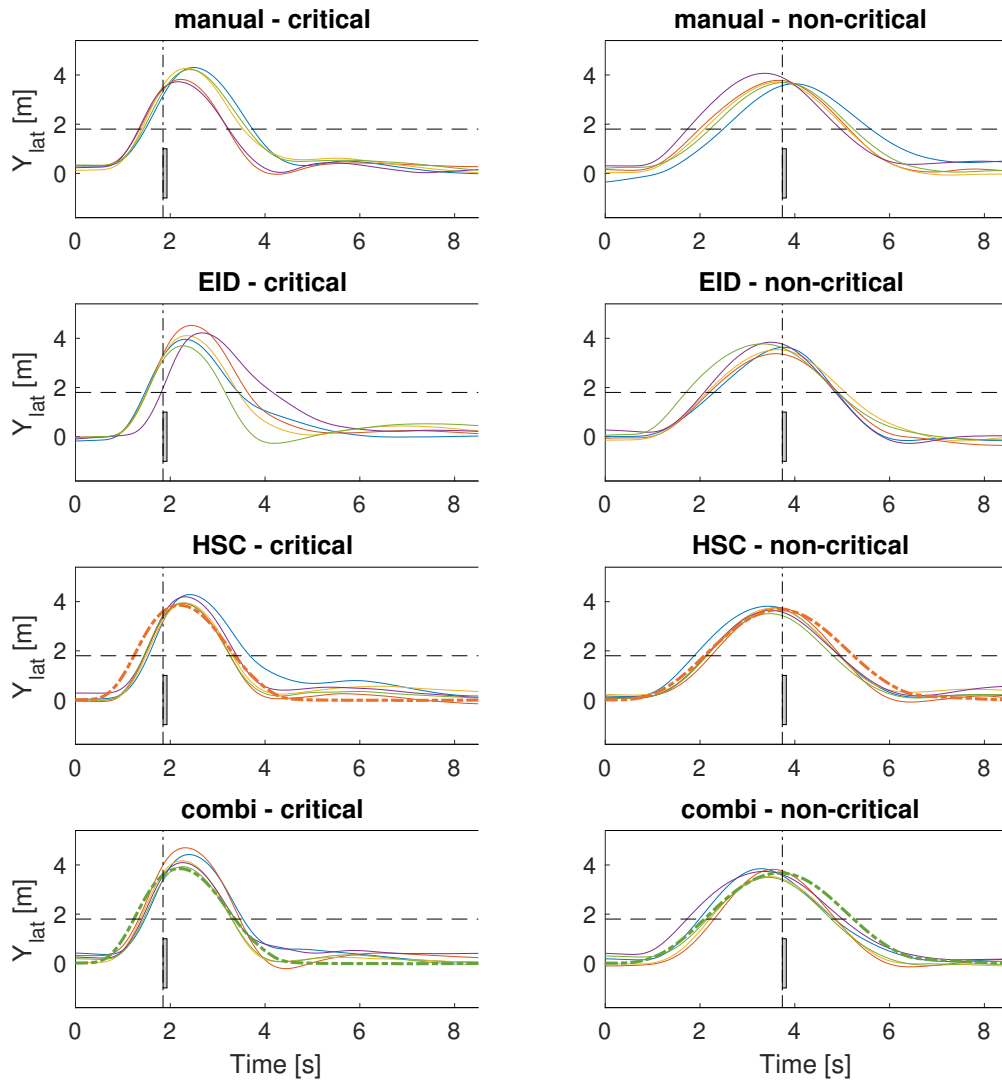


## Steering Wheel Torques - Non-Critical

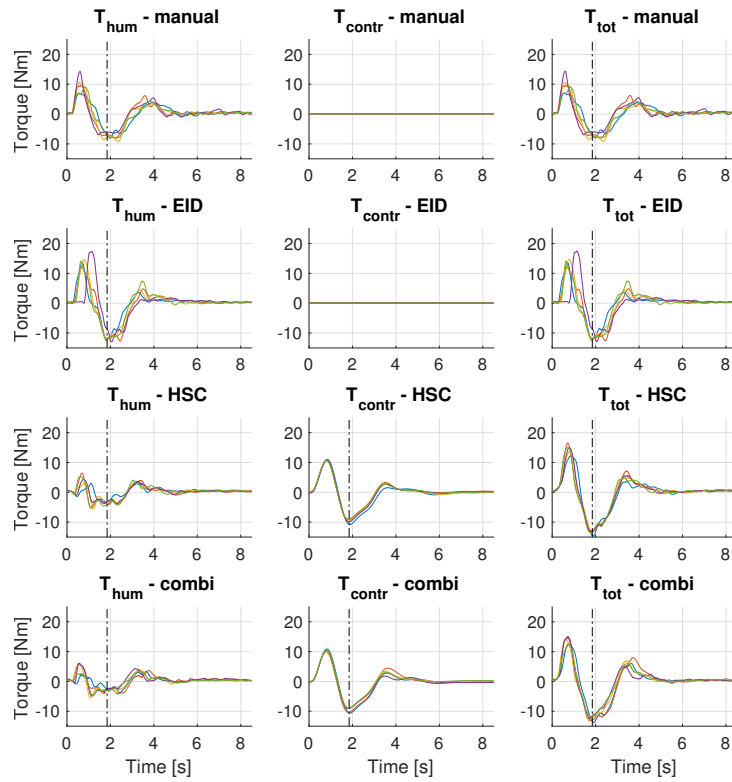


# P19 - Raw data results

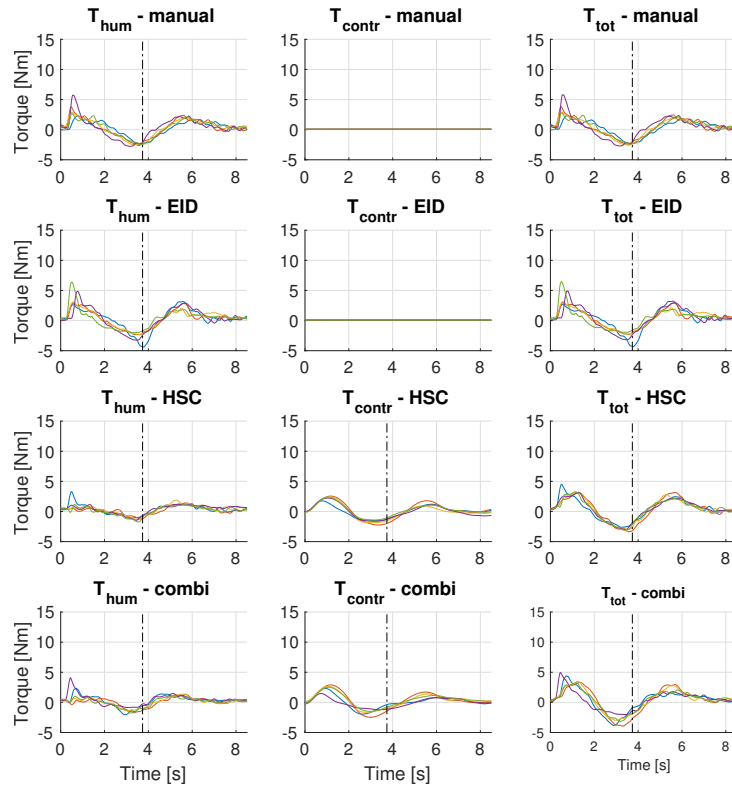
## Trajectories



## Steering Wheel Torques - Critical

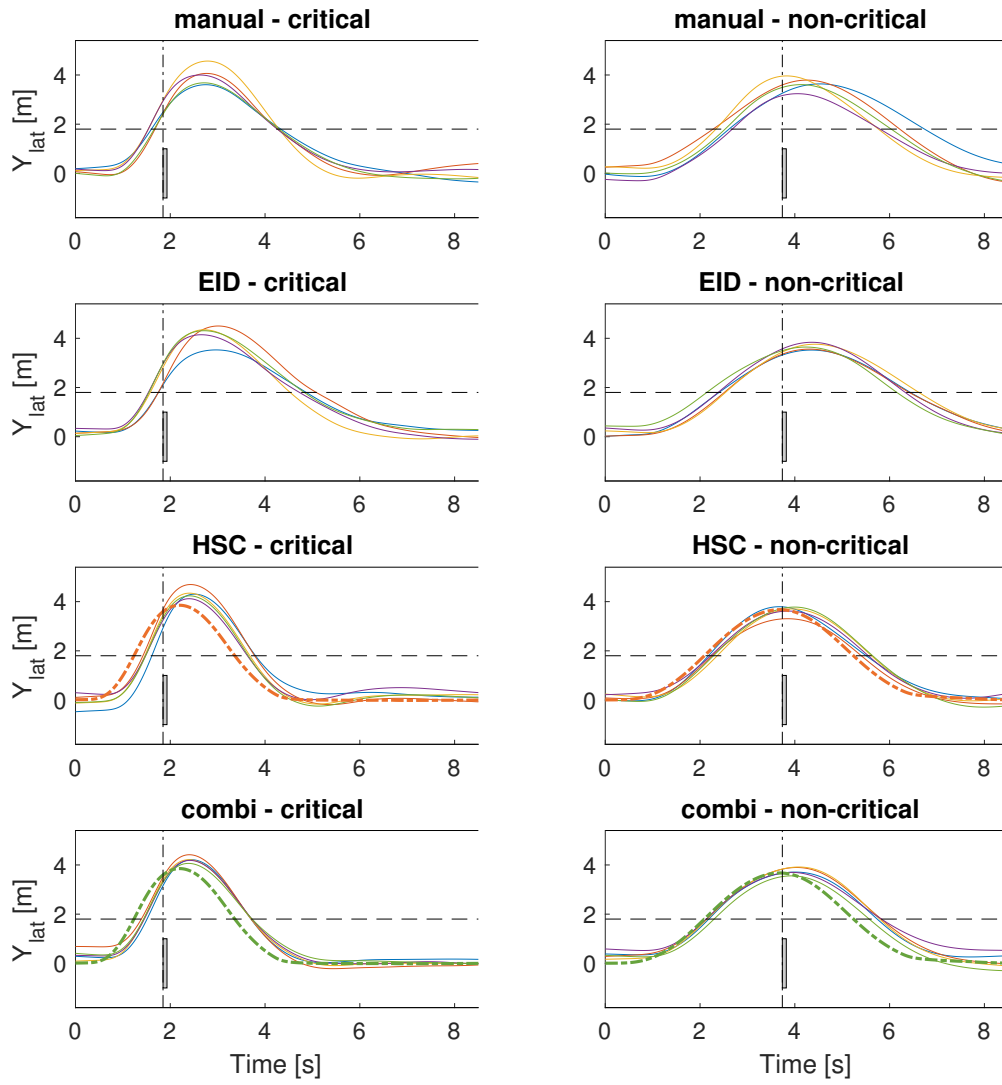


## Steering Wheel Torques - Non-Critical

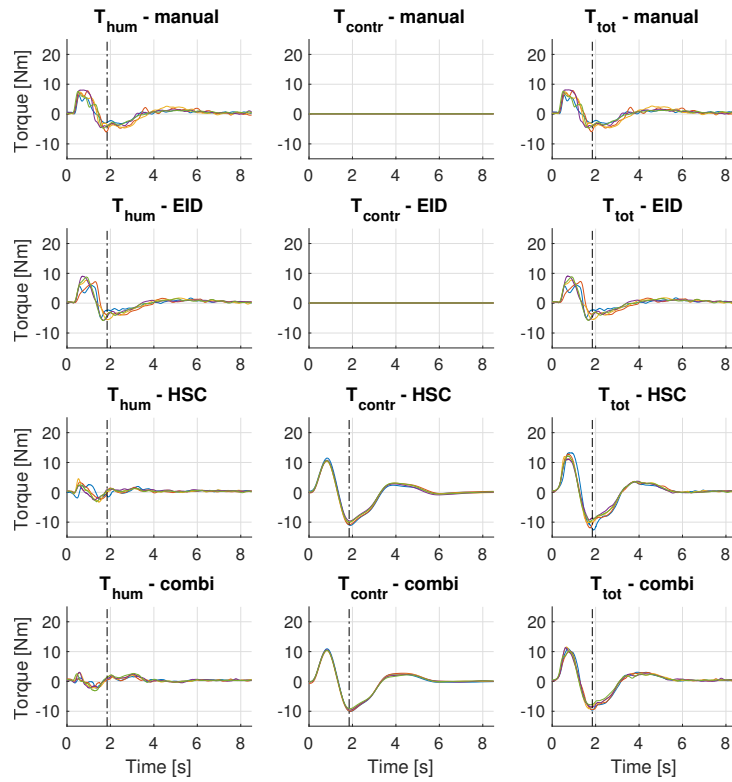


## P20 - Raw data results

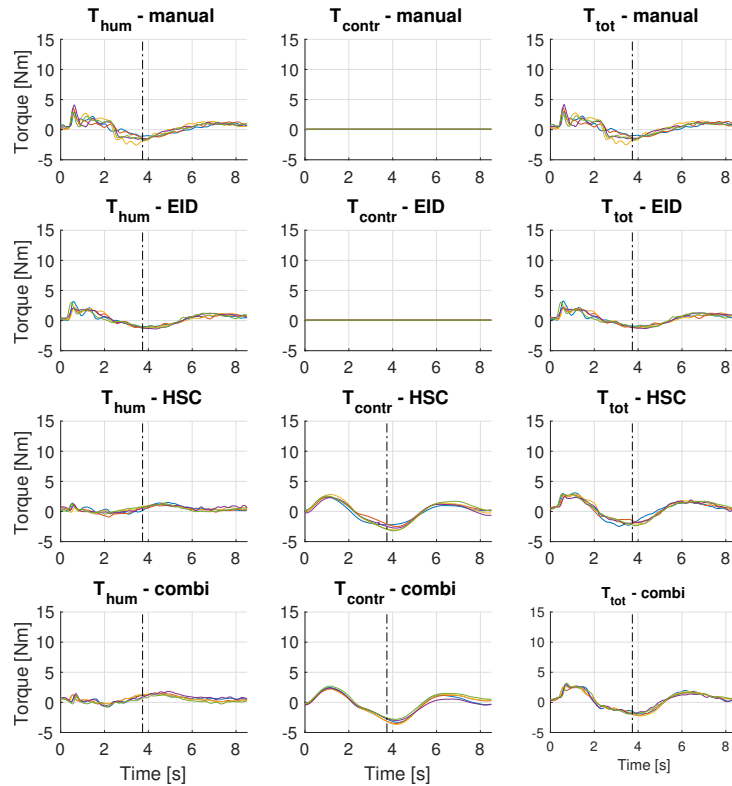
### Trajectories



## Steering Wheel Torques - Critical

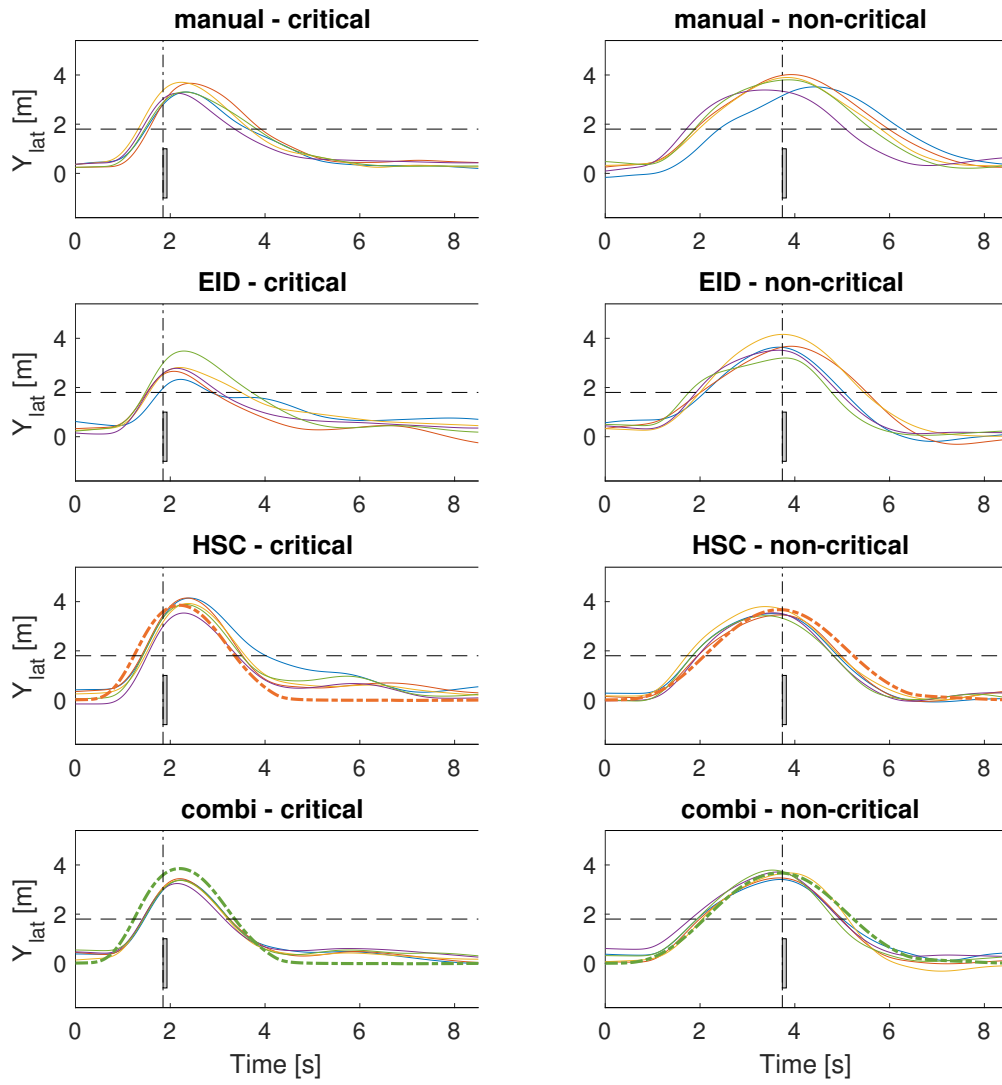


## Steering Wheel Torques - Non-Critical

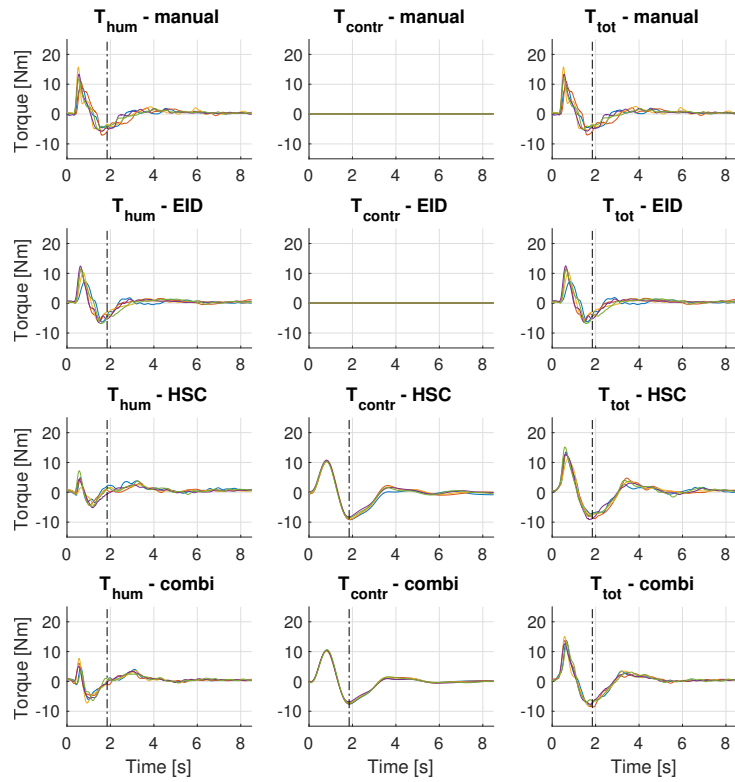


## P21 - Raw data results

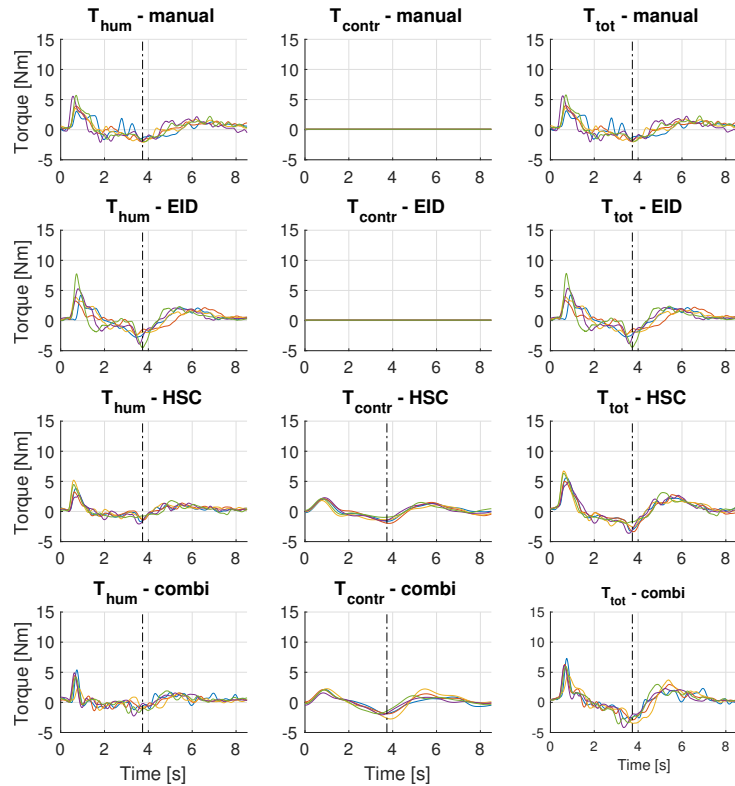
### Trajectories



## Steering Wheel Torques - Critical

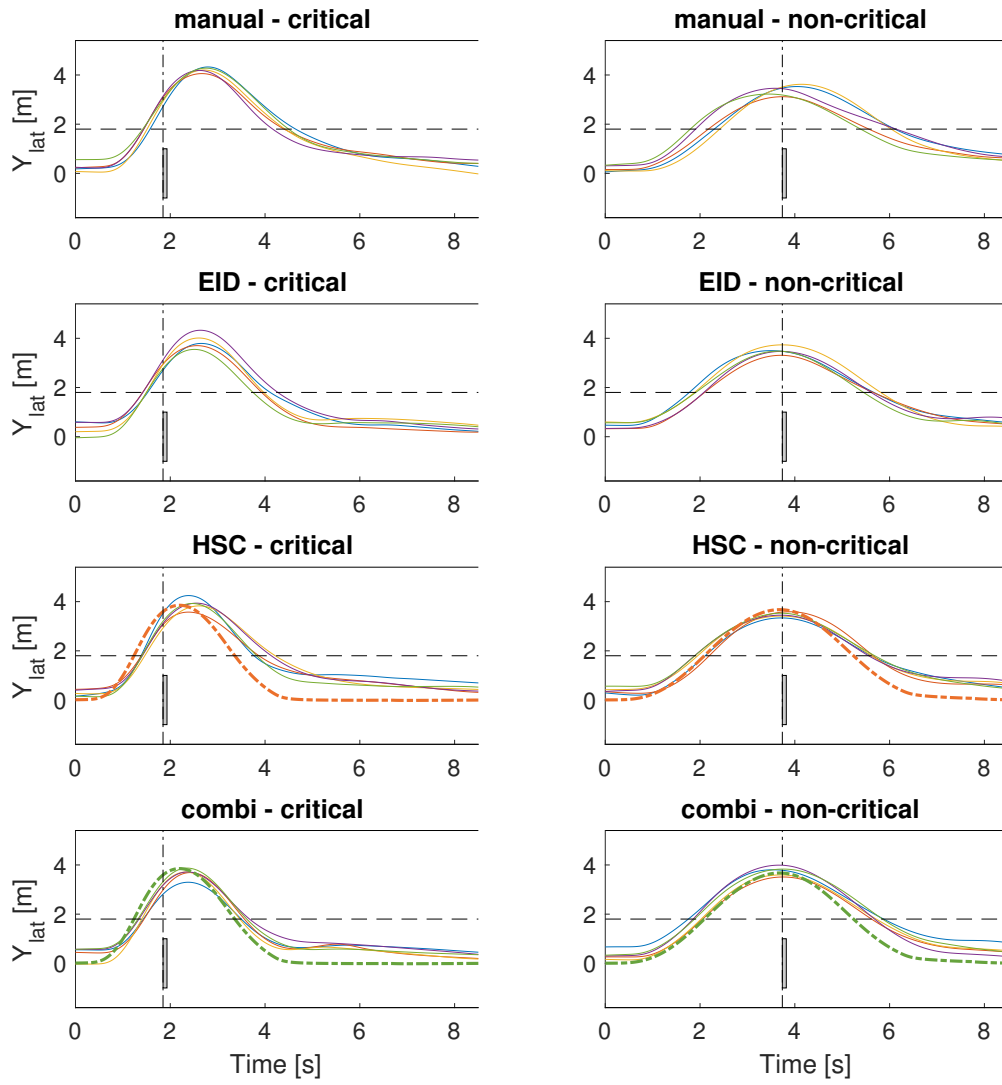


## Steering Wheel Torques - Non-Critical

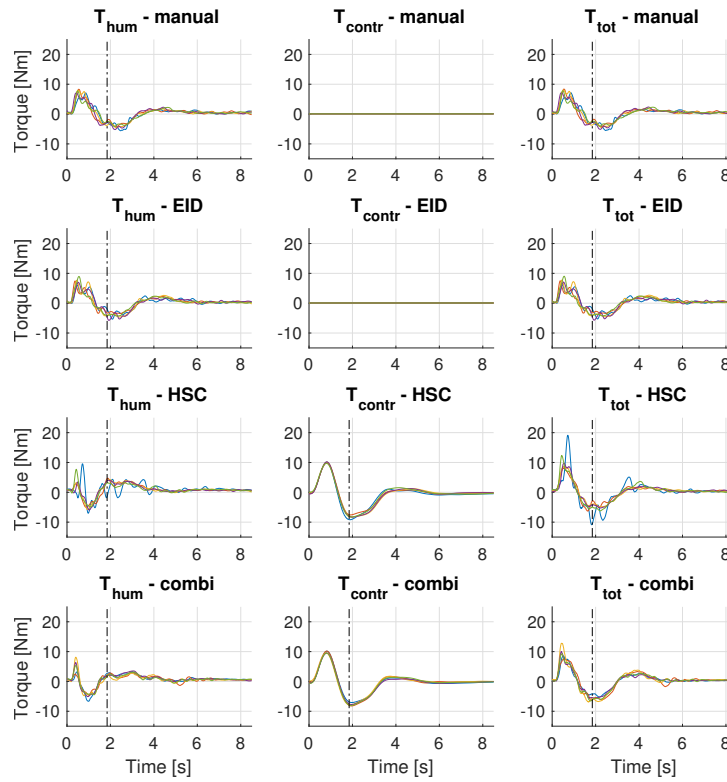


## P22 - Raw data results

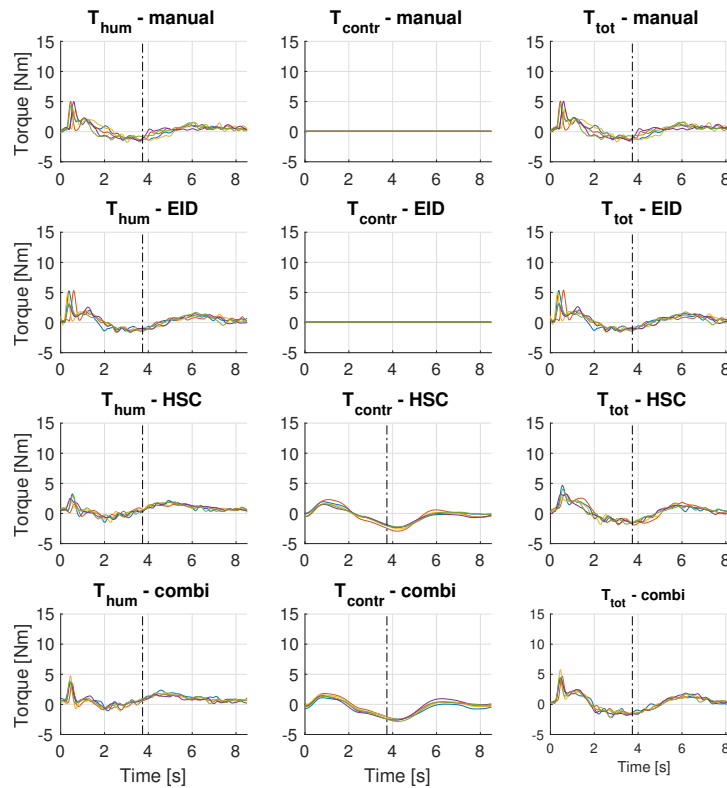
### Trajectories



## Steering Wheel Torques - Critical

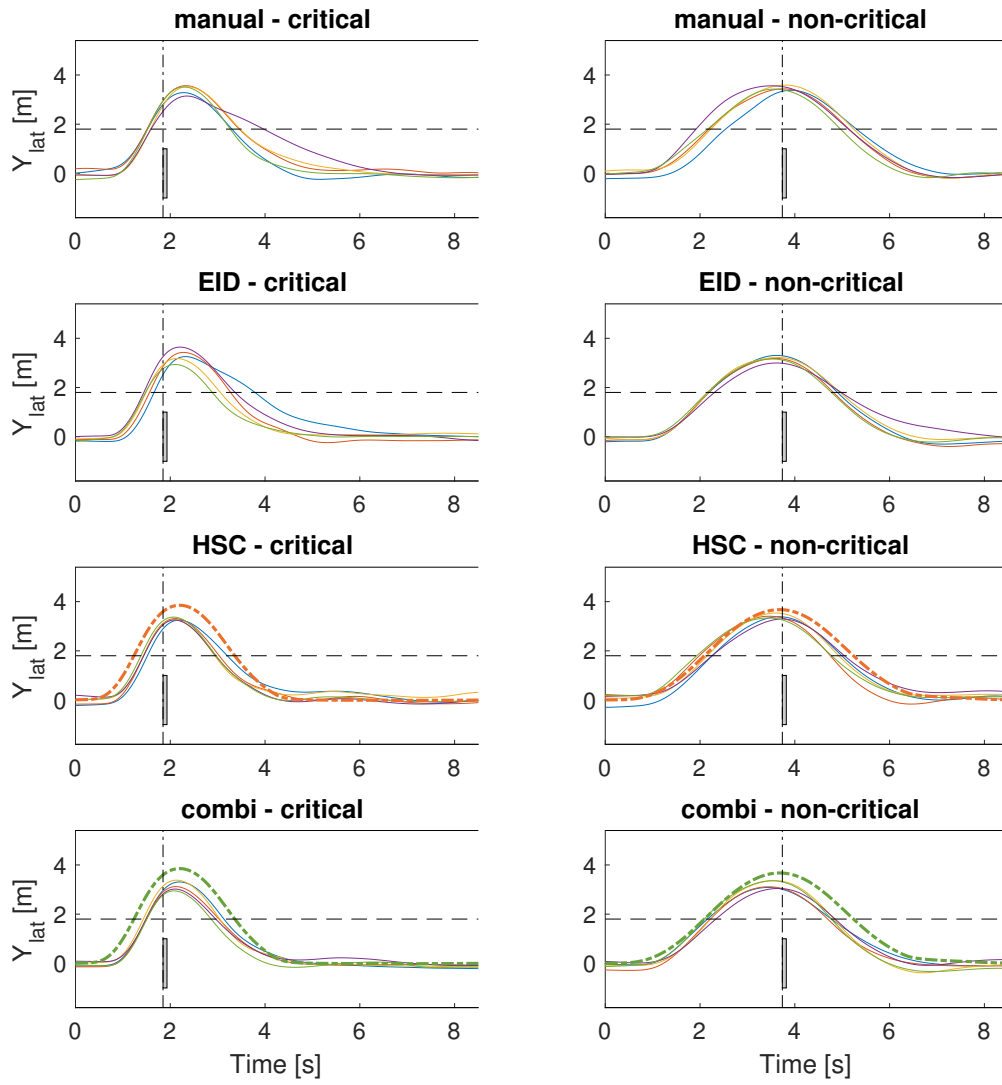


## Steering Wheel Torques - Non-Critical

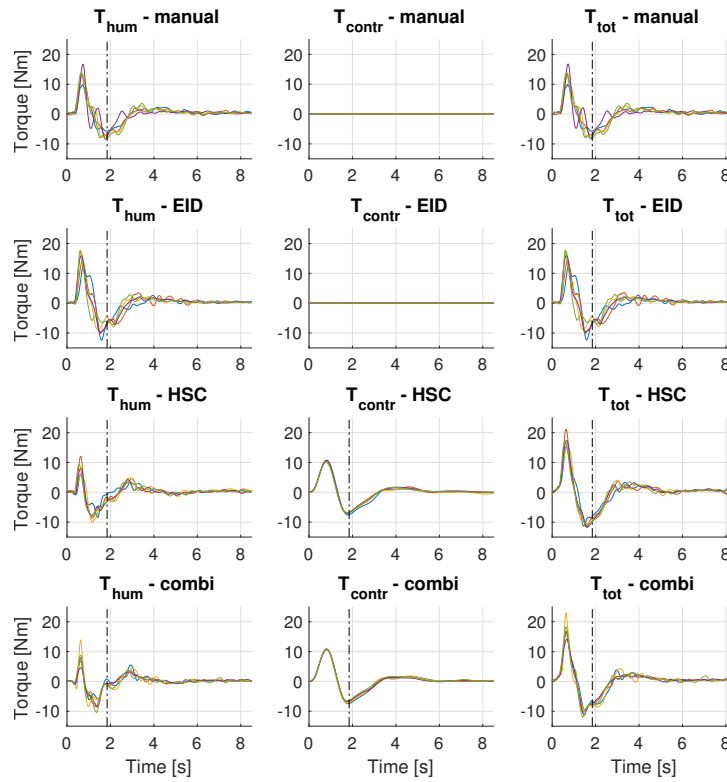


## P23 - Raw data results

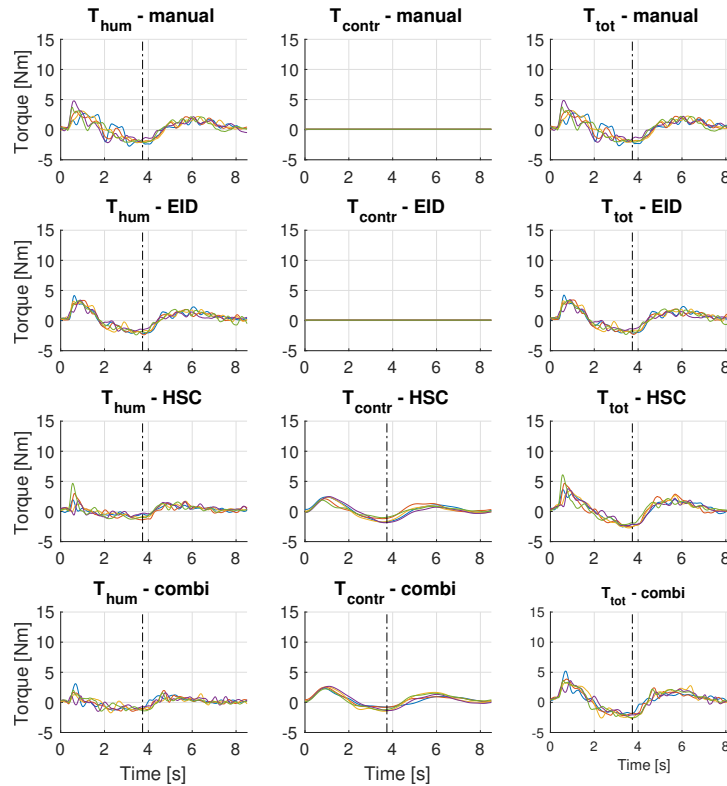
### Trajectories



## Steering Wheel Torques - Critical

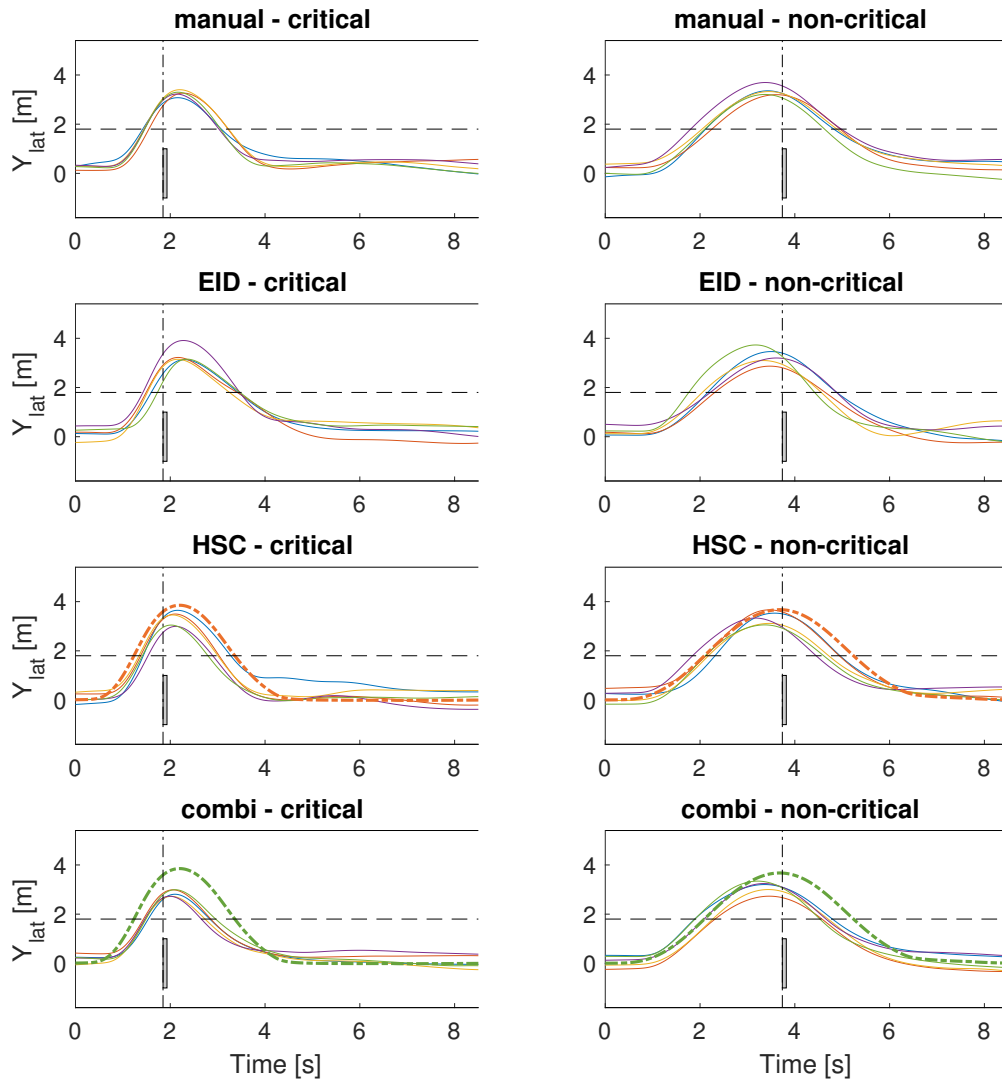


## Steering Wheel Torques - Non-Critical

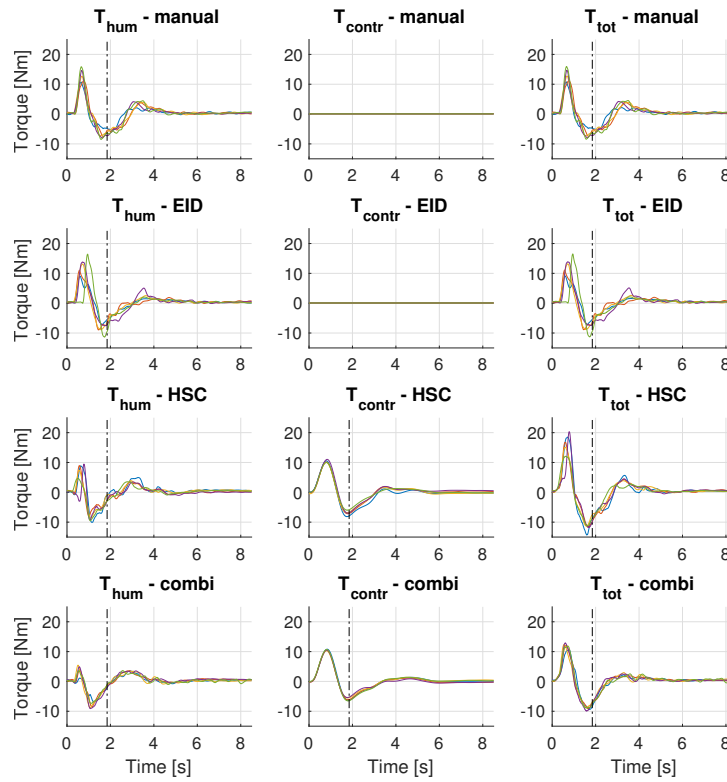


## P24 - Raw data results

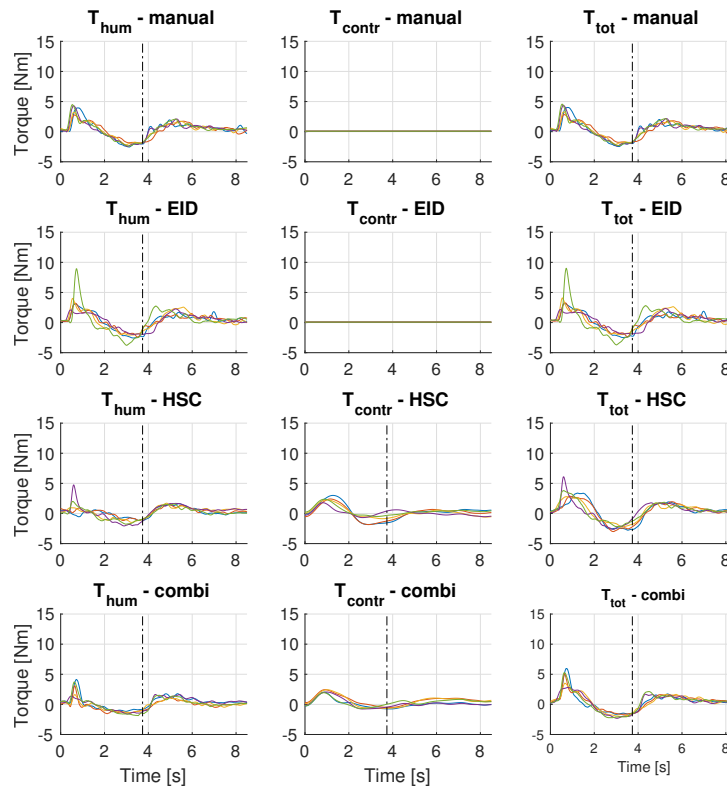
### Trajectories



## Steering Wheel Torques - Critical

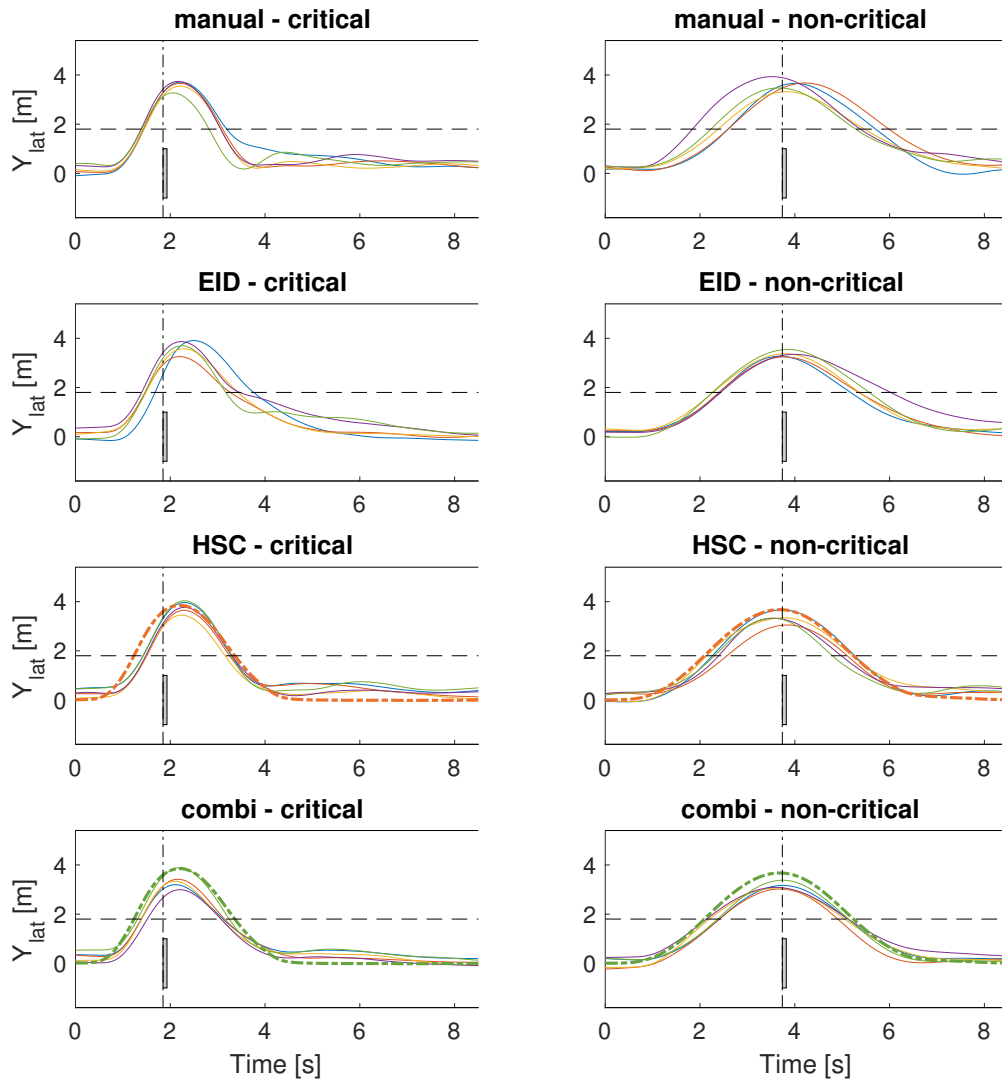


## Steering Wheel Torques - Non-Critical

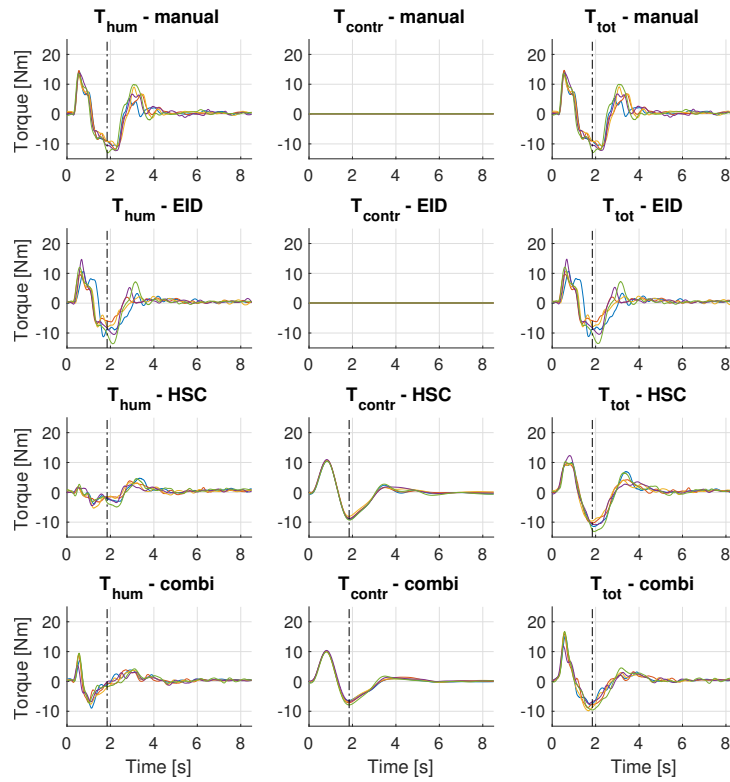


## P25 - Raw data results

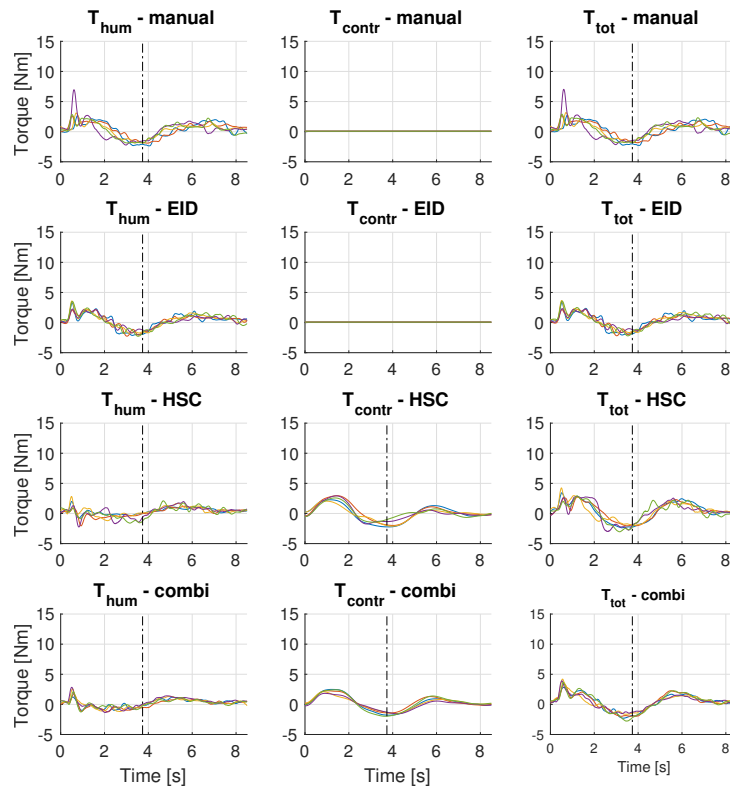
### Trajectories



## Steering Wheel Torques - Critical

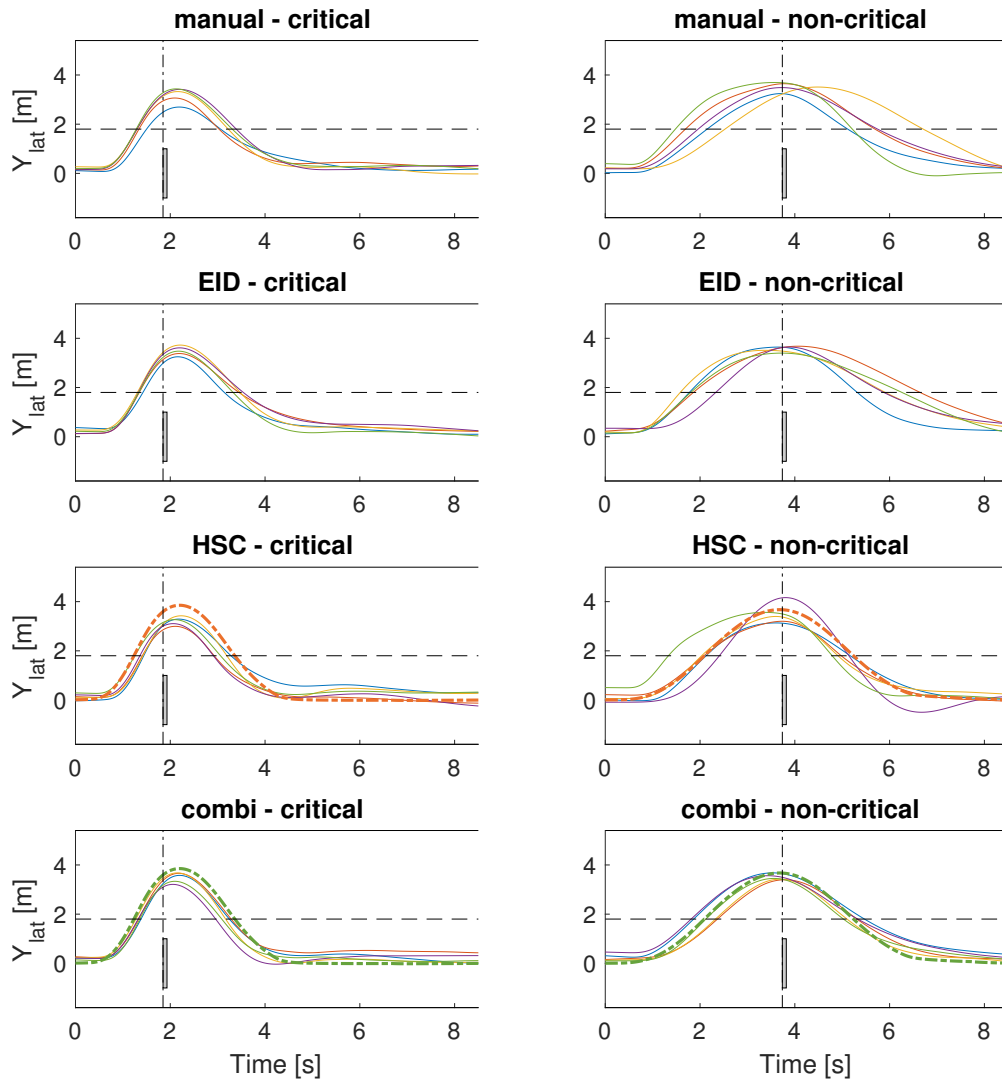


## Steering Wheel Torques - Non-Critical

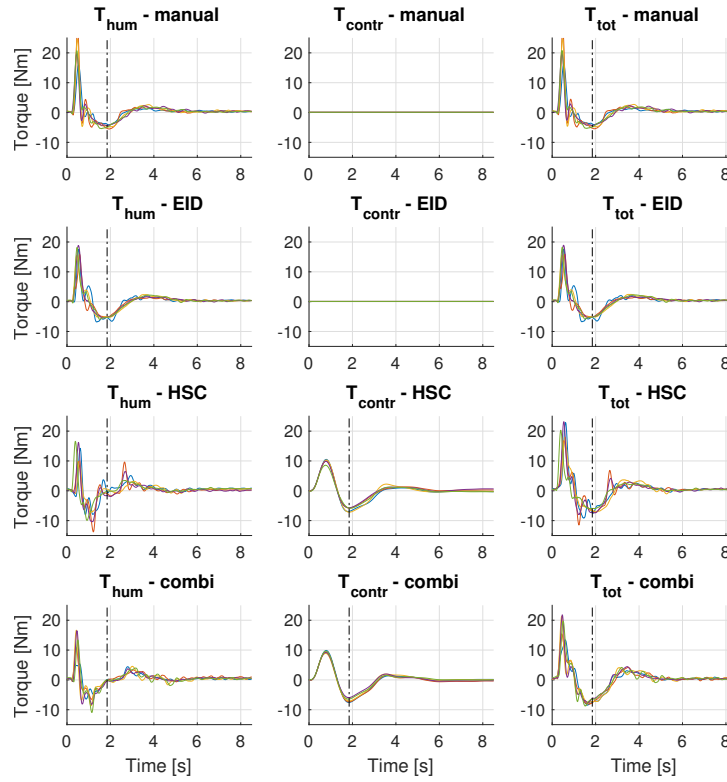


## P26 - Raw data results

### Trajectories



## Steering Wheel Torques - Critical



## Steering Wheel Torques - Non-Critical

